

**Supporting Information for:**

## **Innovative Chalcogenide Transfer Agent for Improved Aqueous Quantum Dot Synthesis**

Guillaume Petit,<sup>[a]</sup> Cédric Malherbe,<sup>[b]</sup> Pauline Bianchi,<sup>[a]</sup> and Jean-Christophe M. Monbaliu\*<sup>[a,c]</sup>

<sup>a</sup>. Center for Integrated Technology and Organic Synthesis (CiTOS), MoISys Research Unit, University of Liège, B-4000 Liège (Sart Tilman), Belgium

[jc.monbaliu@uliege.be](mailto:jc.monbaliu@uliege.be) | [www.citos.uliege.be](http://www.citos.uliege.be)

<sup>b</sup>. Mass Spectrometry Laboratory, MoISys Research Unit, University of Liège, B-4000 Liège (Sart Tilman), Belgium

<sup>c</sup>. WEL Research Institute, Avenue Pasteur 6, B-1300 Wavre, Belgium

## Contents

1. General Information .....	5
2. Reagents and Solvents .....	5
3. Continuous flow setups .....	6
3.1. Microfluidic setups and parts .....	6
3.1.1. Pumps.....	6
3.1.2. PFA tubing .....	6
3.1.3. SS tubing.....	6
3.1.4. Connectors, ferrules and mixers .....	7
3.1.5. Check valves .....	7
3.1.6. Back pressure regulators.....	7
3.1.7. Thermoregulatory devices .....	7
3.1.8. Setup flow parts and vendors .....	7
3.2. Mesofluidic setup and parts .....	8
3.2.1. Pumps.....	8
3.2.2. PFA tubing .....	8
3.2.3. SS tubing.....	8
3.2.4. Connectors, ferrules and mixers .....	8
3.2.5. Back pressure regulator .....	8
3.2.6. Thermoregulatory devices .....	8
4. Setups and protocols .....	9
4.1. Batch optimization of TCEP=S.....	9
4.2. Batch optimization of TCEP=Se.....	10
4.3. Batch optimization of TCEP=Te .....	10
4.4. Stability study for TCEP=X (X = Se, Te).....	10
4.4.1. Stability of TCEP=Se vs NaHSe in water (open flask) .....	10
4.4.2. Stability study for TCEP=Te .....	11
4.5. Raman monitoring of TCEP=X formation .....	11
4.5.1. Preliminary pH optimization .....	11
4.5.2. Experimental setup for <i>in-situ</i> Raman monitoring.....	13
4.5.3. Monitoring of TCEP=S formation .....	13
4.5.4. Monitoring of TCEP=Se formation .....	14

4.5.5.	Monitoring of TCEP=Te formation .....	14
4.6.	Transposition in flow of TCEP=X synthesis (lab scale).....	14
4.6.1.	Design of the chalcogenide packed-bed column .....	14
4.6.2	TCEP feed preparation .....	16
4.7.	Concatenated microfluidic preparation of QDs synthesis.....	16
4.7.1.	Setup.....	16
4.7.2.	In-line monitoring.....	17
4.7.3.	Concatenated preparation of CdS.....	18
4.7.4.	Concatenated preparation of CdSe.....	19
4.7.5.	Concatenated preparation of CdTe.....	19
4.8.	Preparation of type I CdSe@ZnS core-shell QDs.....	19
4.8.1.	Setup.....	20
4.8.2.	Preparation of the feed solutions .....	20
4.8.3.	Modus operandi .....	21
4.9.	Flow synthesis of CdTe .....	21
4.9.1.	Preparation of the feed solutions .....	21
4.9.2.	Setup.....	22
4.9.3.	Sample analysis .....	22
4.9.4.	Data analysis.....	22
4.10.	Mesofluidic synthesis of CdTe .....	23
4.10.1.	Detailed setup for the pilot scale production of CdTe .....	23
4.10.2.	Heat exchanger.....	24
4.10.3.	Feed preparation .....	24
4.10.4.	Modus operandi .....	24
5.	Additional experimental details.....	25
5.1.	Stability study for TCEP=Te.....	25
5.2.	Determination of the optimum pH.....	26
5.3.	Raman monitoring for the formation of TCEP=S.....	26
5.4.	Raman monitoring for the formation of TCEP=Se.....	28
5.5.	TCEP=Te Raman monitoring .....	29
5.6.	Establishment of a kinetic model .....	31
5.7.	Transposition of the TCEP=X synthesis in flow (microfluidic scale) .....	34
5.8.	Productivity of TCEP=Te over time .....	34

5.9.	Control experiment for the preparation of CdS .....	35
5.10.	Determination of reaction yield.....	36
5.11.	Sample preparation for QDs characterization .....	37
5.11.1.	High-Resolution Transmission Electron Microscopy (HRTEM).....	37
5.11.2.	X-Ray Powder Diffraction (PXRD) .....	37
5.11.3.	Diffusion-Ordered NMR Spectroscopy (DOSY).....	37
5.11.4.	X-Ray Photoelectron Spectroscopy (XPS).....	37
5.12.	Additional experimental details for CdSe/ZnS QDs .....	37
5.13.	Isotopic labeling .....	41
5.13.1.	TCEP <sup>16</sup> O reference synthesis .....	41
5.13.2.	Isotopic labeling for CdTe QDs synthesis.....	41
5.13.3.	HPLC-MS method.....	43
5.14.	Compounds characterization.....	44
5.15.	Copy of the spectra (NMR, Raman or UV/Vis, photoluminescence).....	45
5.15.1.	TCEP .....	45
5.15.2.	TCEP=O .....	45
5.15.3.	TCEP=S .....	47
5.15.4.	TCEP=Se .....	49
5.15.5.	TCEP=Te .....	52
5.15.6.	CdS .....	54
5.15.7.	CdSe core .....	56
5.15.8.	CdSe\ZnS.....	58
5.15.9.	CdTe .....	59
5.16.	DFT calculations .....	62
6.	References .....	64

## 1. General Information

High-field NMR experiments (structural identification of intermediates and determination of NMR conversions for the batch experiments) were carried out with a Bruker Avance III 400 MHz spectrometer in D<sub>2</sub>O. The chemical shifts ( $\delta$ ) are reported relative to the solvent residual peak or to H<sub>3</sub>PO<sub>4</sub> (<sup>31</sup>P NMR). In-line monitoring with low-field <sup>31</sup>P NMR experiments was carried out with a Magritek Spinsolve Ultra Phosphorus 43 MHz equipped with a flow-through glass cell (Spinsolve RM2 kit).

Transmission electron microscopy (TEM) was performed with a LaB6-Tecnai G2 under 180 kV acceleration voltage, in bright field mode, on 200 mesh carbon-coated copper grids.

X-ray powder diffraction (XRD) was used to characterize the crystal structure (Bruker AXS D8 Discover) using Cu K radiation. The samples were analyzed on a zero background substrate.

Absorbance measurements were recorded on an AvaSpec-ULS2048XL EV spectrometer (Ultra-low Stray light Fiber optic Spectrometer, 75 mm AvaBench, 2048 large 500  $\mu$ m pixel back-thinned CCD detector), equipped with an AvaLight-DH-S light source (Deuterium-Halogen light source, 190-2500 nm, incl. TTL shutter). In-line absorbance measurements were carried out with an Avantes CUV-ALL/UV/VIS cuvette sample holder (10x10 mm), equipped with a flow-through cell (3 in 1, Hellma 176-760-15-40). Offline analyses were performed in PMMA cells with the same spectrometer. The source, the holder, and the analyzer were connected using Avantes FCB-UVIR400 fiber optic cables (bifurcated cable 2x400  $\mu$ m, 2 or 1 m length, SMA terminations).

Photoluminescence experiments were recorded offline with a Shimadzu RF-6000 Spectrofluorimeter in Fluorescence quartz-made macro cells (Hellma 101-10-40).

The XPS experiments were conducted with a SSX 100/206 spectrometer from Surface Science Instruments (USA) using a monochromatized and micro focused Al-K $\alpha$  X-ray beam operated at 10 kV, a parking chamber, and an automatic sample analysis.

**Caution:** This work involves the use of heavy metals (cadmium) and chalcogens (sulfur, selenium, tellurium). These compounds should be handled under a fume hood and with appropriate personal protective equipment (PPE). All the effluents generated must be disposed in appropriate containers with special labels following the instruction of EH&S authorities. All glassware must be cleaned with commercial bleach (aqueous sodium hypochlorite for chalcogen decontamination).

## 2. Reagents and Solvents

The reagents and solvents were purchased from commercial sources. These compounds are used without purification (Table S1).

Table S1: Solvents, chemicals and suppliers

Solvents	Purity (%)	CAS number	Supplier
Deuterium Oxide	99.90 %	7789-20-0	Eurisotop

Ethanol (absolute)	>99%	64-17-5	VWR
Water HiPerSolv CHROMANORM®	/	7732-18-5	VWR
Chemicals	Purity (%)	CAS number	Supplier
3-Mercaptopropionic acid	99%	107-96-0	Alfa Aesar
Cadmium acetate dihydrate	98%	5743-04-4	Sigma Aldrich
Fluoresceine sodium salt	NA	518-47-8	Sigma Aldrich
Oxalic acid anhydrous	≥97%	144-62-7	Fluka Analytical
Rhodamine 6G	99%	989-38-8	Sigma Aldrich
Rhodamine 101	99%	116450-56-7	Sigma Aldrich
Selenium powder 200 mesh	99.999%	7782-49-2	Alfa Aesar
Sodium borohydride	≥98%	16940-66-2	TCI
Sodium hydroxide	≥97%	1310-73-2	VWR
Sulfur	99.98%	7704-34-9	Aldrich
Tellurium 200 mesh	99.8%	13494-80-9	Aldrich Chemistry
Tellurium -18+60 mesh	99.999%	13494-90-9	Alfa Aesar
Thiourea	98%	62-56-6	UCB
Tris-(carboxyethyl)phosphine hydrochloride	99.5%	51805-45-9	Chem-Impex
Zinc chloride	N.A.	7646-85-7	Federa

Cadmium acetate and sodium borohydride must be stored under anhydrous conditions and tris-(carboxyethyl)phosphine (TCEP) hydrochloride must be stored at 4 °C.

### 3. Continuous flow setups

#### 3.1. Microfluidic setups and parts

All microfluidic setups were assembled with commercially available parts.

##### 3.1.1. Pumps

Knauer AZURA P 4.1S HPLC pumps were used to handle all the liquid streams for microfluidic experiments.

##### 3.1.2. PFA tubing

PFA coil reactors and collection lines were constructed from PFA tubing (high purity PFA; 1.58 mm outer diameter, 500 µm internal diameter).

##### 3.1.3. SS tubing

The stainless tubing reactors were built with 316 stainless steel tubing (1.58 mm outer diameter, 500 or 750 µm internal diameter).

### 3.1.4. Connectors, ferrules and mixers

Sections of the reactor that were not subjected to high temperatures and pressures were equipped with coned PEEK fittings and micromixers. Sections of the reactor that were subjected to high temperatures and pressures were equipped with Valco SS fittings, ferrules and unions. Connectors, ferrules and unions were purchased from IDEX/Upchurch or from VICI (details in Table S2).

### 3.1.5. Check valves

Check valves were inserted before the cross junction to prevent cross-contamination of the chalcogen columns and were purchased from IDEX/Upchurch Scientific.

### 3.1.6. Back pressure regulators

To control the pressure inside the reactor, back pressure regulators of 100, 250 and 500 psi were used (IDEX/Upchurch Scientific).

### 3.1.7. Thermoregulatory devices

Thermoregulation of PFA coil reactors was performed with a Heidolph™ MR Hei-Tec® equipped with a Pt-1000 temperature sensor. The stainless steel coil reactors were embedded in a GC oven (Thermo Finnigan Interscience GC trace).

### 3.1.8. Setup flow parts and vendors

Continuous flow parts and vendors are gathered in Table S2.

Table S2: Connectors, ferrules and unions

Part	Details	Vendor	Reference
Connectors	One-Piece Fingertight, PEEK, 10-32 Coned, for 1/16" OD	IDEX/Upchurch Scientific	F-120X
	Super Flangeless Nuts, natural PEEK 1/4-28 thread for 1/16" OD tubing	IDEX/Upchurch Scientific	P-255X
	Super Flangeless Ferrule Tefzel (ETFE) and SS ring 1/4-28 thread for 1/16" OD tubing	IDEX/Upchurch Scientific	P-259X
	303SS 10-32 NUTS for 1/16" o.d.	VICI (Valco Ins. Co. Inc.	Zn1-10
	303SS union for 1/16" o.d. tubing with 0.5 mm BORE	VICI (Valco Ins. Co. Inc.	ZU1M
	316 SS column end fitting 1/4" 1/16" 4 mm 4.6 mm cone, removable 2 µm frit	VICI (Valco Ins. Co. Inc.	CEF 414.6F
Mixers	T-mixer, natural PEEK 1/4-28 thread for 1/16" o.d. tubing, 0.02" through hole	IDEX/Upchurch Scientific	P-712
	Cross assembly, natural PEEK 1/4-28 thread for 1/16" o.d. tubing, 0.02" through hole	IDEX/Upchurch Scientific	P-722

Tubing	High-purity PFA tubing, 1.58 mm outer diameter, 500 $\mu$ m internal diameter	VICI (Valco Ins. Co. Inc.)	JR-T-4002-M25
	316 Stainless steel tubing, 1/16" o.d. tubing, 0.03" through hole	VICI (Valco Ins. Co. Inc.)	TSS-130
	High-purity 1/8" and 1/4" PFA tubing, including appropriate PFA connections	Swagelok	PFA-T2-030-100 PFA-T4-047-100
	316/316L Stainless Steel Seamless Tubing, 1/4 in. od x 0.035 in. Wall	Swagelok	SS-T4-S-035
Check-valve	Check-valve inline 3 psi	IDEX/Upchurch Scientific	CV-3315
Back pressure regulators	BPR Assembly 100, 250, 500 psi	IDEX/Upchurch Scientific	P-787, P-788, P-789, U- 610

### 3.2. Mesofluidic setup and parts

Each mesofluidic setup was assembled with commercially available parts.

#### 3.2.1. Pumps

During the scalability trials at the pilot scale, a Knauer AZURA P 4.1S HPLC pump, an Isco Teledyne 5000D dual syringe pump and a Knauer BlueShadow 80P (with 100 mL pump head), equipped with a Bronkhorst flow meter were used to handle liquids.

#### 3.2.2. PFA tubing

PFA coil reactors and collection lines were constructed from PFA tubing (high purity PFA 1/8"; 3.175 mm outer diameter, 1.65 mm internal diameter or high purity PFA 1/4"; 6.35 mm outer diameter, 3.2 mm internal diameter), and purchased from Swagelok.

#### 3.2.3. SS tubing

The stainless tubing reactors were built with 316 Stainless Steel tubing (3.175 mm outer diameter, 1.14 mm internal diameter), and purchased from Swagelok.

#### 3.2.4. Connectors, ferrules and mixers

Sections of the reactor that were not subjected to high temperatures were equipped with PFA Swagelok connectors. Sections of the reactor that were subjected to high temperatures were equipped with Swagelok SS fittings, ferrules and unions. Connectors, ferrules and unions were purchased from IDEX/Upchurch and from Swagelok PFA fittings (details in Table S3).

#### 3.2.5. Back pressure regulator

The pressure was regulated by an Equilibar BPR (H3P) that was inserted downstream of the pilot scale mesofluidic setup. The cracking pressure setpoints were regulated by a Bronkhorst EL-PRESS (M23211621B) connected to a compressed nitrogen gas cylinder (AirLiquide).

#### 3.2.6. Thermoregulatory devices

The Corning® AFR™ G1 SiC reactor was thermostated by a Lauda XT 280 thermostat (containing HL60) and the heat exchanger was cooled down by a Lauda PRO thermostat (containing water).



Table S3 : Connectors, ferules and unions

Part	Details	Vendor	Reference
Connectors	One-Piece Fingertight, PEEK, 10-32 Coned, for 1/16" OD	IDEX/Upchurch Scientific	F-120X
	Super Flangeless Nuts, natural PEEK 1/4-28 thread for 1/16" OD tubing	IDEX/Upchurch Scientific	P-255X
	316 Stainless Steel Nut for 1/8 in. Tube Fitting	Swagelok	SS-202-1
	316 Stainless Steel Nut for 1/4 in. Tube Fitting	Swagelok	SS-402-1
	316 Stainless Steel Nut for 1/2 in. Swagelok Tube Fitting	Swagelok	SS-812-1
	Tube Fitting, Bulkhead Union, 1/8 in. x 1/4 in. Tube OD	Swagelok	SS-200-61-4
	Stainless Steel Tube Fitting, Reducing Union, 1/2 in. x 1/4 in. Tube OD	Swagelok	SS-810-6-4
	PFA Tube Fitting, 1/4 in. Nut	Swagelok	PFA-422-1
T-junction	Stainless Steel Tube Fitting, Union Tee, 1/8 in. Tube OD	Swagelok	SS-200-3
	Stainless Steel Swagelok Tube Fitting, Reducing Union Tee, 1/2 in. x 1/4 in. x 1/2 in. Tube OD	Swagelok	SS-810-3-4-8
Tubing	High-purity PFA tubing, 1.58 mm outer diameter, 500 µm internal diameter	Swagelok	JR-T-4002-M25
	High-purity 1/8" and 1/4" PFA tubing, including appropriate PFA connections	Swagelok	PFA-T2-030-100 PFA-T4-062-100
	316 Stainless Steel Tubing, 1/8 in. od x 0.040 in. Wall	VICI (Valco Ins. Co. Inc.)	TSS240
	316 Stainless Steel Tubing, ¼ in OD 0.049 in. Wall	Swagelok	SS-T4-S-049-6ME
	316 Stainless Steel Tubing, ½ in OD 0.065 in. Wall	Swagelok	SS-T8-S-065-6ME
Check-valve	Stainless Steel Poppet Check Valve, Fixed Pressure, 1/8 in. Swagelok Tube Fitting, 1 psig (0.07 bar)	Swagelok	SS-2C-1
BPR	High-pressure BPR	Equilibrar	H3P1SNN8

## 4. Setups and protocols

### 4.1. Batch optimization of TCEP=S

An aqueous solution 0.2 M of **TCEP** was prepared by dissolving **TCEP·HCl** (0.573 g, 2 mmol, 1 equiv.) with milliQ water. The pH was adjusted to the desired value (5, 8, 11) with 2 M aqueous NaOH, then the solution was filled up to 10 mL with milliQ water in a volumetric flask. The solution was then quickly transferred into a 25 mL round-bottom flask and degassed with a

flow of Argon for 15 min. The needed amount of chalcogen (S: 0.096 g, 3 mmol, 1.5 equiv.; 0.144 g, 4.5 mmol, 2.25 equiv.; 0.192 g, 6 mmol, 3 equiv.) was added under an inert atmosphere and the solution was stirred (750, 825 and 900 rpm) at room temperature. The reaction was carried out until reaching the desired reaction time (20 min, 40 min, 60 min). Next, 300  $\mu$ L of the mixture was pipetted out and transferred in a NMR tube (syringe equipped with a polysulfone filter 0.5  $\mu$ m to remove the chalcogen particles) and 300  $\mu$ L of degassed D<sub>2</sub>O was added. During the operation, the tube was kept under an argon atmosphere to prevent **TCEP=X** oxidation (to **TCEP=O**). An insert containing H<sub>3</sub>PO<sub>4</sub> as the internal standard was added to the NMR tubes which were analyzed by high field <sup>31</sup>P NMR (162 MHz).

#### 4.2. Batch optimization of TCEP=Se

An aqueous solution 0.2 M of **TCEP** was prepared by dissolving **TCEP·HCl** (0.573 g, 2 mmol, 1 equiv.) with milliQ water. The pH was adjusted to the desired value (7, 8.75, 10.5) with 2 M aqueous NaOH, then the solution was filled up to 10 mL with milliQ water in a volumetric flask. The solution was then quickly transferred into a 25 mL round-bottom flask and degassed with a flow of Argon for 15 min. The needed amount of chalcogen (0.160 g, 2 mmol, 1 equiv.; 0.240 g, 3 mmol, 1.5 equiv.; 0.320 g, 4 mmol, 2 equiv.) was added under an inert atmosphere and the solution was stirred at 750 rpm at room temperature. The reaction was carried out until reaching the desired reaction time (10 min, 15 min, 20 min). Next, 300  $\mu$ L of the mixture was pipetted out and transferred in a NMR tube (syringe equipped with a polysulfone filter 0.5  $\mu$ m to remove the chalcogen particles) and 300  $\mu$ L of degassed D<sub>2</sub>O was added. During the operation, the tube is kept under an argon atmosphere to prevent **TCEP=X** oxidation (to **TCEP=O**). An insert containing H<sub>3</sub>PO<sub>4</sub> as the internal standard was added to the NMR tubes which were analyzed by high field <sup>31</sup>P NMR (162 MHz).

#### 4.3. Batch optimization of TCEP=Te

An aqueous solution 0.2 M of **TCEP** was prepared by dissolving **TCEP·HCl** (1.433 g, 5 mmol, 1 equiv) with milliQ water. The pH was adjusted to 10.7 with 2 M aqueous NaOH, then the solution was filled up to 25 mL with milliQ water in a volumetric flask. The solution was then transferred into a modified three-necked round-bottom flask, see Figure S4, and degassed with a flow of Argon for 15 min. The needed amount of tellurium of various granulometries (18-60 mesh or 200 mesh: 0.9570 g, 7.5 mmol, 1.5 equiv.; 1.4355 g, 11.25 mmol, 2.25 equiv.; 1.9140 g, 15. mmol, 3 equiv.) was added under an inert atmosphere and the solution was stirred (500 or 750 rpm) at room temperature. The Raman probe was inserted into the solution and the mixing started. The reaction was monitored after the addition of tellurium (corresponding to the initial time,  $t_0$ ). Spectra were recorded every 30 s ranging from 326  $\text{cm}^{-1}$  to 1805  $\text{cm}^{-1}$ . The signal of interest is the vibration P-Te at 370  $\text{cm}^{-1}$ . For experimental details, see section S4.5.2.

#### 4.4. Stability study for TCEP=X (X = Se, Te)

##### 4.4.1. Stability of TCEP=Se vs NaHSe in water (open flask)

The stability of **TCEP=Se** was assessed by comparing it to NaHSe. While NaHSe quickly turns red due to oxidation (Figure S1), **TCEP=Se** remains transparent, indicating its higher resilience to oxidation. Deselenization of **TCEP=Se** allows the oxidation of selenide (-II) into selenium (0), forming **TCEP** (P = +III) in solution. **TCEP** is then further oxidized into **TCEP=O** (+V) by the

oxygen in the air. After 16 hours, less than 1% of **TCEP=O** was observed in a 0.02 M solution. In a 0.5 M solution at room temperature, after 4 weeks, 98% of **TCEP=Se** and 2% of **TCEP=O** were detected (by  $^{31}\text{P}$  NMR), demonstrating the much higher stability of **TCEP=Se** compared to NaHSe. This stability is advantageous for the subsequent formation of quantum dots.

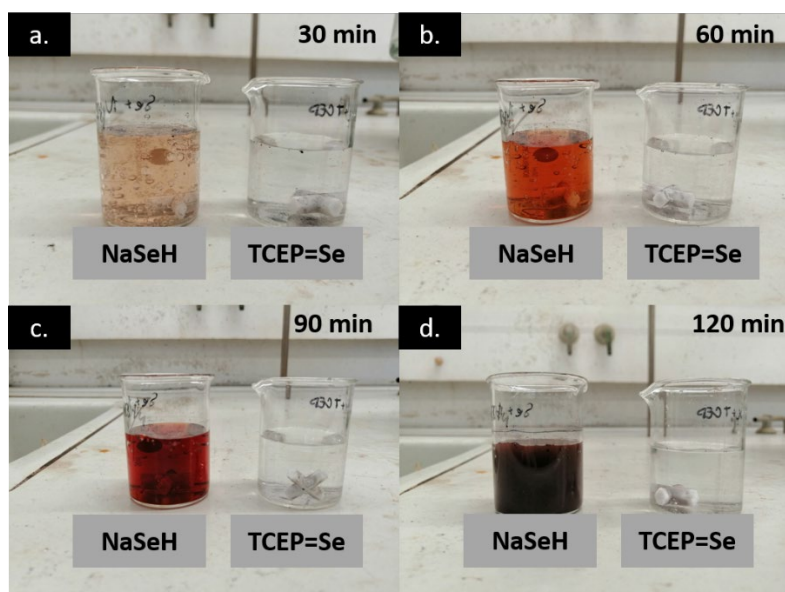


Figure S1. Stability of **TCEP=Se** (right) vs **NaHSe** (left) in aqueous solutions left open to air after a) 30 min, b) 60 min, c) 90 min, d) 120 min

#### 4.4.2. Stability study for **TCEP=Te**

An aqueous solution 0.08 M of **TCEP** was prepared by dissolving **TCEP·HCl** (1.1464 g, 4 mmol, 1 equiv.) with milliQ water. The pH was adjusted to 10 with 1 M aqueous NaOH, then the solution was filled up to 50 mL with milliQ water in a volumetric flask. The solution was then quickly transferred into a 100 mL round-bottom flask and degassed with a flow of Argon for 15 min. The needed amount of tellurium (1.5312 g, 12 mmol, 3 equiv.) was added under an inert atmosphere and the solution was stirred at 50 °C under 800 rpm mixing. After 10 min of reaction, the conversion of **TCEP** into **TCEP=Te** was confirmed by  $^{31}\text{P}$ -NMR (162 MHz). Finally, the stopper was removed and a sample was collected every 10 min for 110 min. 300  $\mu\text{L}$  of the mixture was pipetted out and transferred in a NMR tube (syringe equipped with a polysulfone filter 0.5  $\mu\text{m}$  to remove the chalcogen particles) and 300  $\mu\text{L}$  of degassed  $\text{D}_2\text{O}$  was added.

### 4.5. Raman monitoring of **TCEP=X** formation

#### 4.5.1. Preliminary pH optimization

Preliminary tests have shown that the pH had a major influence on the conversion rate towards **TCEP=X** species. The optima found with the model generated with the DoE were for sulfur 7.5-9 and for selenium 8-9.5. However, the use of these ranges led to a lower conversion rate than predicted. Prior to the kinetic experiments, pH was optimized to set optimal values for the 3 precursors (**TCEP=S**, **TCEP=Se**, **TCEP=Te**).

##### 4.5.1.1. Sulfur

To determine the optimum pH, experiments were conducted by varying the pH while keeping the other parameters constant (rt = 15 min, 0.2 M of **TCEP** [prepared by dissolving **TCEP·HCl** (0.5732 g, 2 mmol, 1 equiv.) with milliQ water], chalcogen excess = 1.5 equiv. [0.0962 g, 3

mmol], mixing = 850 rpm). The pH of the **TCEP** solution was adjusted by adding 2 M NaOH to reach pH values of 9.84, 10.34, 10.72, 10.88, and 11.35. The corresponding solutions were degassed for 15 min with argon, prior to the addition of sulfur. After 15 min of reaction, the mixing was stopped and then, 300  $\mu\text{L}$  of the mixture was pipetted out and transferred into a NMR tube (syringe equipped with a polysulfone filter 0.5  $\mu\text{m}$  to remove the chalcogen particles), and 300  $\mu\text{L}$  of degassed  $\text{D}_2\text{O}$  was added. During the operation, the NMR tube was kept under an argon atmosphere to prevent oxidation. An  $\text{H}_3\text{PO}_4$  insert was added as the internal standard, and the sample was analyzed by high field  $^{31}\text{P}$  NMR (162 MHz). The results are provided in Figure S2.

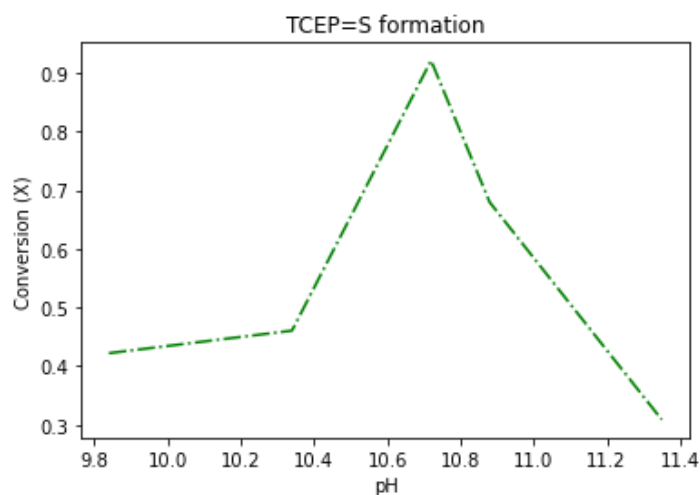


Figure S2. pH optimization for **TCEP=S** formation

#### 4.5.1.2. Selenium

To determine the optimum pH, experiments were conducted by varying the pH while keeping the other parameters constant (rt = 15 min, 0.2 M of **TCEP** [prepared by dissolving **TCEP·HCl** (0.5732 g, 2 mmol, 1 equiv.) with milliQ], chalcogen excess = 1.5 equiv. [0.2369 g, 3 mmol], mixing = 850 rpm). The pH of the **TCEP** solution was adjusted by adding 2 M NaOH to reach pH values of 10.11, 10.46, 11.07, or 11.53. Each solution was degassed for 15 min with argon, prior to the addition of selenium. After 15 min of reaction, 300  $\mu\text{L}$  of the mixture was pipetted out and transferred in a NMR tube (syringe equipped with a polysulfone filter 0.5  $\mu\text{m}$  to remove the chalcogen particles). 300  $\mu\text{L}$  of degassed  $\text{D}_2\text{O}$  was added under an argon atmosphere to prevent oxidation. An  $\text{H}_3\text{PO}_4$  insert was added as the internal standard, and the sample was analyzed by high field  $^{31}\text{P}$  NMR (162 MHz). The results are provided in Figure S3.

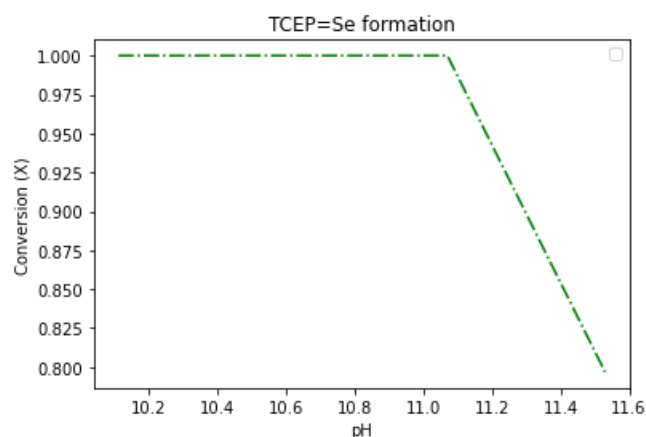


Figure S3. pH optimization for TCEP=Se formation

#### 4.5.2. Experimental setup for *in-situ* Raman monitoring

*In situ* reaction and kinetic monitoring for the formation of TCEP=X (X = S, Se, Te) were carried out in a modified 3-neck round bottom flask for the hosting of a 5/8" Raman probe (Avaraman-PRB-FIP-532 from Avantes, Figure S4). The spectra were recorded with a Raman spectrometer (Horiba Labram-300) excited with a DPSS laser emitting at 532 nm (CNI optoelectronics MLL-U-532, 300 mW).

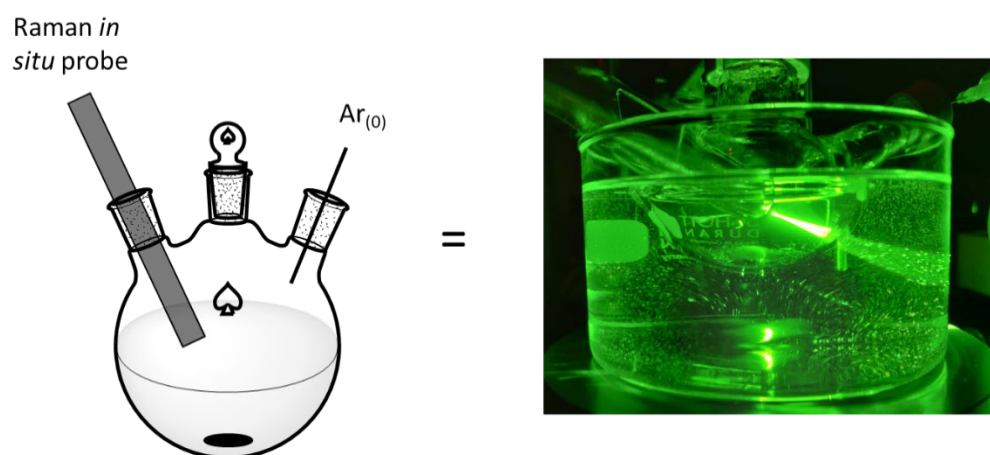


Figure S4. Scheme and picture of the modified round-bottom flask for the Raman monitoring

#### 4.5.3. Monitoring of TCEP=S formation

A 0.2 M aqueous solution of TCEP was prepared by dissolving TCEP·HCl (1.433 g, 5 mmol, 1 equiv.) with milliQ water. The pH was adjusted to 10.7 with 2 M aqueous NaOH, then the solution was filled up to 25 mL with milliQ water in a volumetric flask. The solution was then transferred into a modified 3-neck round-bottom flask (Figure S4), degassed with a flow of argon for 15 min and immersed into a thermostated water bath (at 30 °C, 40 °C, or 50 °C) for 10 min. Next, sulfur (0.4812 g, 15 mmol, 3 equiv.) was added in one portion. The Raman probe was then inserted into the solution and the mixing restarted. The reaction was monitored after the addition of sulfur (corresponding to the initial time,  $t_0$ ). Spectra were recorded every 30 s for 2 h, in the wavenumber range from 513  $\text{cm}^{-1}$  to 1961  $\text{cm}^{-1}$ . The signal of interest is the vibration P-S at 570  $\text{cm}^{-1}$ .

#### 4.5.4. Monitoring of TCEP=Se formation

An aqueous solution 0.2 M of **TCEP** was prepared by dissolving **TCEP·HCl** (1.433 g, 5 mmol, 1 equiv.) with milliQ water. The pH was adjusted to 10.7 with 2 M aqueous NaOH, then the solution was filled up to 25 mL with milliQ water in a volumetric flask. The solution was then transferred into a modified 3-neck round-bottom flask (Figure S4), and degassed with a flow of argon for 15 min. The reactor was thermostated at various temperatures (at 30 °C, 40 °C, 50 °C, and 60 °C) for 10 min. Next, selenium (0.5922 g, 7.5 mmol, 1.5 equiv.) was added. The reaction was monitored after the addition of selenium (corresponding to the initial time,  $t_0$ ). Spectra were recorded every 15 s for 2 h, in the wavenumber range from 316  $\text{cm}^{-1}$  to 1805  $\text{cm}^{-1}$ . The signal of interest is the vibration P-Se at 428  $\text{cm}^{-1}$ .

#### 4.5.5. Monitoring of TCEP=Te formation

An aqueous solution 0.2 M of **TCEP** was prepared by dissolving **TCEP·HCl** (1.433 g, 5 mmol, 1 equiv.) with milliQ water. The pH was adjusted to 10.7 with 2 M aqueous NaOH then the solution was filled up to 25 mL with milliQ water in a volumetric flask. The solution was then transferred into a modified 3-neck round-bottom flask (Figure S4), degassed with a flow of argon for 15 min, and thermostated at various temperatures (at 30 °C, 40 °C, 50 °C, and 60 °C) for 10 min. Next, tellurium (0.9570 g, 7.5 mmol, 1.5 equiv.) was added. The reaction was monitored after the addition of tellurium (corresponding to the initial time,  $t_0$ ). Spectra were recorded every 15 s for 2 h, in the wavenumber range from 326  $\text{cm}^{-1}$  to 1805  $\text{cm}^{-1}$ . The signal of interest is the vibration P-Te at 376  $\text{cm}^{-1}$ .

### 4.6. Transposition in flow of TCEP=X synthesis (lab scale)

#### 4.6.1. Design of the chalcogenide packed-bed column

The reactors used for the flow synthesis of **TCEP=X** species were constructed from SS tubing (15 cm length, SS-T4-S-065 from Swagelok) with a 2.46 mL internal volume. Both ends of the packed-bed columns were equipped with a column end fitting encompassing a 2  $\mu\text{m}$  frit at the outlet (CEF 414.6F) for preventing chalcogenide leaching. The 3 columns were filled with sulfur (1.91 g), selenium (3.74 g) and tellurium (7.29 g), respectively. For each column, the dead volume was measured, and based on that, the porosity ( $\epsilon$ ) of each column was estimated to  $\epsilon = 0.287, 0.098, 0.434$ , respectively. The reduction of elemental chalcogen (S, Se, Te) was carried out by infusing a **TCEP** aqueous solution (pH = 10.7) with a Knauer Azura P4.1S HPLC pump (10 mL stainless steel head). The **TCEP** feed solution was redirected through a selector valve (Vici C25-3186), enabling the switch between the 3 packed-bed columns filled with sulfur, selenium or tellurium, respectively. The outlet of each column was also equipped with a check valve (IDEX/Upchurch Scientific CV-3315) to prevent backflow and cross-contamination. The reaction effluents converged to a cross-junction mixer and were monitored by in-line  $^{31}\text{P}$  NMR (Benchtop 43 MHz Spinsolve™ spectrometer from Magritek® equipped with a flow-through cell). The system is illustrated in Figure S5. A detailed experimental setup is provided in Figure S6.

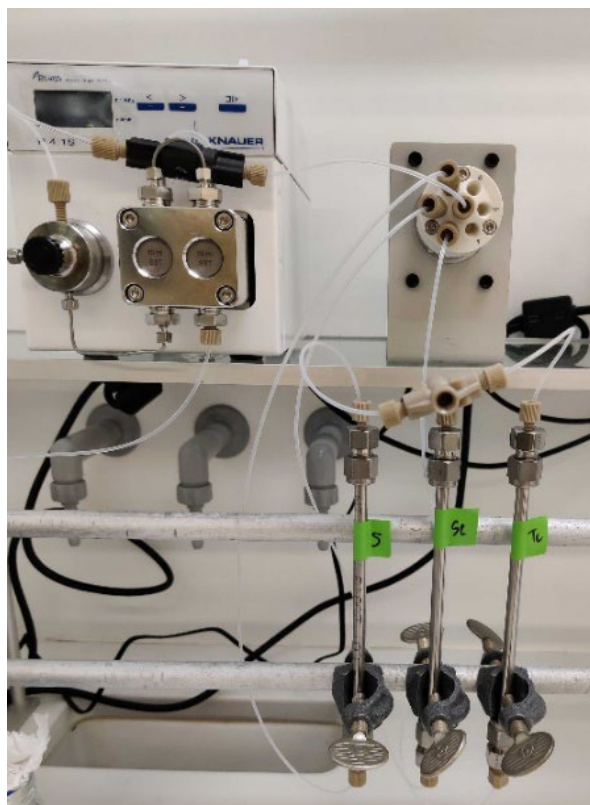


*Figure S5. Column design in the flow setup*

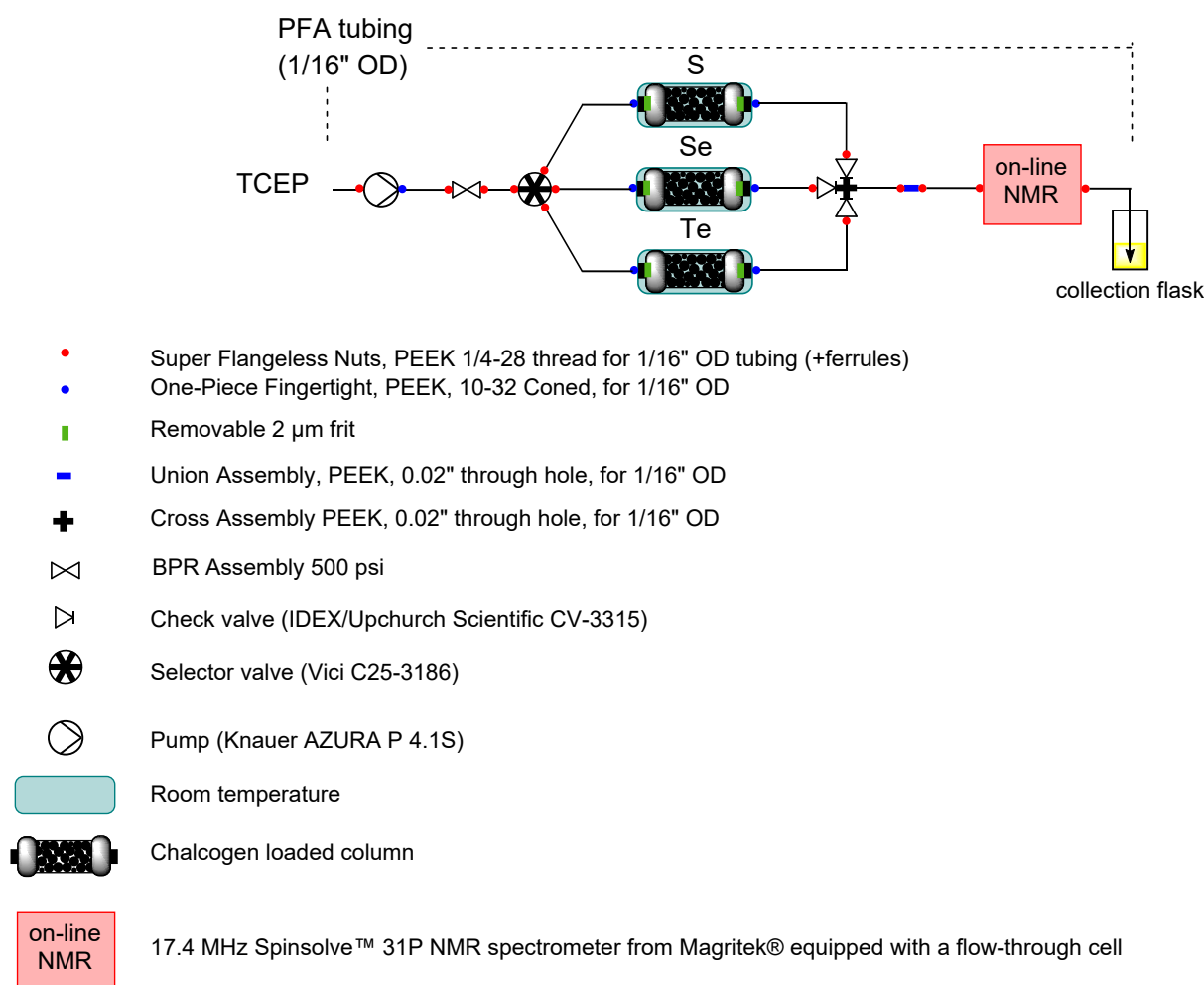


Figure S6. Scheme of the overall setup for the transposition in flow of the TCEP=X (X = S, Se, Te) synthesis

#### 4.6.2 TCEP feed preparation

An aqueous solution 0.2 M of TCEP was prepared by dissolving TCEP·HCl (14.33 g, 50 mmol, 1 equiv.) with milliQ water. The pH was adjusted to 10.7 with 2 M aqueous NaOH, then the solution was filled up to 250 mL with milliQ water in a volumetric flask. The solution was then transferred into a 250 mL round-bottom flask and degassed with argon for 20 min.

#### 4.7. Concatenated microfluidic preparation of QDs synthesis

The setup for the concatenated synthesis of the CdX QDs (X=S, Se, Te) consisted in two main modules: (a) the first module relied mostly on the packed-bed system illustrated in Figure S5 and Figure S6 for the reduction of chalcogens; (b) the second module concerned the transfer of chalcogens to a cadmium source for the synthesis of the QDs. A cooling loop was inserted downstream of the second module for thermal quenching prior to in-line analysis by UV/Vis spectroscopy (Figure S7).

##### 4.7.1. Setup

The elemental chalcogen reduction was carried out by infusing a TCEP aqueous solution (pH = 10.7) with a Knauer Azura P4.1S pump (10 mL stainless steel head). The TCEP feed solution was redirected through a selector valve (Vici C25-3186) allowing to switch among 3 packed-



bed columns filled with sulfur, selenium or tellurium, respectively. To prevent the leaching of the elemental chalcogen, a 2  $\mu\text{m}$  frit was added at the outlet of the columns. The outlet of each column was also equipped with a check valve (IDEX/Upchurch Scientific CV-3315) to prevent backflow and cross-contamination. The freshly prepared solution of **TCEP=X** is mixed in a T mixer with the aqueous feed of **Cd(3-MPA)<sub>2</sub>** (handled through a Knauer Azura P4.1S pump, 10 mL stainless steel head). Note that to ensure a stable flow rate, both the Knauer pumps were equipped with a 250 psi BPR. The microfluidic SS coil reactor was thermoregulated with a Thermo Finnigan Interscience GC oven, which allowed to reach the desired temperatures under a back pressure of 500 psi (IDEX/Upchurch Scientific P-788). The reactor effluent was thermally quenched and analyzed by in-line UV/Vis spectroscopy (AvaSpec-ULS2048XL EV spectrometer equipped with a Charge-Coupled Device detector and a deuterium-halogen light source), as depicted in Figure S7.

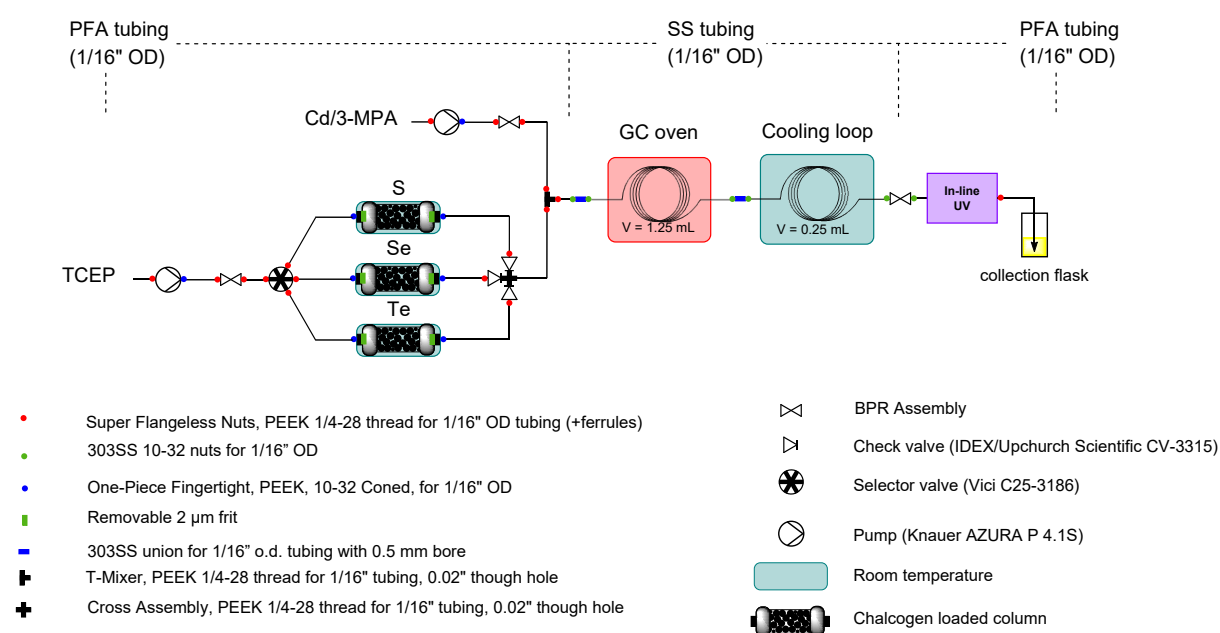


Figure S7. Scheme of the setup for the concatenated synthesis of **CdX** QDs ( $X=S, Se, Te$ )

#### 4.7.2. In-line monitoring

The in-line monitoring was performed inside a flow-through cell (3 in 1) from Hellma Analytics (176-760-15-40) allowing to perform UV/Vis and/or photoluminescence (5 and 10 mm pathlength) measurements independently or at once. This flow cell was placed inside a cuvette holder (Avantes CUV-ALL-UV/VIS) connected to both sources (UV/Vis: Avalight DH-S-BAL and PL: Avalight HPLED-385) with a 600  $\mu\text{m}$  core optical fibers (FC-UVIR600-1). A second type of in-line measurement was performed by measuring directly through a PFA tubing (500  $\mu\text{m}$  ID), sandwiched by 2 3D-printed blocs of PLA including two SMA screws to fit the optical fibers. The signal was monitored by a spectrophotometer (Avaspec-ULS2048XL-EVO-RS-UA) and treated with Avasoft software. Illustrations of the various configurations are provided in Figure S8.

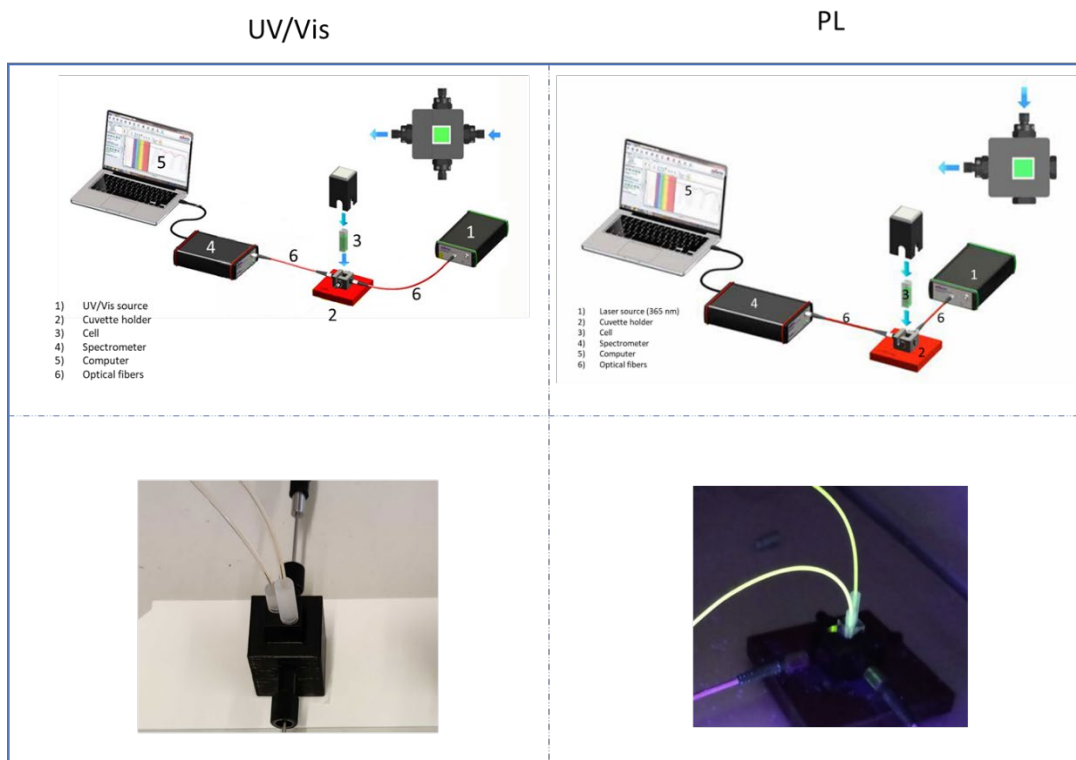


Figure S8. Schemes and pictures of experimental configuration for UV/Vis and PL measurements (scheme adapted from <https://pro-lite.co.uk/products-services-index/spectroscopy/spectrometers/fibre-optic-spectroscopy/avantes-bundles/>)

### 4.7.3. Concatenated preparation of CdS

#### 4.7.3.1. Preparation of the feed solutions

A 0.02 M aqueous solution of **TCEP** was prepared by dissolving **TCEP·HCl** (0.5732 g, 2 mmol, 1 equiv.) with milliQ water. The pH was adjusted to 10.7 with 2 M aqueous NaOH, then the solution was filled up to 100 mL with milliQ water in a volumetric flask. The solution was transferred into a round-bottom flask and degassed with a flow of argon for 15 min.

The cadmium precursor feed solution was prepared by dissolving **Cd(Ac)<sub>2</sub>** (0.3332 g, 1.25 mmol, 1 equiv.) and **3-MPA** (0.3317 g, 3.125 mmol, 2.5 equiv.) in milliQ water. The pH of the solution was adjusted to 11 by the addition of 1 M aqueous NaOH. The solution was next filled up to 250 mL with milliQ water in a volumetric flask.

#### 4.7.3.2. Modus operandi

The **TCEP** feed solution was infused (flow rates of 0.25 mL min<sup>-1</sup> and 0.33 mL min<sup>-1</sup>) through a column filled with elemental sulfur (1.991 g, 62.2 mmol). The resulting stream of **TCEP=S** was mixed through a T-mixer with the cadmium precursor feed solution that was infused at a flow rate of 1 mL min<sup>-1</sup> or 1.33 mL min<sup>-1</sup>. The SS reactor coil (1.25 mL, 1/16" SS tubing) was heated up to 170 °C, 180 °C, 190 °C and 200 °C under a downstream pressure of 500 psi. Residence times were fixed at 45 s and 60 s, respectively. The reactor effluent was thermally quenched and analyzed by in-line UV/Vis spectroscopy (0.5 mm light path).

#### 4.7.4. Concatenated preparation of CdSe

##### 4.7.4.1. Preparation of the feed solutions

A 0.02 M aqueous solution of **TCEP** was prepared by dissolving **TCEP·HCl** (0.5732 g, 2 mmol, 1 equiv.) with milliQ water. The pH was adjusted to 10.7 with 2 M aqueous NaOH, then the solution was filled up to 100 mL with milliQ water in a volumetric flask. The solution was then transferred into a round-bottom flask and degassed with a flow of argon for 15 min.

The cadmium precursor feed solution was prepared by dissolving **Cd(Ac)<sub>2</sub>** (0.6663 g, 2.5 mmol, 1 equiv.) and **3-MPA** (0.6634 g, 6.25 mmol, 2.5 equiv) with milliQ water. The pH was adjusted to 11 by the addition of 1 M aqueous NaOH, then the solution was filled up to 500 mL with milliQ water in a volumetric flask.

##### 4.7.4.2. Modus operandi

The **TCEP** feed solution was infused (flow rates of 0.25 mL min<sup>-1</sup> and 0.33 mL min<sup>-1</sup>) through a column filled with elemental selenium (3.743 g, 47.4 mmol). The resulting stream of **TCEP=Se** was mixed through a T-mixer with the cadmium precursor feed solution that was infused at a flow rate of 1 mL min<sup>-1</sup> or 1.33 mL min<sup>-1</sup>. The SS reactor coil (1.25 mL, 1/16" SS tubing) was heated up to 160 °C, 170 °C and 180 °C under a downstream pressure of 500 psi. Residence times were fixed at 45 s and 60 s, respectively. The reactor effluent was thermally quenched and analyzed by in-line UV/Vis spectroscopy (0.5 mm light path).

#### 4.7.5. Concatenated preparation of CdTe

##### 4.7.5.1. Preparation of the feed solutions

A 0.003 M aqueous solution of **TCEP** was prepared by dissolving **TCEP·HCl** (0.2150 g, 0.75 mmol, 1 equiv.) with milliQ water. The pH was adjusted to 10.7 with 2 M aqueous NaOH then the solution was filled up to 250 mL with milliQ water in a volumetric flask. The solution was then transferred into a round-bottom flask and degassed with a flow of argon for 15 min.

The cadmium precursor feed solution was prepared by dissolving **Cd(Ac)<sub>2</sub>** (0.9995 g, 3.75 mmol, 5 equiv.) and **3-MPA** (0.9951 g, 9.375 mmol, 12.5 equiv.) with milliQ water. The pH was adjusted to 10.7 by the addition of 1 M aqueous NaOH, then the solution was filled up to 250 mL with milliQ water in a volumetric flask.

##### 4.7.5.2. Modus operandi

The **TCEP** feed solution was infused (flow rates of 0.625 mL min<sup>-1</sup> and 0.833 mL min<sup>-1</sup>) through a column filled with elemental tellurium (7.290 g, 57.4 mmol). The resulting stream of **TCEP=Te** was mixed through a T-mixer with the cadmium precursor that which was infused at a flow rate of 0.625 mL min<sup>-1</sup> or 0.833 mL min<sup>-1</sup>, respectively. The SS reactor coil (1.25 mL, 1/16" SS tubing) was heated up to 140 °C, 145 °C and 150 °C under a downstream pressure of 500 psi. Residence times were fixed at 45 s and 60 s, respectively. The reactor effluent was thermally quenched and analyzed by in-line UV/Vis spectroscopy (0.5 mm light path).

#### 4.8. Preparation of type I CdSe@ZnS core-shell QDs

A solution was sought to improve the emissivity properties of **CdSe** QDs obtained through our **TCEP**-based concatenated protocol (see Figure S56). A common way reported in the literature to improve QD emission consists of surface passivation. One of the most efficient methods for

surface passivation relies on the addition of a **ZnS** shell.<sup>S1</sup> It was therefore envisioned to concatenate **CdSe** core synthesis with **ZnS** shell enclosure. To achieve this goal, careful selection of the sulfur source was paramount. Indeed, to avoid competition with potential leftovers of **TCEP=Se** from the upstream **CdSe** synthesis, a sulfur source reacting at a lower temperature than **TCEP=Se** must be selected. **Thiourea**<sup>S2</sup> emerged as a convenient and widely available sulfur source. A concatenated setup was built accordingly (Figure S9).

#### 4.8.1. Setup

A freshly prepared solution of **TCEP=Se** (see section S4.6) was infused with a Knauer Azura P4.1S pump (10 mL stainless steel head) and mixed through a T-mixer with the feed aqueous solution of **Cd(3-MPA)<sub>2</sub>** (handled through a Knauer Azura P4.1S pump, 10 mL stainless steel head). Note that to ensure a stable flow rate, both the Knauer pumps were equipped with a 250 psi BPR. Both feeds reacted in a microfluidic SS coil reactor (1 mL internal volume) thermoregulated with a Thermo Finnigan Interscience GC oven operated at 190 °C under 250 psi. The reactor effluent was thermally quenched through an air-cooled SS coil (0.2 mL), before being blended with an aqueous feed of **ZnCl<sub>2</sub>/3-MPA** through a T-mixer. The **ZnCl<sub>2</sub>/3-MPA** feed solution was handled through a Knauer Azura P4.1S pump, equipped with a 10 mL stainless steel head. The reaction medium reacted next in a microfluidic PFA coil reactor (6 mL internal volume) operated at 120 °C < T < 160 °C (heating with a silicone oil bath) under 100 psi of counterpressure. The reactor effluent was collected and analyzed by UV/Vis spectroscopy.

A detailed setup is depicted in Figure S9.

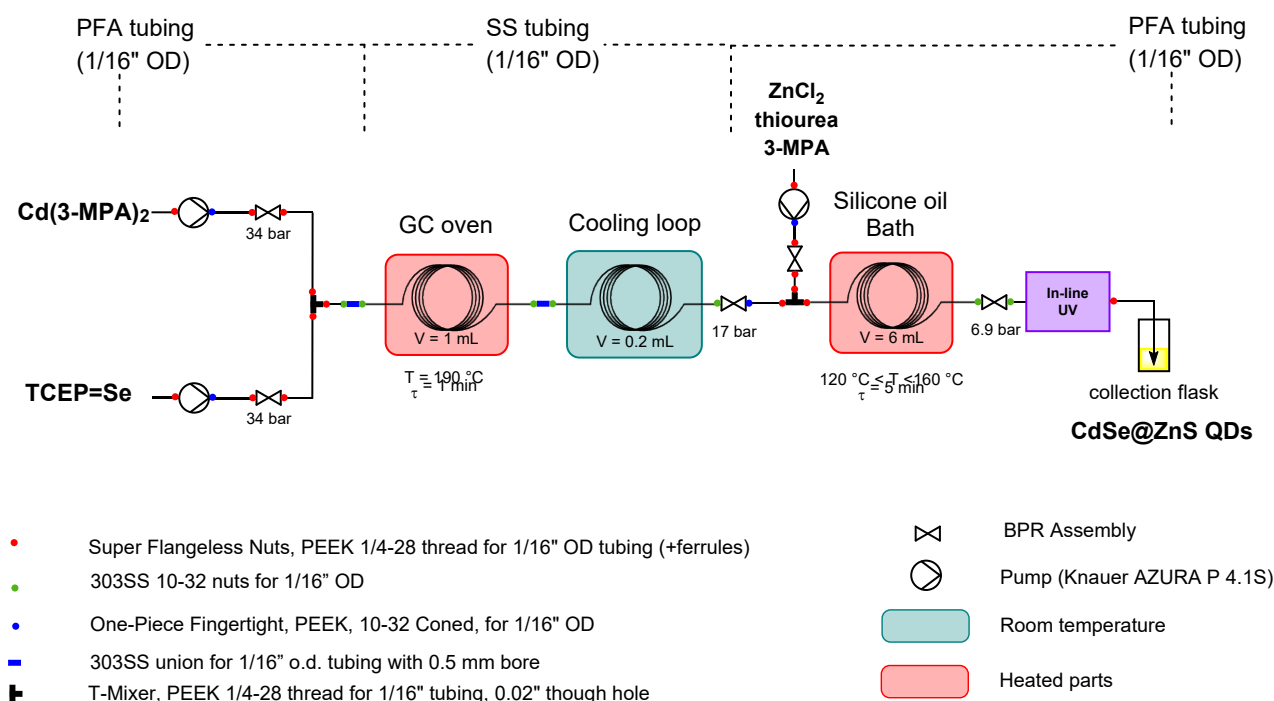


Figure S9. Concatenated setup for the preparation of **CdSe@ZnS**

#### 4.8.2. Preparation of the feed solutions

The cadmium precursor **Cd(3-MPA)<sub>2</sub>** feed solution was prepared by dissolving **Cd(OAc)<sub>2</sub>** (0.1333 g, 5 mmol, 5 equiv. vs TCEP) and **3-MPA** (0.1327 g, 12.5 mmol, 2.5 equiv.) with milliQ

water. The pH was adjusted to 11 by the addition of 1 M aqueous NaOH, then the solution was filled up to 100 mL with milliQ water in a volumetric flask.

The feed solution of **TCEP=Se** (0.02 M) was prepared according to the procedure described in section S4.7.4 and involved the reaction of elemental selenium (0.1579 g, 2 mmol, 2 mmol, 2 equiv.) with an aqueous solution of **TCEP** (0.2866 g, 1 mmol, 1 equiv.), prepared in a 50 mL volumetric flask (pH increased to 11 with NaOH 1 M)

The zinc shell precursor feed solution was prepared by dissolving **ZnCl<sub>2</sub>** (0.1363 g, 1 mmol, 1 equiv.), **thiourea** (0.0761 g, 1 mmol, 1 equiv.) and **3-MPA** (0.3184 g, 3 mmol, 3 equiv.) in milliQ water. The pH was then adjusted to 11 with the addition of 3.6 mL 1 M aqueous NaOH, then the solution was filled up to 50 mL with milliQ water in a volumetric flask.

#### 4.8.3. Modus operandi

The 0.02 M **TCEP=Se** feed solution and the 0.05 M **Cd(3-MPA)<sub>2</sub>** feed solution were infused at 200 and 800  $\mu\text{L}\cdot\text{min}^{-1}$ , respectively, through a PEEK T-mixer and reacted at 190 °C for 1 min of residence time under 250 psi of counterpressure. After cooling down to room temperature, the reactor effluent containing **CdSe** QDs was then mixed through a PEEK T-mixer with the zinc shell precursor feed solution, infused at 200  $\mu\text{L}\cdot\text{min}^{-1}$ . **CdSe/ZnS** core-shell QDs occurred at 160 °C (100 psi) within 5 min of residence time. See additional experimental details in section S5.10.

#### 4.9. Flow synthesis of CdTe

Following the successful transposition of the concatenated process for **CdTe** QDs synthesis in flow, preliminary results indicated that **CdTe** had the most promising core. Consequently, an optimization phase was undertaken. For this optimization, the impacts of temperature, residence time, and Cd:Te ratio were assessed.

##### 4.9.1. Preparation of the feed solutions

A 0.003 M aqueous solution of **TCEP** was prepared by dissolving **TCEP·HCl** (0.2150 g, 0.75 mmol, 1 equiv.) with milliQ water. The pH was adjusted to 10.7 with 2 M aqueous NaOH, then the solution was filled up to 250 mL with milliQ water in a volumetric flask. The solution was then transferred into a round-bottom flask and degassed with an argon flow for 15 min.

- Cd:Te ratio 5

The cadmium precursor feed solution was prepared by dissolving **Cd(Ac)<sub>2</sub>** (0.9995 g, 3.75 mmol, 5 eq) and **3-MPA** (0.9951 g, 9.375 mmol, 12.5 equiv.) with milliQ water. The pH was adjusted to 10.7 by the addition of 1 M aqueous NaOH, then the solution was filled up to 250 mL with milliQ water in a volumetric flask.

- Cd:Te ratio 7.5

The cadmium precursor feed solution was prepared by dissolving **Cd(Ac)<sub>2</sub>** (1.4992 g, 5.625 mmol, 7.5 eq) and **3-MPA** (1.4926 g, 14.063 mmol, 18.75 equiv.) with milliQ water. The pH was adjusted to 10.7 by the addition of 1 M aqueous NaOH, then the solution was filled up to 250 mL with milliQ water in a volumetric flask.

#### 4.9.2. Setup

See setup in section S4.7.1.

#### 4.9.3. Sample analysis

Each sample produced was treated as follows:

- Dilution: crude sample 100  $\mu\text{L}$  + 1000  $\mu\text{L}$  milliQ water
- Absorbance measurement: between 350 nm to 1000 nm
- Recording of 3D emission spectra: excitation (460 nm to 560 nm, 5 nm step), emission (470 nm to 900 nm, step 0.5 nm)

#### 4.9.4. Data analysis

The measurements obtained in section S4.9.3. allow the calculation of various metrics that help to characterize the QDs samples: the peak position (absorbance and emission), the size distribution (full width at half maximum (FWHM)), and the relative quantum yield. These metrics were calculated using a Python script working as follows:

- For each sample, importation of the absorbance and 3D emission spectra
- Data smoothing
- Peak position calculation:
  - o Absorbance: peak detection based on extrema by looking for derivatives equal to zero (1<sup>st</sup>: valley, 2<sup>nd</sup>: peak)
  - o Emission: detection of the maximum value in 3D by reporting the index of the emission peak position
- Size distribution:
  - o Emission: intersections (right and left) at half of the peak intensity
- Relative quantum yields:

The determination of relative photoluminescence quantum yields (PLQY) is a challenging step and follows two protocols.<sup>S3,4</sup>

- o Comparison between sample emission and reference emission peak (Fluoresceine, Rhodamine 6G, and Rhodamine 101) and stamping of the sample with the closest reference.
- o Depending on the reference with which the sample is compared, attribution of the excitation wavelength at 470 nm for fluoresceine, 505 nm for Rhodamine 6G, and 560 nm for Rhodamine 101.
- o Collection of the absorbance of the sample and its reference at this wavelength (the ratio must be as close as possible to 1)
- o Collection of the emission spectrum of the sample and the reference spectra at the defined excitation wavelength and calculation of the emission surface.
- o Application of the following formula

$$PLQY(\%) = QY_{ref} \cdot \frac{S_{sample}}{S_{ref}} \cdot \frac{(1 - 10^{-A_{ref}})}{(1 - 10^{-A_{sample}})} \cdot \frac{n_{sample}^2}{n_{ref}^2} \cdot 100$$

Where: QY is the reference quantum yield (Fluoresceine = 89 %, Rhodamine 6G = 91 %, Rhodamine 101 = 91.5%), S is the integration of the emission peak, A is the absorbance at the excitation wavelength and n is the refractive indices: NaOH 0.1

M = 1.360 (for samples and fluoresceine), ethanol = 1.335 (for Rhodamine 6G and 101)

#### 4.10. Mesofluidic synthesis of CdTe

The scalability of our protocol was validated for the production of **CdTe** QDs. The pilot scale setup featured the upstream preparation of **TCEP=Te**, its dilution with milliQ water, and tellurium transfer with a **Cd(3-MPA)<sub>2</sub>** aqueous feed. The transfer of tellurium to cadmium occurred at temperatures ranging from 130 °C to 190 °C in a commercial mesofluidic Corning<sup>®</sup> AFR<sup>™</sup> G1 SiC reactor operated under 15.5 bar (225 psi) of counterpressure. The reactor effluent was thermally quenched through a tube-in-tube heat exchanger, prior to in-line UV/Vis spectroscopy. A detailed flow chart is depicted in Figure S10.

##### 4.10.1. Detailed setup for the pilot scale production of CdTe

The aqueous feed solution of **TCEP** was pumped with a Knauer Azura P4.1S HPLC pump (10 mL stainless steel head) through a packed-bed column filled with tellurium (see Section S4.8.2 for the detailed description). The aqueous effluent containing **TCEP=Te** was then diluted with a stream of water through a SS T-mixer (Swagelok). The water feed was dosed with a Knauer BlueShadow equipped with a Bronkhorst flow meter. Both devices were connected to LabVision, which provided a PID feedback loop to ensure a constant flow rate. After dilution, the stream of **TCEP=Te** was then mixed with the aqueous cadmium feed, which was pumped by an Isco Teledyne 5000D dual syringe pump. Both solutions then reacted in a mesofluidic Corning<sup>®</sup> AFR<sup>™</sup> G1 SiC reactor equipped with 6 Silicon Carbide fluidic modules (10 mL internal volume each) connected in series. The temperature of the reactor was controlled by a Lauda XT 280 thermostat (using HL 60 thermal fluid) at temperatures ranging from 130 °C to 190 °C. The entire pilot scale setup was operated under 15.5 bar (225 psi) of counterpressure (Equilibar H3P) regulated by a Bronkhorst EL-PRESS. The reactor effluent was thermally quenched through a tube-in-tube heat exchanger (15 mL internal volume, operated at 4 °C) prior to in-line UV/Vis analysis (Avantes Flow cell-1/4", 5 mm pathlength).

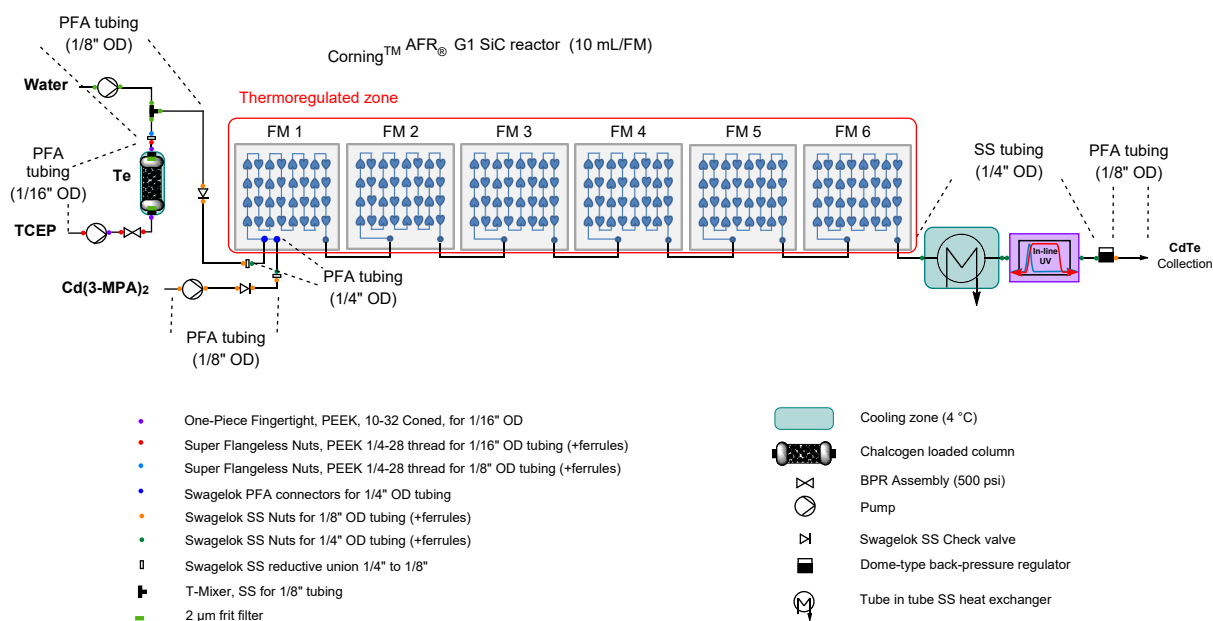


Figure S10. Detailed setup for the scalability trials toward CdTe

#### 4.10.2. Heat exchanger

Downstream of the mesofluidic reactor, a thermal quench is performed through a heat exchanger, which consists of a tube-in-tube exchanger. To maximize heat dissipation, the system is entirely made of stainless steel. The exchanger itself consists of 1 m of  $\frac{1}{4}$  " tube surrounded, over 83 cm, by a  $\frac{1}{2}$  " tube. Cooled water (setpoint at 4 °C) circulates in the volume around the  $\frac{1}{4}$  " pipe. A scheme of this system is provided in Figure S11. The heat exchange efficiency is assessed downstream by a thermocouple. The measured temperature remained between 20 °C and 30 °C throughout the experiments.

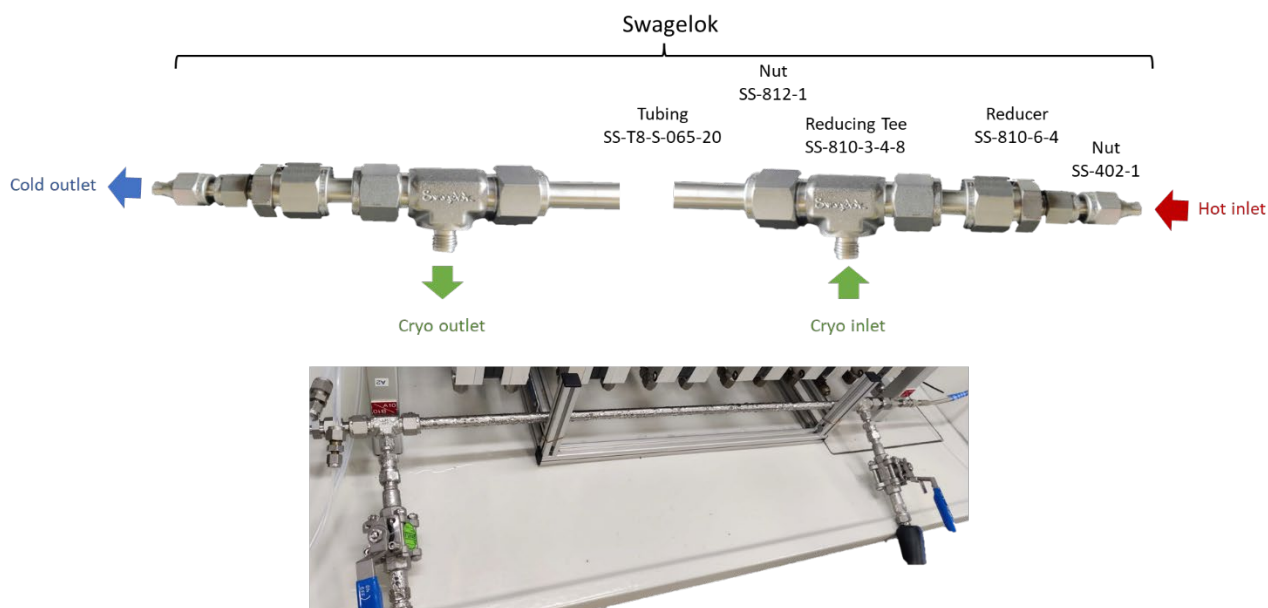


Figure S11. Detailed setup of the tube-in-tube heat exchanger

#### 4.10.3. Feed preparation

A 2 M aqueous stock solution (300 mL) of NaOH was prepared by dissolving 24.00 g (0.6 mol) of NaOH in milliQ water in a volumetric flask.

A 0.2 M aqueous solution of **TCEP** was prepared by dissolving **TCEP.HCl** (5.732 g, 20 mmol, 1 equiv.) with milliQ water. The solution was prepared by adding 54 mL with NaOH 2 M and then filling up to 100 mL with water in a volumetric flask. The solution was then transferred into a round-bottom flask and degassed with an argon flow for 15 min.

The cadmium precursor feed solution was prepared by dissolving **Cd(OAc)<sub>2</sub>** (29.9846 g, 0.112 mol, 1 equiv.) and **3-MPA** (29.85 g, 0.281 mol, 2.5 equiv.) in milliQ water. The pH was then adjusted with the addition of 220 mL 2 M aqueous NaOH, then the solution was filled up to 5000 mL with milliQ water in a volumetric flask.

#### 4.10.4. Modus operandi

The 0.2 M **TCEP** feed solution was infused at a flow rate of 0.45 or 0.6 mL min<sup>-1</sup> through a column filled with elemental tellurium (7.34 g, 57.8 mmol). The resulting stream of **TCEP=Te** was diluted with a stream of milliQ water in a T-mixer (flow rate of 29.6 mL min<sup>-1</sup> or 39.4 mL min<sup>-1</sup>). After dilution, the stream of **TCEP=Te** was then mixed with the aqueous cadmium feed, which was injected at a flow rate of 30 or 40 mL min<sup>-1</sup>. **CdTe** QDs were obtained at process



temperatures ranging from 130 °C to 190 °C (15.5 bar – 225 psi – of counterpressure), with a residence time of 45 s or 60 s.

## 5. Additional experimental details

### 5.1. Stability study for TCEP=Te

The experimental details are available in Section S4.4.2. The samples were analyzed by  $^{31}\text{P}$  NMR (162 MHz) and exhibited two peaks at  $\delta = 58.7$  ppm (**TCEP=O**) and  $\delta = -4.88$  ppm (**TCEP=Te**) after quantitative conversion of **TCEP** ( $\delta = -26.27$  ppm) with tellurium (Figure S12).

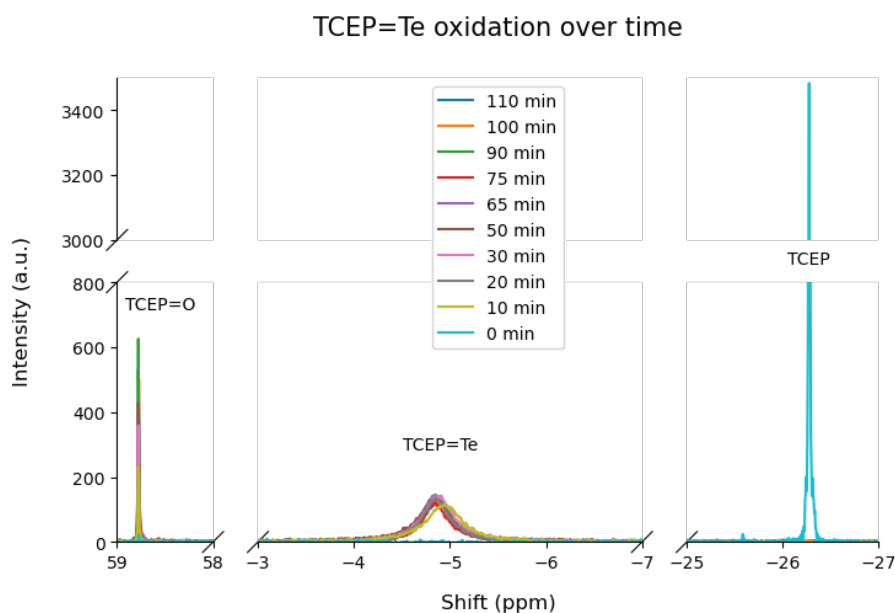


Figure S12. Crude results of TCEP=Te degradation ( $^{31}\text{P}$  NMR, 162 MHz)

The  $^{31}\text{P}$  NMR peaks for **TCEP=O** and **TCEP=Te** were monitored and integrated over time, as depicted in Figure S13. As the conversion of **TCEP=Te** increased, the appearance of a layer of  $\text{Te}_0$  was noticed.

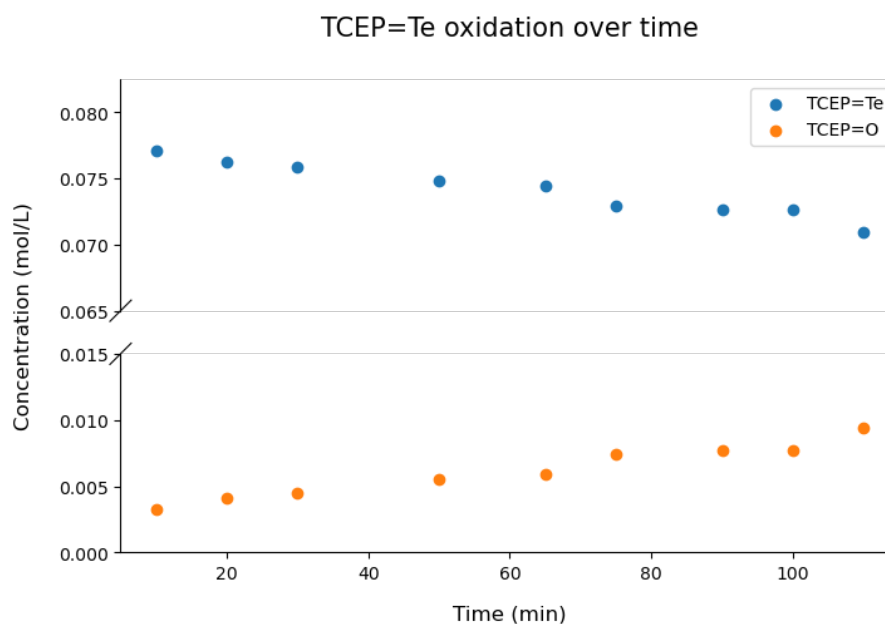


Figure S13. Oxidation over time of TCEP=Te into TCEP=O

The increase of TCEP=O over ~2 h emphasized the critical importance of degassing and maintaining solutions and working under argon to protect the integrity of TCEP=X (X=S, Se, Te).

### 5.2. Determination of the optimum pH

Figure S14 was obtained upon stacking the graphs from the pH optimization of TCEP=S, Se (section S4.5.1) and the deprotonation rate of the TCEP. An optimum pH appeared at 10.7, mostly due to TCEP=S formation's limitations.

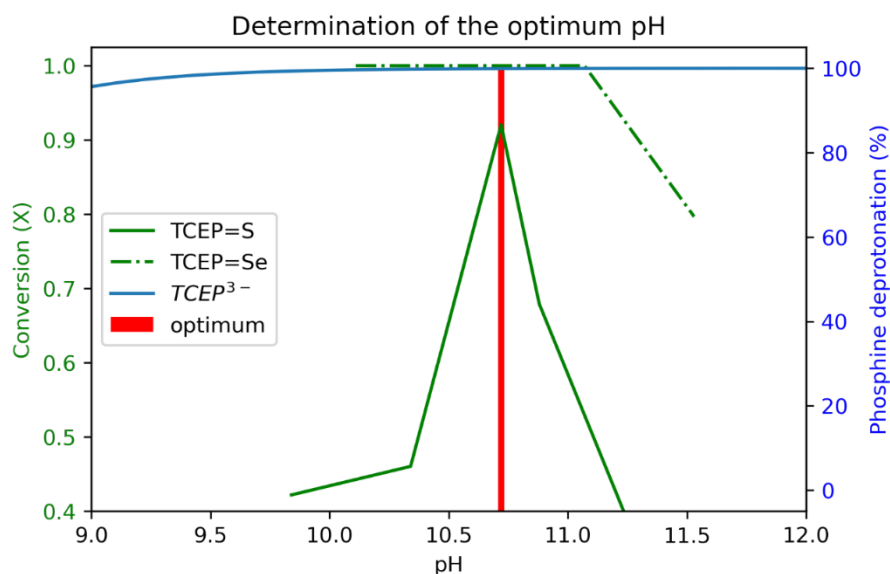


Figure S14. pH optimum for TCEP=X (X=S, Se, Te) formation

### 5.3. Raman monitoring for the formation of TCEP=S

The formation of TCEP=S was monitored in batch through Raman spectroscopy. The raw data were treated with a 6<sup>th</sup>-order polynomial Savitsky-Golay baseline correction and

normalization of the intensity (based on the signal of water, assumed to remain constant, from  $1635\text{ cm}^{-1}$  to  $1655\text{ cm}^{-1}$ ). Experimental data were then concatenated in a 3D matrix and plotted as a heatmap (Figure S15). From Figure S15, it became clear that 4 signals were evolving during the experiment, at  $875\text{ cm}^{-1}$  and  $825\text{ cm}^{-1}$  (both signals seem to be related to an intermediate hypothesized as the adsorbed form TCEP on the sulfur surface), at  $657\text{ cm}^{-1}$  (associated with the P-C bond, and thus the disappearance of TCEP), and at  $578\text{ cm}^{-1}$  (associated with the P=S bond and thus the appearance of TCEP=S).

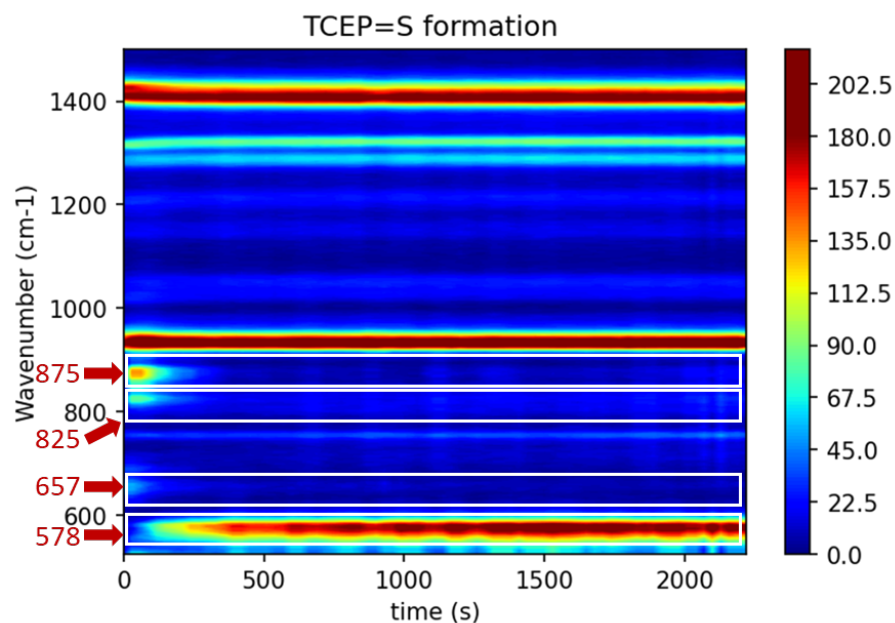


Figure S15: Heatmap for the formation of TCEP=S at  $40\text{ }^{\circ}\text{C}$

Based on these observations, the intensity profile was extracted at  $875\text{ cm}^{-1}$ ,  $657\text{ cm}^{-1}$  and  $578\text{ cm}^{-1}$  (the intensities are obtained as the average on the 3 points closest to the maximum height of the band). Then, based on the mass balance, the intensities are converted into a concentration profile (Figure S16).

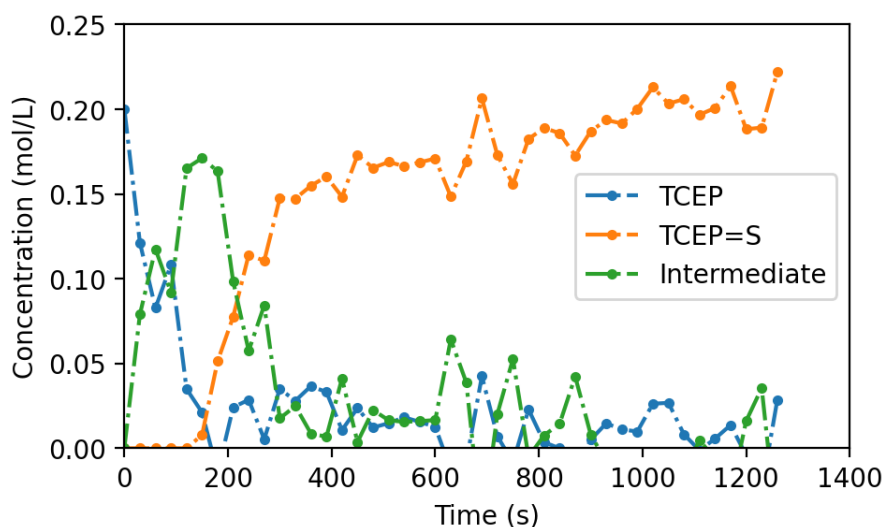


Figure S16. Concentration profiles for the formation of TCEP=S at 40 °C

#### 5.4. Raman monitoring for the formation of TCEP=Se

The formation of TCEP=Se was monitored in batch through Raman spectroscopy. The raw data were treated with a 6<sup>th</sup>-order polynomial Savitsky-Golay baseline correction and normalization of the intensity (based on the signal of water, assumed to remain constant, from 1635 cm<sup>-1</sup> to 1655 cm<sup>-1</sup>). Experimental data were then concatenated in a 3D matrix and plotted as a heatmap (Figure S17). From Figure S17, it became clear that 3 signals were evolving during the experiment, at 653 cm<sup>-1</sup> (associated with the P-C bond, and thus the disappearance of TCEP) and at 428 cm<sup>-1</sup> and 455 cm<sup>-1</sup> (associated with the P=Se bond and thus the appearance of TCEP=Se).

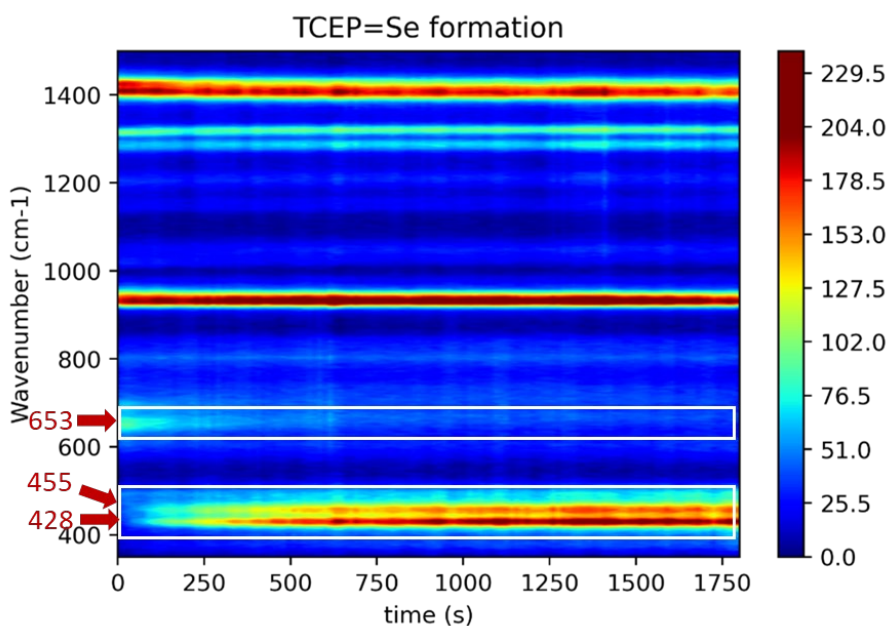


Figure S17. Heatmap for the formation of TCEP=Se at 40 °C

Based on these observations, the intensity profile was extracted at  $653\text{ cm}^{-1}$  and  $428\text{ cm}^{-1}$  (average on the 3 points closest to the maximum). Then, based on the mass balance, the intensities are converted into a concentration profile (Figure S18).

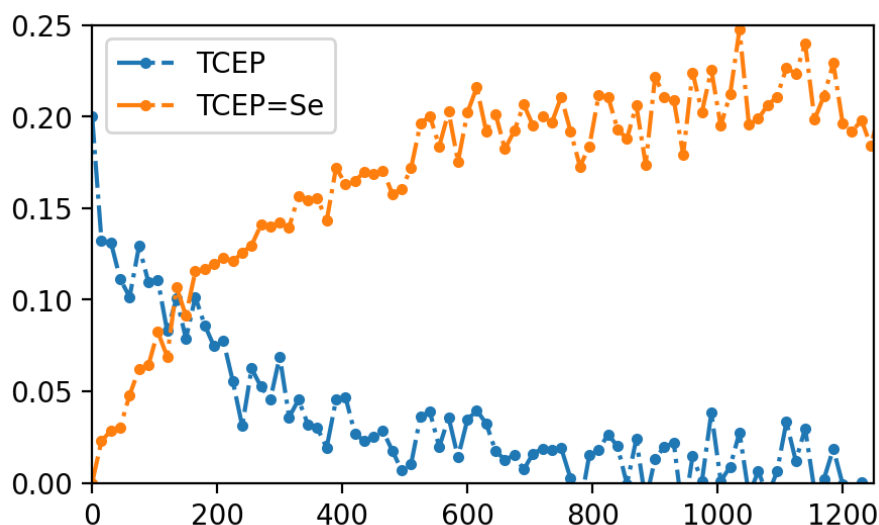


Figure S18. Concentration profiles for the formation of **TCEP=Se** at  $40\text{ }^{\circ}\text{C}$

### 5.5. TCEP=Te Raman monitoring

The formation of **TCEP=Te** was monitored in batch through Raman spectroscopy. The raw data were treated with a 6<sup>th</sup>-order polynomial Savitsky-Golay baseline correction and normalization of the intensity (based on the signal of water, assumed to remain constant, from  $1635\text{ cm}^{-1}$  to  $1655\text{ cm}^{-1}$ ). Experimental data were then concatenated in a 3D matrix and plotted as a heatmap (Figure S19). From Figure S19, it became clear that 5 signals were evolving during the experiment, at  $494\text{ cm}^{-1}$  and  $715\text{ cm}^{-1}$  (matrix effect, probably due to tellurium dioxide<sup>55</sup>),  $649\text{ cm}^{-1}$  (disappearance of **TCEP**), and at  $376\text{ cm}^{-1}$  and  $418\text{ cm}^{-1}$  (associated with the P=Te bond and thus the appearance of **TCEP=Te**).

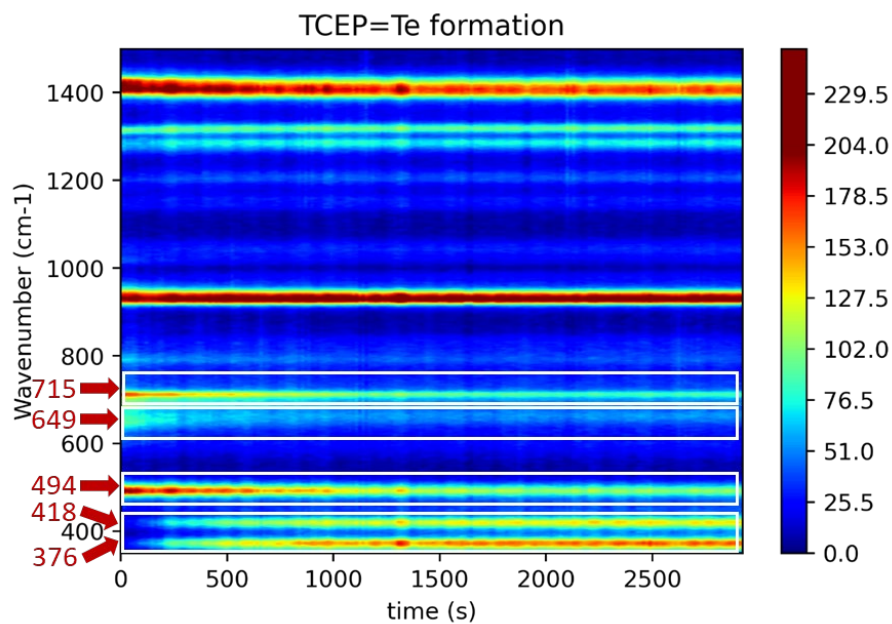


Figure S19. Heatmap for the formation of TCEP=Te at 40 °C

Based on these observations, the intensity profile was extracted at 649 cm<sup>-1</sup> and 376 cm<sup>-1</sup> (average on the 3 points closest to the maximum). Then, based on the mass balance, the intensities are converted into a concentration profile (Figure S20).

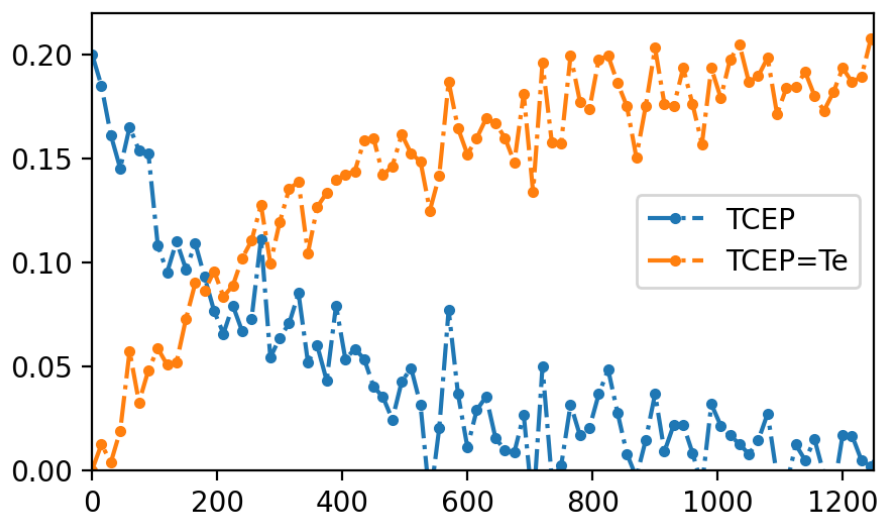


Figure S20. Concentration profiles for the formation of TCEP=Te at 40 °C

## 5.6. Establishment of a kinetic model

Three models were originally developed to fit the experimental data. For the discussion of the models, the following assumptions were made: (a) the reaction occurs at the interface between the chalcogen and the aqueous liquid phase when a phosphine molecule is adsorbed on the surface; and (b) the constants  $k_{adsorption}$  and  $k_{desorption}$  of **TCEP** are far more important than the constant rate ( $k_r$ ) (Figure S21).

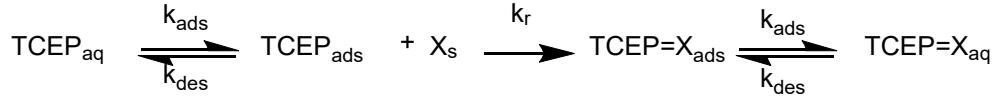


Figure S21: fundamental step of **TCEP=X** formation

With the previous assumptions, the general kinetic equation is:

$$r = -k_r \cdot \theta_{TCEP} \cdot \theta_X$$

Where  $\theta_{TCEP}$  is the covering rate of **TCEP** and  $\theta_X$  is the covering rate of the chalcogen.

- First scenario:

In this scenario, since the powder is composed of the chalcogen, the assumption is made that the covering rate of chalcogen  $\theta_X = 1$ . The second assumption is that phosphine is adsorbed on the surface according to a Langmuir Isotherm. The kinetic equation then becomes:

$$r = -k_r \cdot \frac{k_a \cdot C}{1 + k_a \cdot C}$$

Where  $k_r$  is the constant rate and  $k_a$  is the affinity constant of the **TCEP**.

- Second scenario:

The surface of the chalcogen is still saturated, but all sites are not equivalent. In this case, the hypothesis that  $\theta_X = 1$  is not met, expressing the non-homogeneity of the sites on the surface. Here again, the assumption is made that the **TCEP** is adsorbed following a Langmuir Isotherm. Accordingly, the kinetic equation becomes as follows:

$$\begin{aligned} r &= -k_r \cdot \frac{k_x \cdot k_{TCEP} \cdot C_x \cdot C_{TCEP}}{(1 + k_x \cdot C_x + k_{TCEP} \cdot C_{TCEP})^2} = -\frac{k_1 \cdot C_{TCEP}}{(k_2 + k_3 \cdot C_{TCEP})^2} \\ &= -\frac{k_1 \cdot C_{TCEP}}{(k_2^2 + 2 \cdot k_2 \cdot k_3 \cdot C_{TCEP} + k_3^2 \cdot C_{TCEP}^2)} \end{aligned}$$

Where  $k_r$  is the constant rate,  $k_x$  is the affinity constant of the chalcogen for itself,  $k_{TCEP}$  is the affinity constant of the **TCEP** for the chalcogen and  $C_x$  is the concentration of chalcogen.

- Third scenario:

In this scenario, the main hypothesis is that the covering rate of chalcogen  $\theta_X = 1$ , but in this case, the phosphine adsorbs according to a BET isotherm, which leads to the following equation:

$$r = -k_r \cdot \frac{k_s \cdot C_{TCEP}}{(1 - k_L \cdot C_{TCEP}) \cdot (1 - k_L \cdot C_{TCEP} + k_s \cdot C_{TCEP})}$$

Where  $k_r$  is the constant rate,  $k_s$  is the affinity constant of the first layer of TCEP adsorbed on the chalcogen and  $k_L$  is the affinity constant of the upper layers of TCEP

To efficiently segregate these three models, the decision was made to compare them under the form  $C_{TCEP}/r$ . Indeed, under this form, equation 1 becomes a straight line, equation 2 becomes a parabola with all coefficients of the same sign, and equation 3 becomes a parabola with variable sign coefficients. These equations are summarized below:

$$\frac{C_{TCEP}}{r} = \frac{1}{k_r \cdot k_a} \frac{1}{k_r} \cdot C \quad (1)$$

$$\frac{C_{TCEP}}{r} = \frac{k_2^2}{k_1} C - \frac{2 \cdot k_2 \cdot k_3}{k_1} C + \frac{k_3^2}{k_1} C^2 \quad (2)$$

$$\frac{C_{TCEP}}{r} = \frac{1}{k_r \cdot k_s} C + \frac{2 \cdot k_L - k_s}{k_r \cdot k_s} C - \frac{k_L^2 - k_L \cdot k_s}{k_r \cdot k_s} C^2 \quad (3)$$

Based on these assumptions, the expressions of  $C(t)/dC$   $f(C(t))$  were plotted. The first observation is that the values of  $C(t)/dC$  tend quickly towards a vertical asymptote. The first attempts to fit all the data with the three models failed. At best, if the fit is limited to low conversion values *i.e.*,  $C < 0.1$  mol/L, the early stage of the reaction can be fitted with relative success (Figure S22).

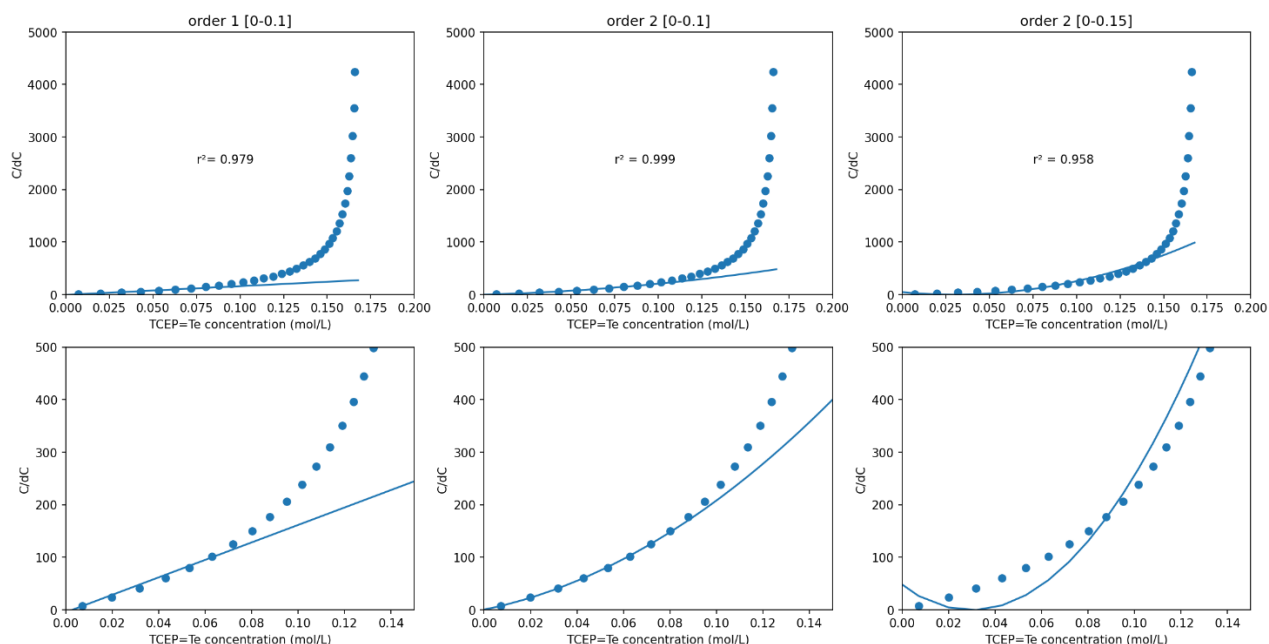


Figure S22. Trials to fit the  $C(t)/dC(t)$   $f(C(t))$  with first and second degree polynomials

The first row shows  $C(t)/dC(t)$  up to 5000, while the second row is limited to 500 to emphasize the fit quality in the early stages of the reaction. Generally speaking, the second-order



polynomial fit (second and third columns) provides a better-fit quality with a higher R<sup>2</sup>. The first-order fit (first column) only fits a much earlier stage for the reaction.

With such poor fit quality, it became apparent that none of these models could explain the kinetics from experimental data. These models work at best for the early stages of the experiments, then deviate significantly from the theoretical model. Such a deviation clearly emphasizes that the experimental kinetics slow down faster than what is predicted by all three models.

To take this observation into account, we hypothesized that surface deactivation was involved. Since deactivation is impossible strictly speaking with a reactive solid, it seemed more coherent to explain this reaction rate decrease with decreasing surface accessibility. The latter probably arises as a consequence of an increase in surface roughness. Therefore, a decreasing exponential contribution was empirically added to establish a new model (Figure S23).

$$r = k_r \cdot \frac{k_a \cdot C(t)}{1 + k_a \cdot C(t)}$$

- Adsorption Langmuir
- $\theta_x = 1$

Available sites f(time) ➔

$$r = k_r \cdot \frac{k_a \cdot C(t)}{1 + k_a \cdot C(t)} \cdot e^{-k_{dea} \cdot C(t)}$$

$$\frac{C(t)}{r} = \frac{1}{k_r \cdot k_a} + \frac{1}{k_r} \cdot C(t) + e^{k_{dea} \cdot C(t)}$$

Figure S23: Modification of a first-order kinetic with a decreasing surface availability

The experimental kinetics data were fitted with the revised model, as illustrated in Figure S24, with a significant improvement. The revised models cannot explain the decreasing rate for the late stages of the reaction but provided excellent regressions ( $r^2 > 0.999$ ) up to 0.15 mol/L (X = 0.75)

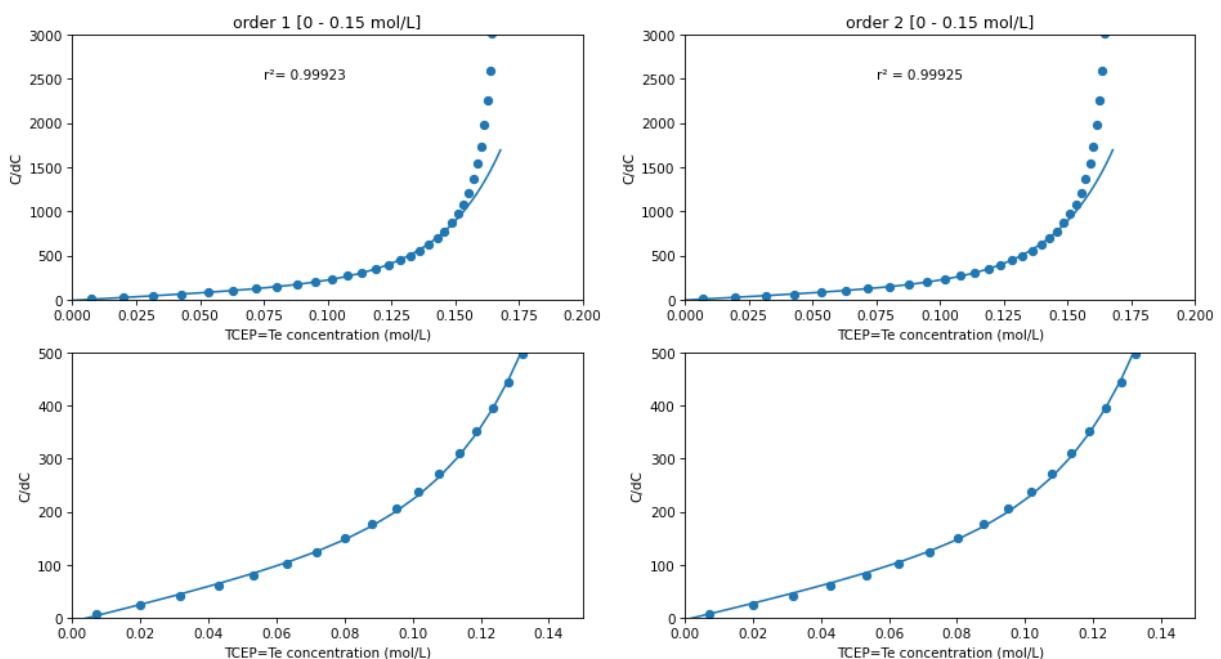


Figure S24. kinetic fitting with modified 1<sup>st</sup> and 2<sup>nd</sup> order Langmuir kinetics

The merits of the fits for 1<sup>st</sup> and 2<sup>nd</sup> order being very close to each other, we decided to fit all the experimental kinetics with the first-order law (Figure S23). From there,  $k_{reac}$  was extracted at each temperature and led to the experimental determination of the corresponding activation barriers for the formation of **TCEP=X** (X= S, Se, Te).

### 5.7. Transposition of the TCEP=X synthesis in flow (microfluidic scale)

To estimate the interest of the transposition in flow, the metric used is the Space-Time Yield (STY). This metric is a practical way to compare the productivity of reactors using various designs. STY is calculated as follows:

$$STY = \frac{m'}{V_{reactor}} = \frac{C \cdot MM \cdot V'_{max}}{V_{reactor}}$$

Where:

- $m'$ : mass product flow rate at the outlet of the reactor
- $V_{reactor}$ : volume of the bed packed reactor
- $C$ : product concentration
- $MM$ : molar mass of the product
- $V'_{max}$ : flow max at which total conversion was observed

### 5.8. Productivity of TCEP=Te over time

The purpose of this experiment was to monitor the production of **TCEP=Te** over time and assess whether this packed-bed approach is amenable for long runs. Reaction monitoring was carried out by in-line <sup>31</sup>P NMR (Figure S25). The results show that up to 200 min, the conversion of **TCEP** towards **TCEP=Te** reached completion without the formation of any degradation product (**TCEP=O**). The packed-bed column setup was therefore validated to sustain a constant production of **TCEP=Te** for long runs.

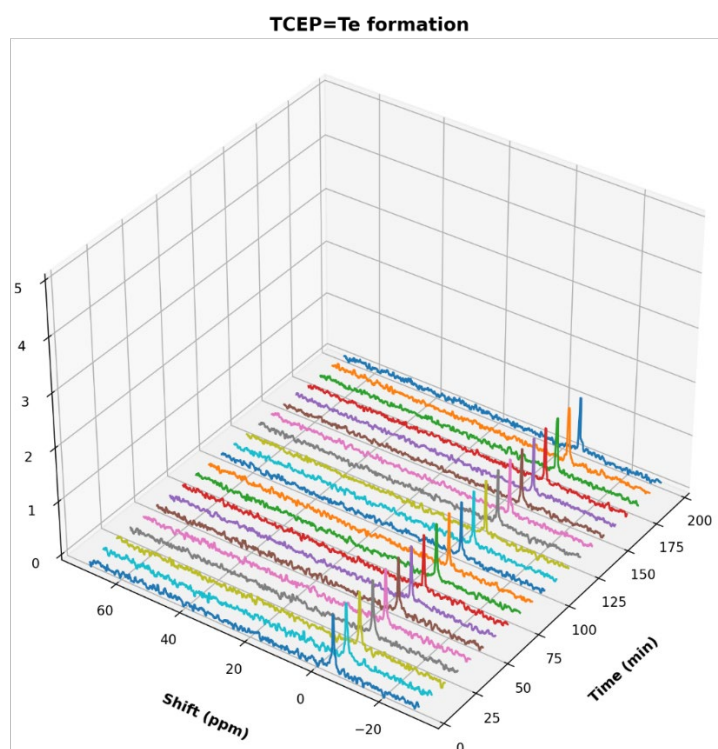


Figure S25. Monitoring of the productivity toward **TCEP=Te**

## 5.9. Control experiment for the preparation of CdS

To rule out the potential contribution of **3-MPA** (3-mercaptoproionic acid) as a potential source of sulfur in the production of **CdS** QDs, a control experiment was performed in the absence of **TCEP=S**. Indeed, **3-MPA** is used as a capping agent and chelates the cadmium source, and could therefore potentially transfer sulfur to cadmium under high temperatures.

The control experiment was conducted as follows: an aqueous feed of **Cd(3-MPA)<sub>2</sub>** was prepared by dissolving **Cd(OAc)<sub>2</sub>** (0.3332 g, 1.25 mmol, 1 equiv.) and **3-MPA** (0.4644 g, 4.375 mmol, 3.5 equiv.) in an aqueous NaOH solution (pH = 11) contained in a 250 mL volumetric flask. The resulting feed solution was injected in the same reactor setup (Figure S26) as for the **CdS** QDs synthesis (section S4.7.1).

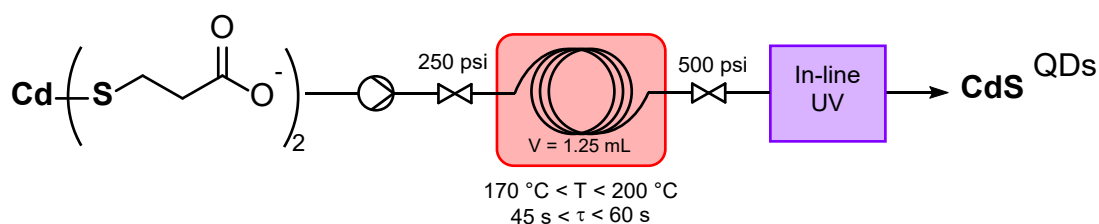


Figure S26. Control experiment for the preparation of **CdS** QDs in the absence of **TCEP=S**

A comparison between the control results of these experiments and the **CdS** synthesis with **TCEP=S** is depicted in Figure S27. Each plot contains the UV/Vis (left) and the photoluminescence results (right). The comparison of these two plots leads to the following observations:

- The use of **3-MPA** allows the formation of **CdS** QDs. They exhibit a larger size and narrower size distribution than those synthesized with **TCEP=S**, under the same conditions. However, the use of **TCEP=S** allows the generation of more nanoparticles (see UV/Vis spectra).
- The **CdS** QDs synthesized with **TCEP=S** as the chalcogen transfer agent are endowed with stronger photoluminescence than QDs obtained with **3-MPA**. Both have broad emissions.

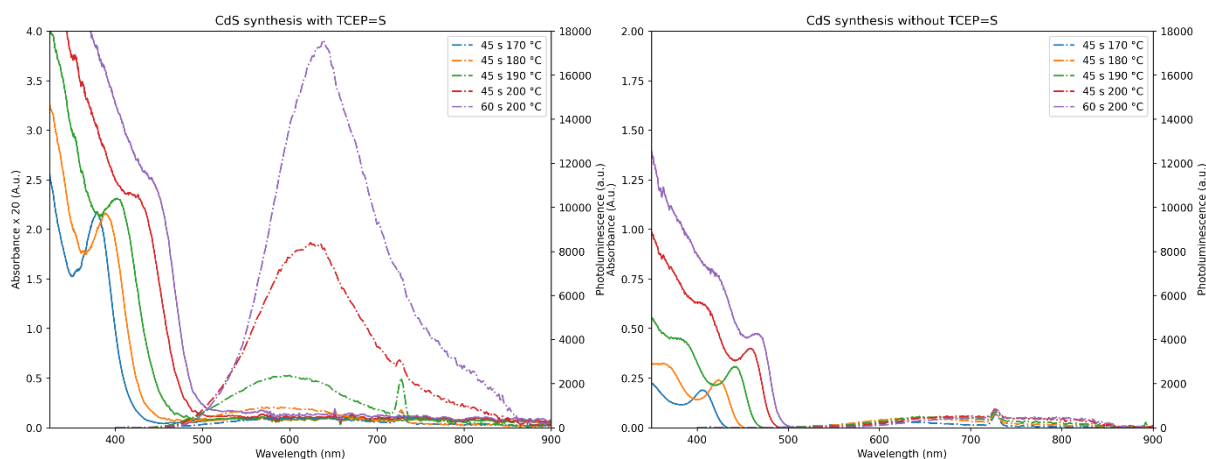


Figure S27. UV/Vis and fluorescence plots for right: **CdS** synthesis with **TCEP=S**, left: **CdS** synthesis with **3-MPA**, (A.u. = Absorbance units). Note that the UV/Vis data from the left plot were obtained from a tube through a flow cell (500  $\mu\text{m}$  light path). The data were therefore multiplied by 20 for easier comparison with the right plot.

In conclusion, **3-MPA** can potentially play the role of sulfur agent under basic conditions<sup>S6</sup> at high temperatures. It allows an efficient transfer of sulfur to cadmium (narrower size distribution and larger QDs), however, they exhibit lower emission properties and generate fewer particles than **TCEP=S**. It seems therefore that the use of **TCEP=S** improves the emission properties of the **CdS** QDs and increases the particle concentration.

### 5.10. Determination of reaction yield

The protocol developed to estimate the reaction yield was executed as follows:

- Extended production of a given QD type (**CdS**, **CdSe**, or **CdTe**) to obtain more or less 150 mL of crude QDs
- Purification of 20 mL of the crude mix (volumetric pipette) by selectively precipitating the QDs through the addition of 25 mL of ethanol (antisolvent) followed by centrifugation (10 min at 5000 rpm)
- Removal of the supernatant
- Drying of the solid residue under vacuum
- Weighting of the container with the dried powder
- Removal of the QDs from the container
- Weighting of the empty container

This operation is repeated at least 4 times. The tare executed allows to calculate the QD mass. It is hypothesized that the weight so obtained is only composed of the crystal material (**CdS**, **CdSe**, or **CdTe**). The theoretical yield is calculated as follows:

$$weight_{th} = \frac{n'_{limiting}}{V'_{tot}} \cdot V_{sample} \cdot MM_{crystal}$$

Where  $n'$  is the molar flow of the limiting reagent,  $V'_{tot}$  is the total flow rate in the reactor,  $V_{sample}$  is the sample volume and  $MM_{crystal}$  is the molar weight for the considered crystal (3<sup>rd</sup> column in Table S4). Finally, the yield results are presented in Table S4.

Table S4: Summary of the yield results and key values

Crystal type	$\delta$ (g.cm <sup>-3</sup> )	MM (g.mol <sup>-1</sup> )	Experimental conditions	Yield (%)
CdS	4.826	144.48	Rt = 45 s, T = 190 °C	40.3±8.8
CdSe	5.816	191.37	Rt = 45 s, T = 180 °C	74.5±6.5
CdTe	5.850	240.01	Rt = 45 s, T = 155 °C	64.6±4.0

## 5.11. Sample preparation for QDs characterization

### 5.11.1. High-Resolution Transmission Electron Microscopy (HRTEM)

The samples analyzed by HRTEM were prepared, directly from the crude, by adding 50  $\mu$ L of the sample (except **CdTe** which was less concentrated: 150  $\mu$ L) to 1000  $\mu$ L of milliQ water. These diluted solutions were then mixed with methanol in a 1:1 volume ratio (500  $\mu$ L:500  $\mu$ L). Finally, a drop of the resulting mixtures is deposited on the surface of carbon-coated 200 mesh copper grids and evaporated under atmospheric conditions overnight. The grids were analyzed without any further treatment.

### 5.11.2. X-Ray Powder Diffraction (PXRD)

The QDs to be analyzed by powder XRD were purified using the process described in section S5.10. The obtained powders were finally deposited on a zero-background support and analyzed as it is.

### 5.11.3. Diffusion-Ordered NMR Spectroscopy (DOSY)

The QDs to be analyzed by DOSY NMR were purified using the process described in section S5.10. The purified particles were dissolved in 600  $\mu$ L of D<sub>2</sub>O.

### 5.11.4. X-Ray Photoelectron Spectroscopy (XPS)

The QDs to be analyzed by XPS were purified using the process described in section S5.10. The obtained powders were finally deposited on a square piece of double-sided tape placed on an autosampler. The samples were analyzed after staying three days in a high vacuum chamber (>10<sup>-9</sup> torr).

## 5.12. Additional experimental details for CdSe/ZnS QDs

A series of experiments was carried out with the setup described in section S4.8 (Figure S9). The temperature of the ZnS shell reactor varied from 120 °C to 160 °C. The results are presented in Figure S28.

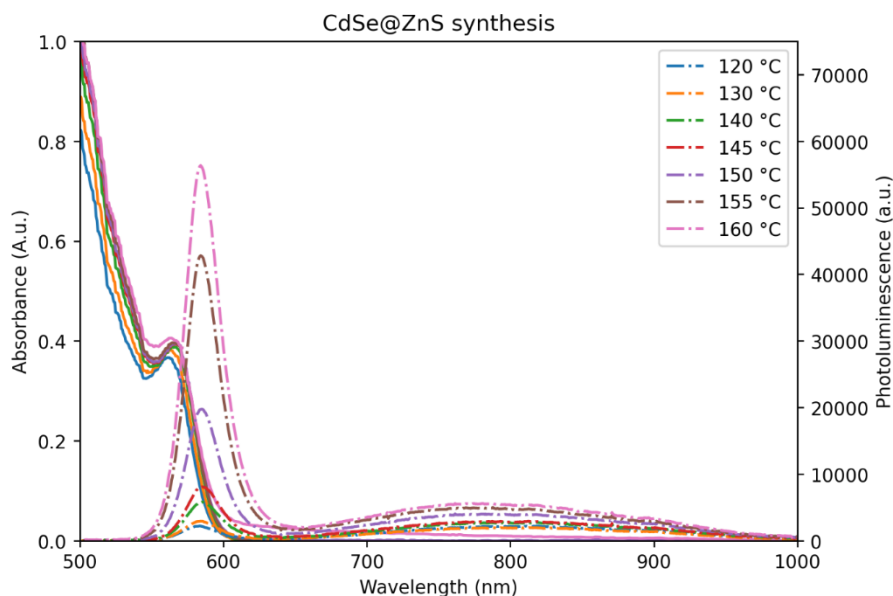


Figure S28. UV/Vis and PL spectra of the **CdSe/ZnS** QDs

It can be seen in Figure S28 (plain lines) that the **ZnS** shell addition on **CdSe** cores leads to a slight red shift of the first excitonic peak (from 561 nm to 566 nm) and an increase of absorbance from 0.365 to 0.406. The photoluminescence of the **CdSe/ZnS** QDs shows a more pronounced effect (Figure S28, dashed lines). Each photoluminescence spectrum features two main peaks: one narrow peak associated with the Stokes fluorescence (585 nm) and one much broader (in the 782-811 nm range) associated with trap states on the surface. As temperatures in the **ZnS** shell reactor increase from 120°C to 160°C, the contribution of Stokes fluorescence significantly rises, while the contribution from trap states on the surface shows minimal increase. This trend was quantified by fitting the photoluminescence spectra with two Gaussian curves (Figure S29).

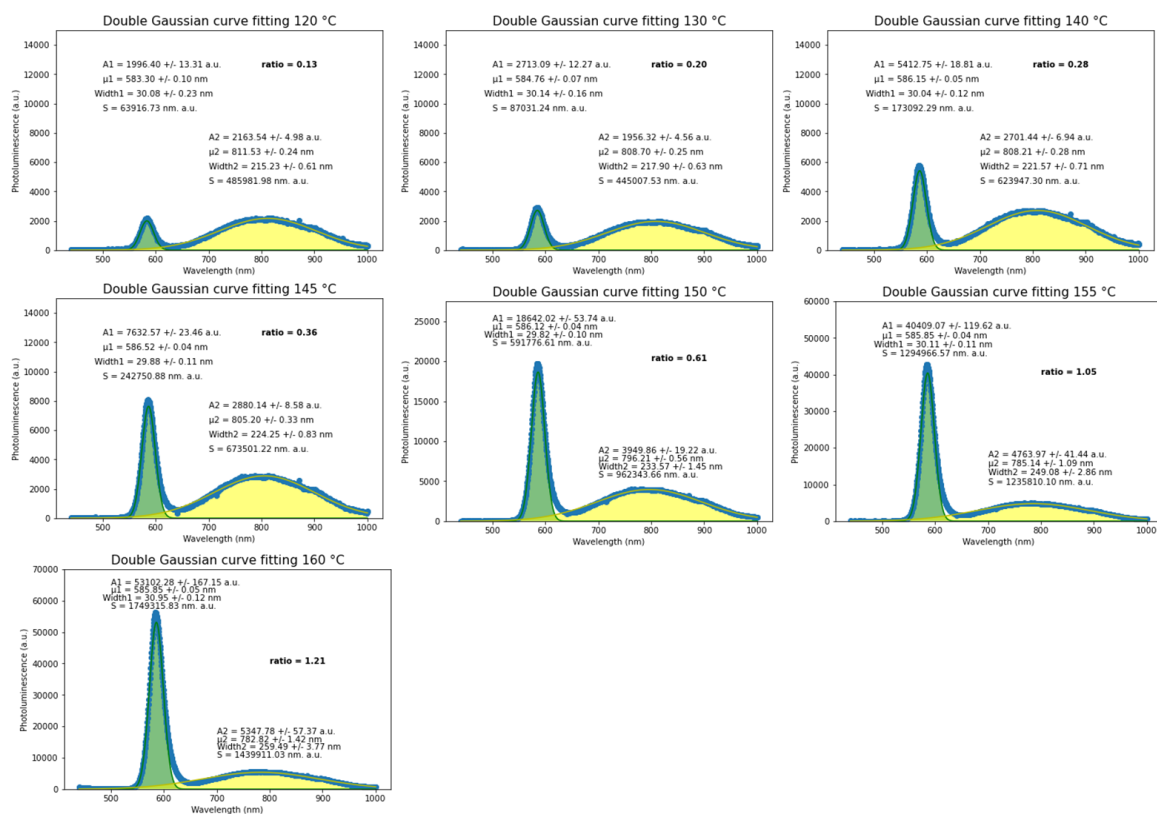


Figure S29. Fitting of the photoluminescence spectra of the CdSe/ZnS QDs

For each data set generated at 120 °C, 130 °C, 140 °C, 145 °C, 150 °C, 155 °C and 160 °C, both Stokes fluorescence and surface trap state peaks were studied, with a particular focus on their intensity (A), position ( $\mu$ ), full width at half maximum (width) and surface peak (S). A metric was defined as the surface ratio between the Stokes fluorescence peak and the trap state emission to evaluate the quality of CdSe (as CdSe/ZnS QDs) QDs generated with the addition of the ZnS shell. The effect of temperature in the second reactor on this metric was plotted, and the results are presented in Figure S30. It emphasizes that from 120 to 155 °C, the fluorescence peak/trap states emission ratio increases exponentially. The last point at 160 °C is slightly out of the trend, likely because TCEP=Se competes with thiourea again for available cations.

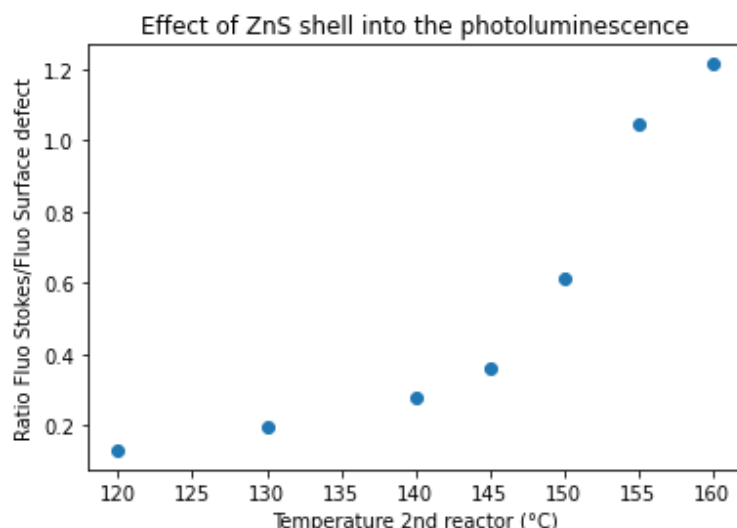


Figure S30. Evolution of the fluorescence ratio over temperature rise

An additional control experiment was carried out without infusing the Zn shell precursor feed to estimate the stability of the stream obtained from the **CdSe** synthesis. The upstream flow of **CdSe** was simply passed through the second reactor operated at 120 °C for 6 min. The results are shown in Figure S31.

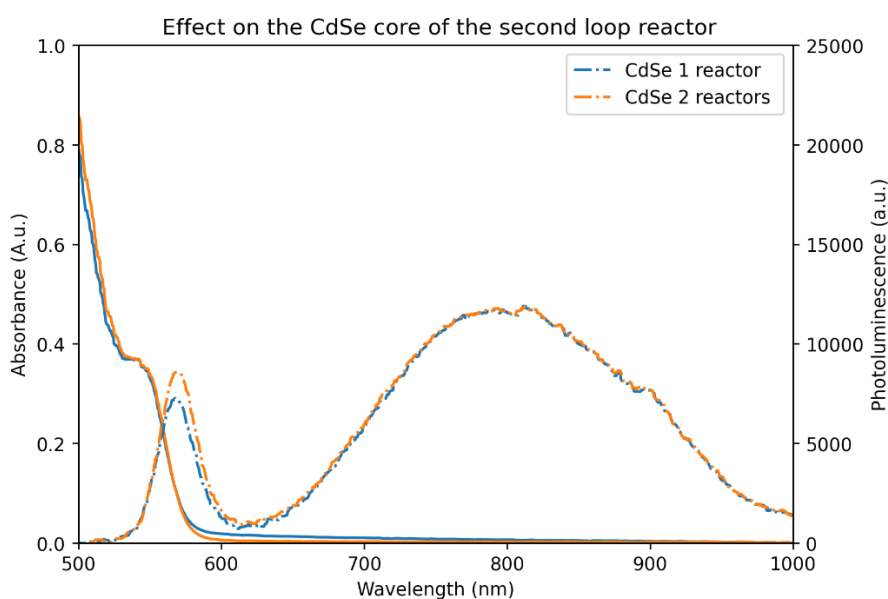


Figure S31. Thermal stability of the **CdSe** stream

The results for the thermal maturation of **CdSe** QDs for an additional 6 min at 120 °C emphasize a slight redshift of the first excitonic peak (absorbance) and of the fluorescence peak (photoluminescence), which is related to a growth phase occurring in the second reactor. These QDs also exhibit a fluorescence/trap state emission ratio that increases slightly with the addition of the second reactor. This is due to the particle growth, which leads to a reduction of the surface/volume of the QDs and therefore to fewer surface defects. However, this effect is limited and cannot explain the improvement of the fluorescence ratio observed in Figure S30. This enhancement is therefore likely to be induced by the formation of the **ZnS** shell.



### 5.13. Isotopic labeling

Before isotopic labeling, a  $\text{TCEP}=\text{}^{16}\text{O}$  reference was synthesized.

#### 5.13.1. $\text{TCEP}^{16}\text{O}$ reference synthesis

The synthesis of  $\text{TCEP}^{16}\text{O}$  was performed by oxidating  $\text{TCEP.HCl}$  with 30 %  $\text{H}_2\text{O}_2$ . A 0.2 M aqueous solution of  $\text{TCEP}$  was prepared by dissolving  $\text{TCEP.HCl}$  (0.0573 g, 0.2 mmol, 1 equiv.) in milliQ water. Then, 30 %  $\text{H}_2\text{O}_2$  (25.5  $\mu\text{L}$ , 0.25 mmol, 1.25 eq) was added to the mixture to oxidize the phosphine and generate  $\text{TCEP}^{16}\text{O}$ . Finally, 20  $\mu\text{L}$  of this solution was added to 1000  $\mu\text{L}$  of milliQ water before the analysis by HPLC-MS. The results of this analysis are provided in Figure S32. It shows two peaks centered at 2 min and 2.3 min. The mass analysis of these peaks matches the expected structure.

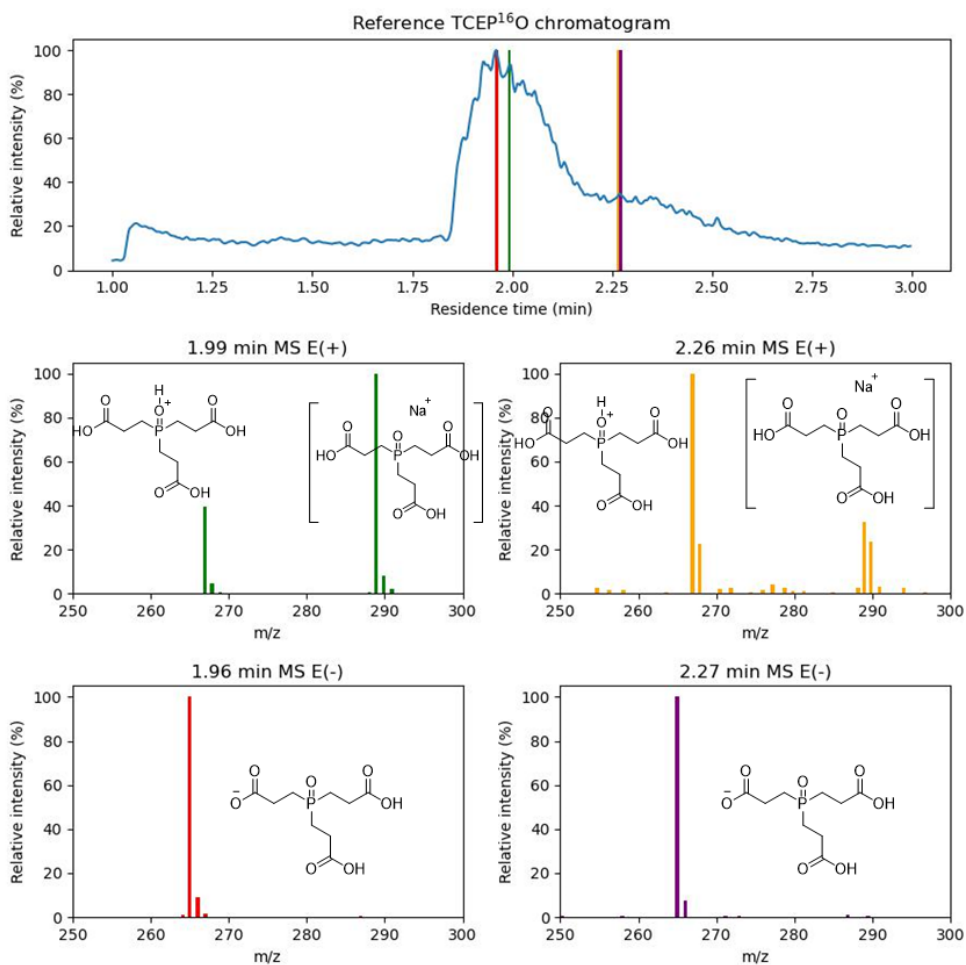


Figure S32. Reference chromatogram of  $\text{TCEP}=\text{O}$  with the representative mass spectra (positive and negative modes) of the two signals (1.97 min and 2.26 min)

#### 5.13.2. Isotopic labeling for CdTe QDs synthesis

The isotopic labeling experiment aimed to determine whether water serves as the oxygen source for the  $\text{TCEP}=\text{O}$  formation, a side product detected during the  $\text{CdTe}$  synthesis. The reaction was therefore conducted in  $\text{H}_2^{18}\text{O}$ , with all solutions saturated with argon and kept under an inert atmosphere.

A 0.2 M aqueous solution of  $\text{TCEP}$  was prepared by dissolving  $\text{TCEP.HCl}$  (0.0573 g, 0.2 mmol, 1 equiv.) and  $\text{NaOH}$  (0.03 g, 0.75 mmol, 3.75 equiv.) with 1 g of  $\text{H}_2^{18}\text{O}$ . The solution was

prepared in a 10 mL flask under argon. Then, **Te** was added (0.0510 g, 0.4 mmol, 2 equiv.) and the solution was stirred for 30 min. The product of the reaction (**TCEP=Te**) was extracted, filtered through a 0.2  $\mu\text{m}$  membrane, and then added to the cadmium precursor solution.

The cadmium precursor solution was prepared by dissolving **Cd(OAc)<sub>2</sub>** (0.0533 g, 0.2 mmol, 1 equiv.), **3-MPA** (0.0531 g, 0.5 mol, 2.5 equiv.), and **NaOH** (0.05 g, 1.25 mmol, 6.25 equiv.) with 1 g of **H<sub>2</sub><sup>18</sup>O**. The solution was purged with argon in a 10 mL flask for 15 min before adding **TCEP=Te**.

The resulting mixture is heated up to 85 °C overnight. The product obtained is a dark viscous liquid that is filtered through a 0.2  $\mu\text{m}$  membrane, leading to a yellowish liquid. 350  $\mu\text{L}$  of this crude is mixed with 350  $\mu\text{L}$  of ethanol, mixed, and centrifugated at 10 000 rpm for 5 min. 50  $\mu\text{L}$  of the supernatant is diluted with 1000  $\mu\text{L}$  of milliQ water and then analyzed by HPLC-MS. The results are shown in Figure S33. The signal at 1.92 min was analyzed and exhibited the same molecular ions but shifted by 2 units compared to Figure S32.

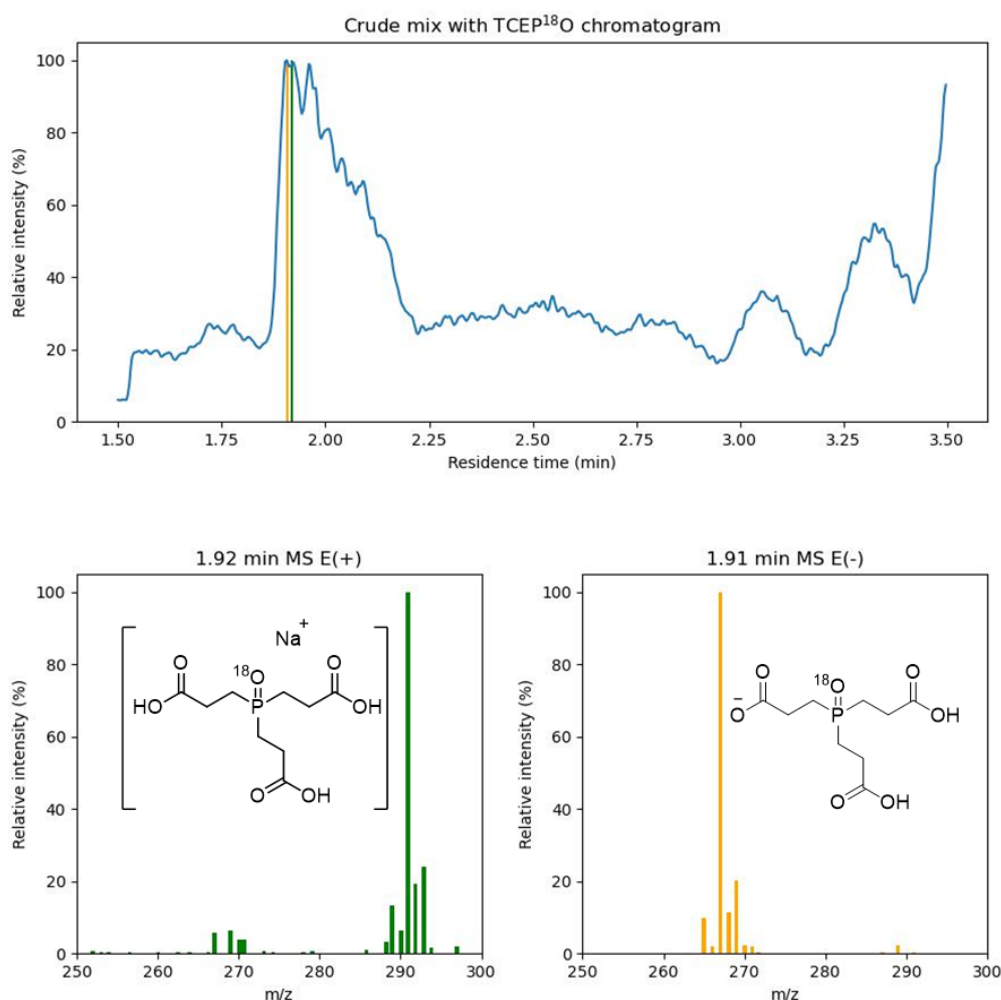


Figure S33. Chromatogram of the **CdTe** QDs crude supernatant with the representative mass spectra (positive and negative modes) of the signal at 1.91 min.

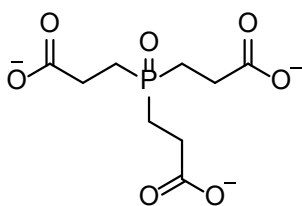
### 5.13.3. HPLC-MS method

HPLC-MS analysis were performed with a Shimadzu LCMS-2020 Single Quadrupole MS equipped with a column C18 (100 x 4.6 mm, 3  $\mu$ m) at 40 °C. A gradient of eluent A (0.1% formic acid in H<sub>2</sub>O, v:v) and B (acetonitrile) was performed

- Eluent: A: 0.1% formic acid in H<sub>2</sub>O; B: Acetonitrile
- Total flow rate: 1 mL min<sup>-1</sup>
- Gradient of the eluents:

<b>Time [min]</b>	<b>A[%]</b>	<b>B[%]</b>
<b>0.00</b>	100	0
<b>10.00</b>	30	70
<b>30.00</b>	20	80
<b>33.00</b>	0	100

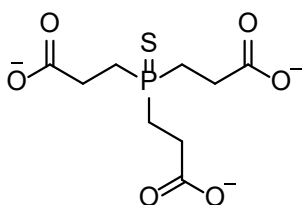
## 5.14. Compounds characterization



$C_9H_{12}O_7P^{3-}$   
MW = 263.163

### 3,3',3''-(oxo- $\lambda^5$ -phosphanetriyl)tripropionate (TCEP=O)

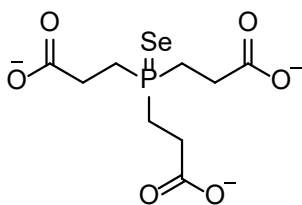
$^1H$  NMR (400 MHz,  $D_2O$ ):  $\delta$  2.48 – 2.27 (m, 2H), 2.20 – 1.98 (m, 2H).  $^{13}C$  NMR (101 MHz,  $D_2O$ ):  $\delta$  180.33 (d,  $J$  = 15.1 Hz), 28.73 (d,  $J$  = 3.5 Hz), 23.22 (d,  $J$  = 65.5 Hz).  $^{31}P$  NMR (162 MHz,  $D_2O$ ):  $\delta$  58.78.



$C_9H_{12}O_6PS^{3-}$   
MW = 279.224

### 3,3',3''-(thioxo- $\lambda^5$ -phosphanetriyl)tripropionate (TCEP=S)

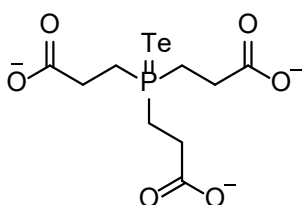
$^1H$  NMR (400 MHz,  $D_2O$ ):  $\delta$  2.52 – 2.40 (m, 2H), 2.29 – 2.16 (m, 2H).  $^{13}C$  NMR (101 MHz,  $D_2O$ ):  $\delta$  180.37 (d,  $J$  = 15.9 Hz), 29.79 (d,  $J$  = 3.4 Hz), 26.09 (d,  $J$  = 50.8 Hz).  $^{31}P$  NMR (162 MHz,  $D_2O$ ):  $\delta$  52.65.



$C_9H_{12}O_6PSe^{3-}$   
MW = 326.136

### 3,3',3''-(selenoxo- $\lambda^5$ -phosphanetriyl)tripropionate

(TCEP=Se).  $^1H$  NMR (400 MHz,  $D_2O$ ):  $\delta$  2.52 – 2.40 (m, 1H), 2.38 – 2.27 (m, 2H).  $^{13}C$  NMR (101 MHz,  $D_2O$ ):  $\delta$  180.17 (d,  $J$  = 16.3 Hz), 30.56 (d,  $J$  = 3.2 Hz), 25.85 (d,  $J$  = 44.4 Hz).  $^{31}P$  NMR (162 MHz,  $D_2O$ )  $\delta$  43.42, 41.47, 39.52 ppm.  $^{77}Se$  NMR (76 MHz,  $D_2O$ ):  $\delta$  -391.09 (d,  $J$  = 630.1 Hz). The NMR data matched those reported in the literature. <sup>57</sup>



$C_9H_{12}O_6PTe^{3-}$   
MW = 374.764

### 3,3',3''-(telluroxo- $\lambda^5$ -phosphanetriyl)tripropionate (TCEP=Te).

$^1H$  NMR (400 MHz,  $D_2O$ ):  $\delta$  2.42 – 2.23 (m, 2H), 2.23 – 2.09 (m, 2H).  $^{13}C$  NMR (101 MHz,  $D_2O$ ):  $\delta$  180.57 (d,  $J$  = 15.4 Hz), 32.53, 24.88 (d,  $J$  = 26.5 Hz).  $^{31}P$  NMR (162 MHz,  $D_2O$ ):  $\delta$  -9.65.

## 5.15. Copy of the spectra (NMR, Raman or UV/Vis, photoluminescence)

### 5.15.1. TCEP

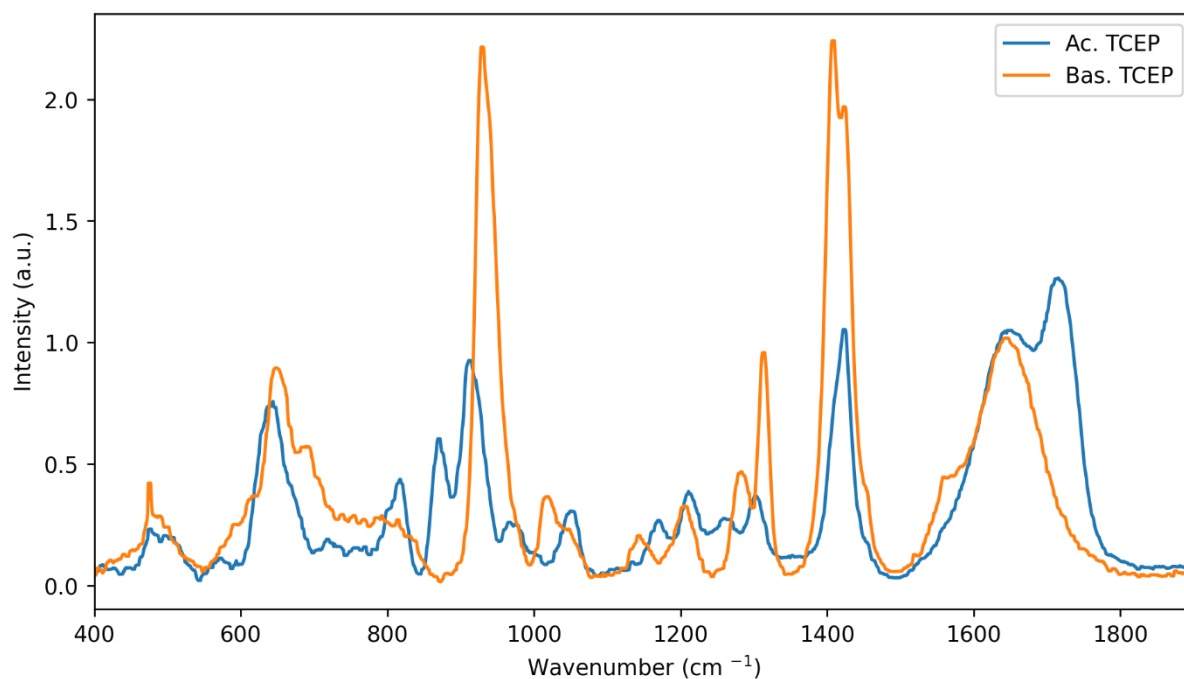


Figure S34. Reference Raman spectra for acidic and basic TCEP, (a.u. = arbitrary units)

### 5.15.2. TCEP=O

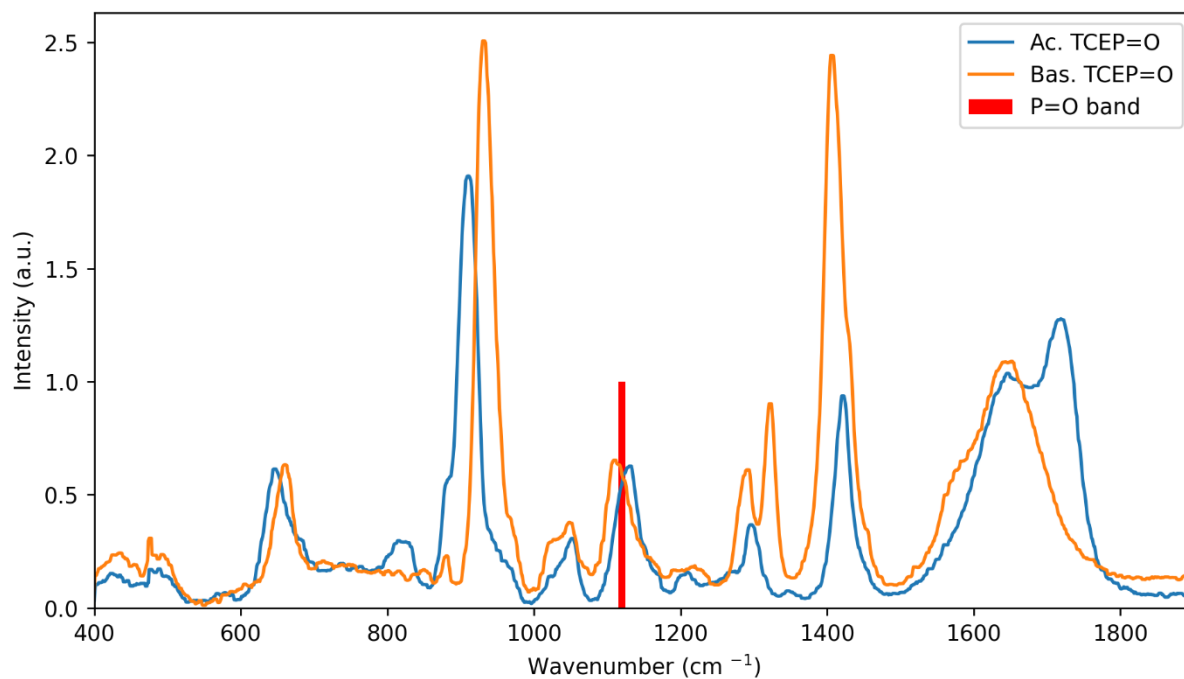


Figure S35. Reference Raman spectra for acidic and basic TCEP=O, (a.u. = arbitrary units)

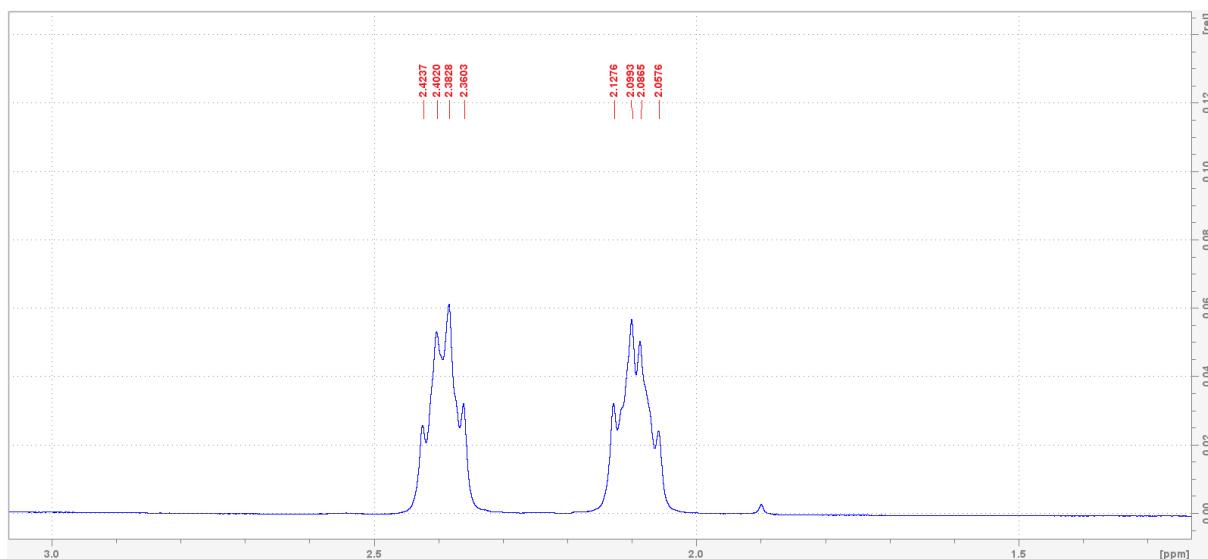


Figure S36:  $^1\text{H}$  NMR (400 MHz,  $\text{D}_2\text{O}$ ), of TCEP=O

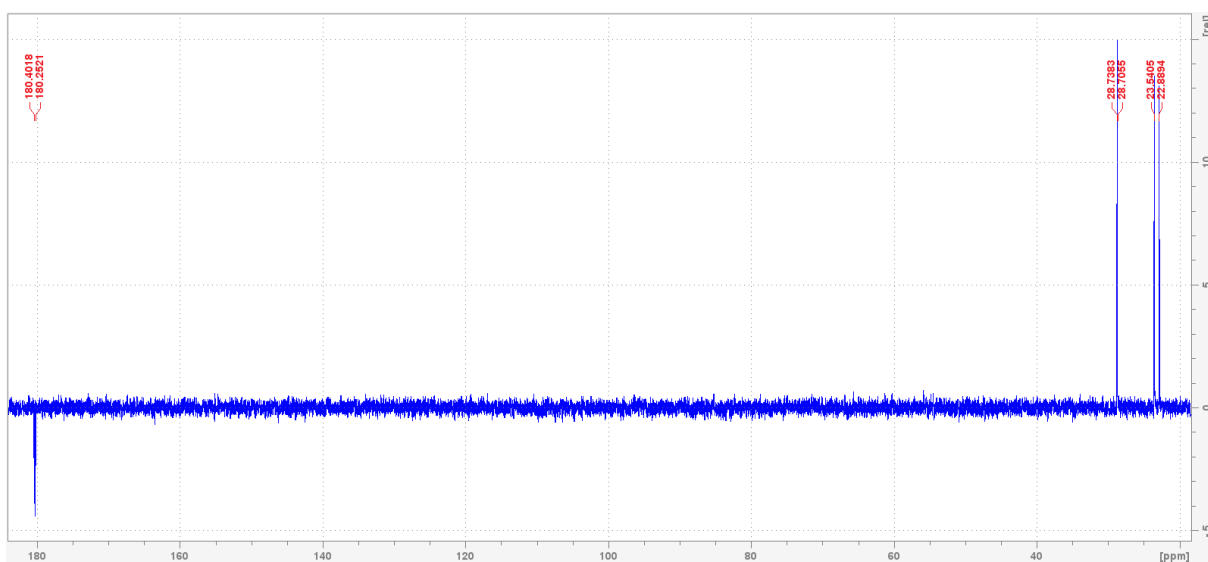


Figure S37.  $^{13}\text{C}$  NMR (101 MHz,  $\text{D}_2\text{O}$ ) of TCEP=O

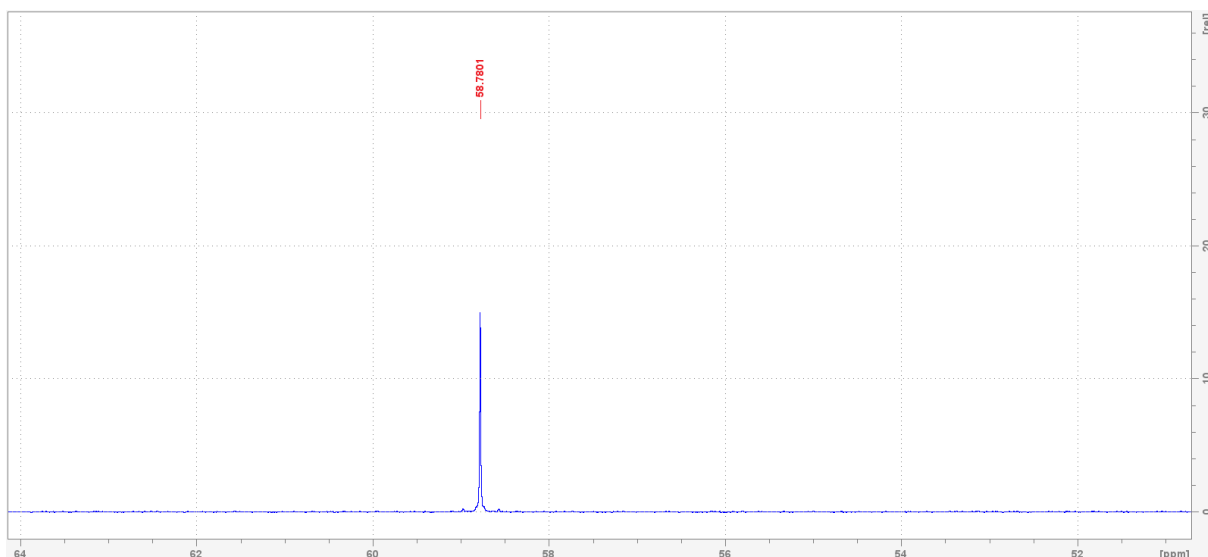


Figure S38.  $^{31}\text{P}$  NMR (162 MHz,  $\text{D}_2\text{O}$ ) of TCEP=O

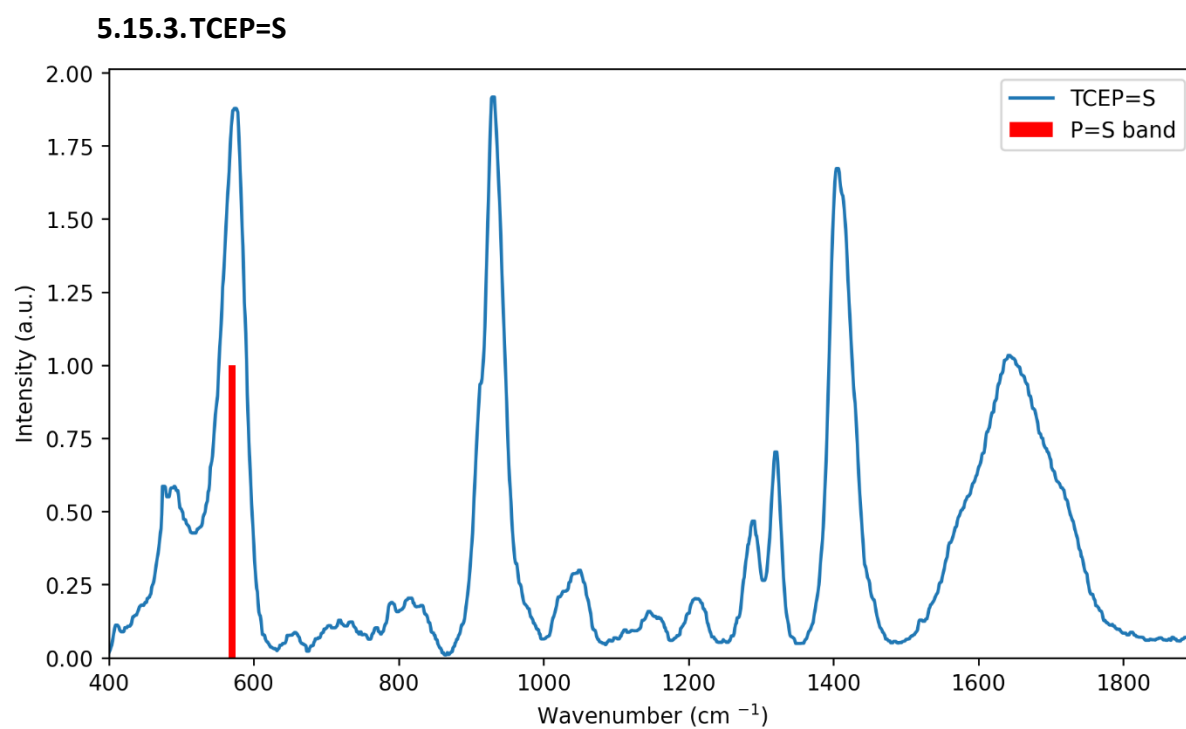


Figure S39. Reference Raman spectrum for TCEP=S, (a.u. = arbitrary units)

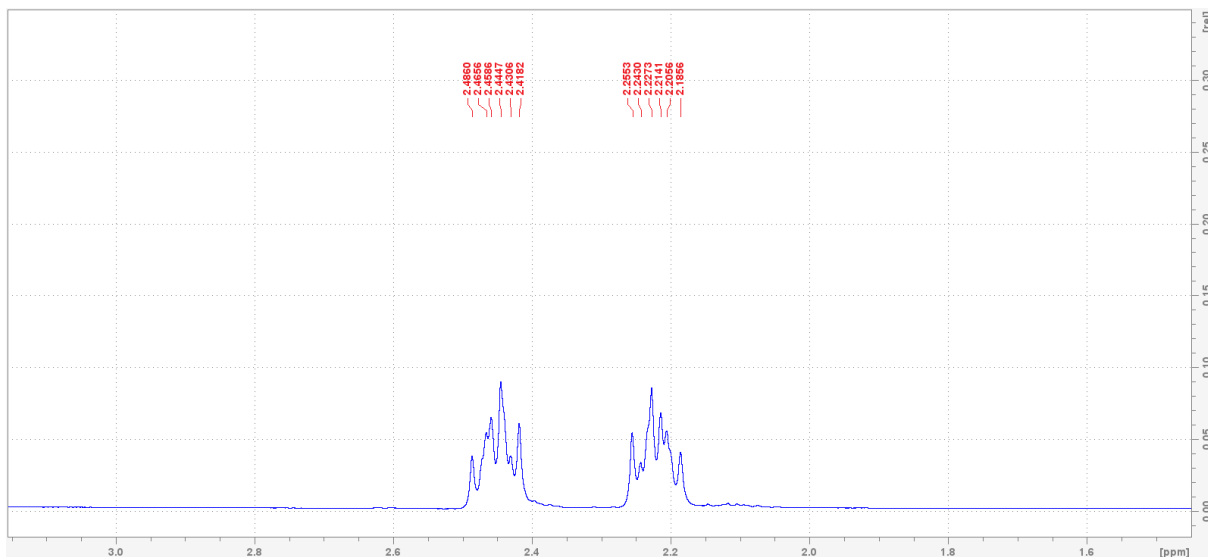


Figure S40.  $^1\text{H}$  NMR (400 MHz,  $\text{D}_2\text{O}$ ), of TCEP=S

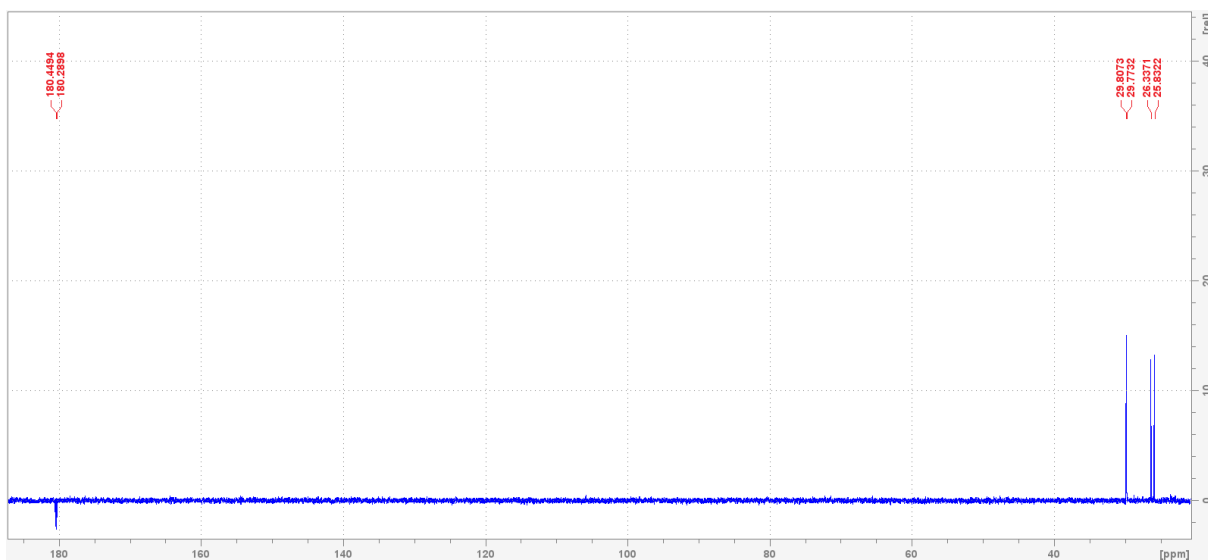


Figure S41.  $^{13}\text{C}$  NMR (101 MHz,  $\text{D}_2\text{O}$ ) of TCEP=S



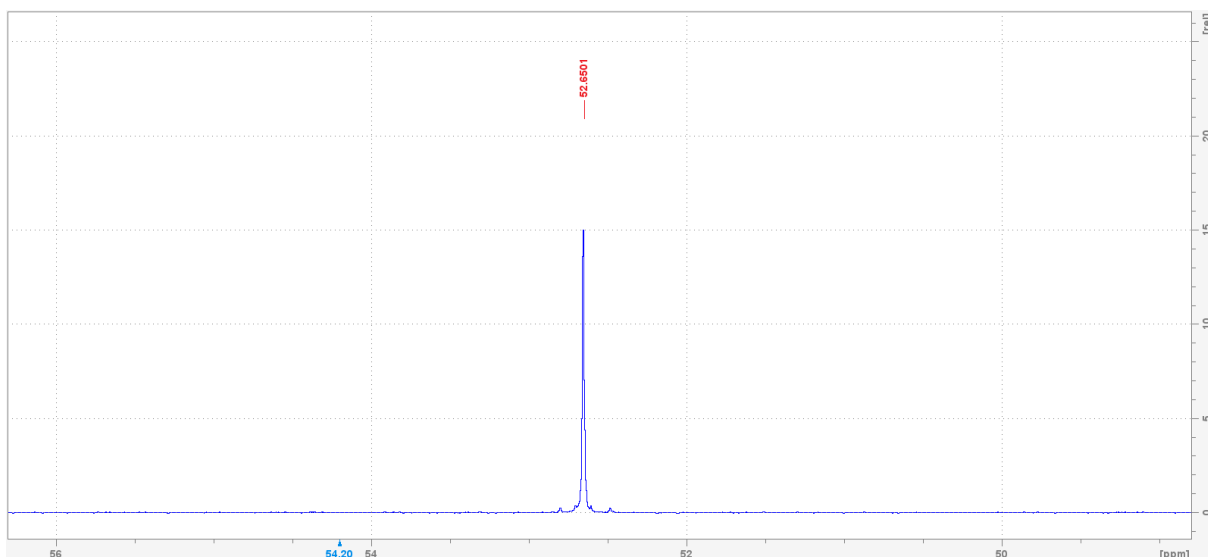


Figure S42.  $^{31}\text{P}$  NMR (162 MHz,  $\text{D}_2\text{O}$ ) of TCEP=S

#### 5.15.4. TCEP=Se

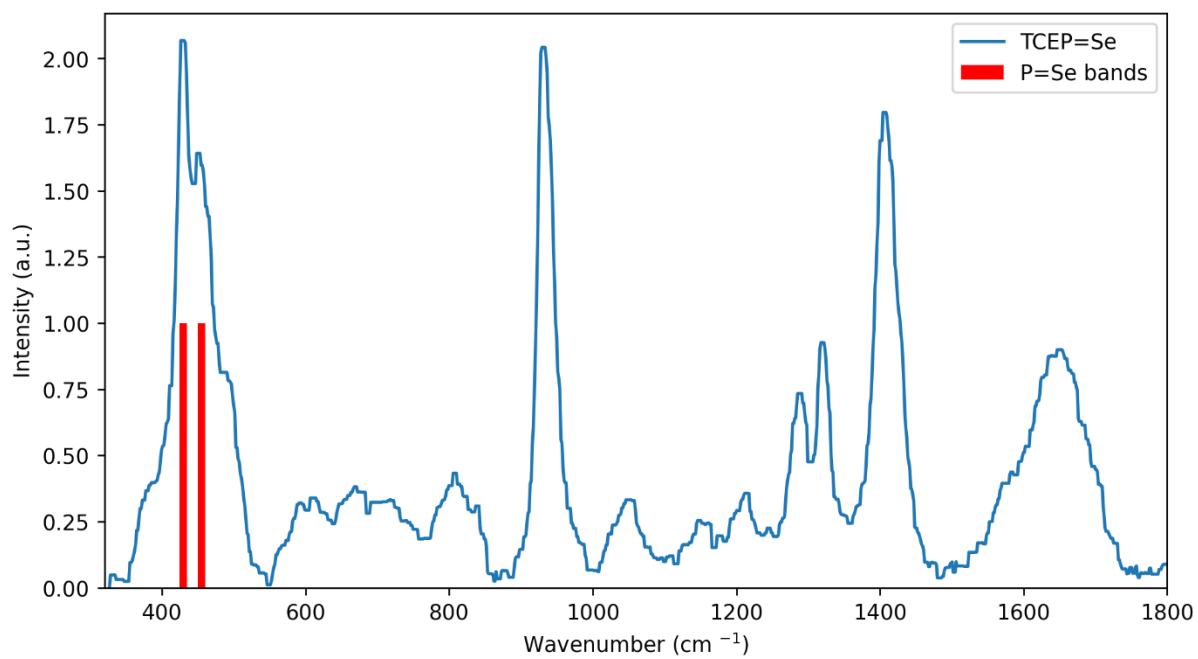


Figure S43. Reference Raman spectrum for TCEP=Se, (a.u. = arbitrary units)

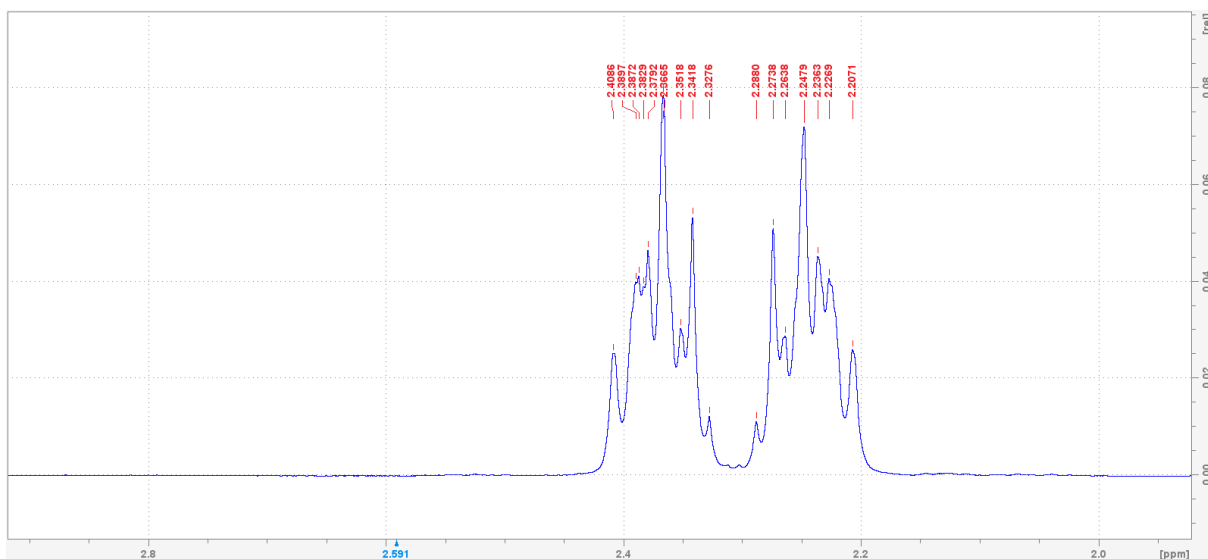


Figure S44.  $^1\text{H}$  NMR (400 MHz,  $\text{D}_2\text{O}$ ) of TCEP=Se

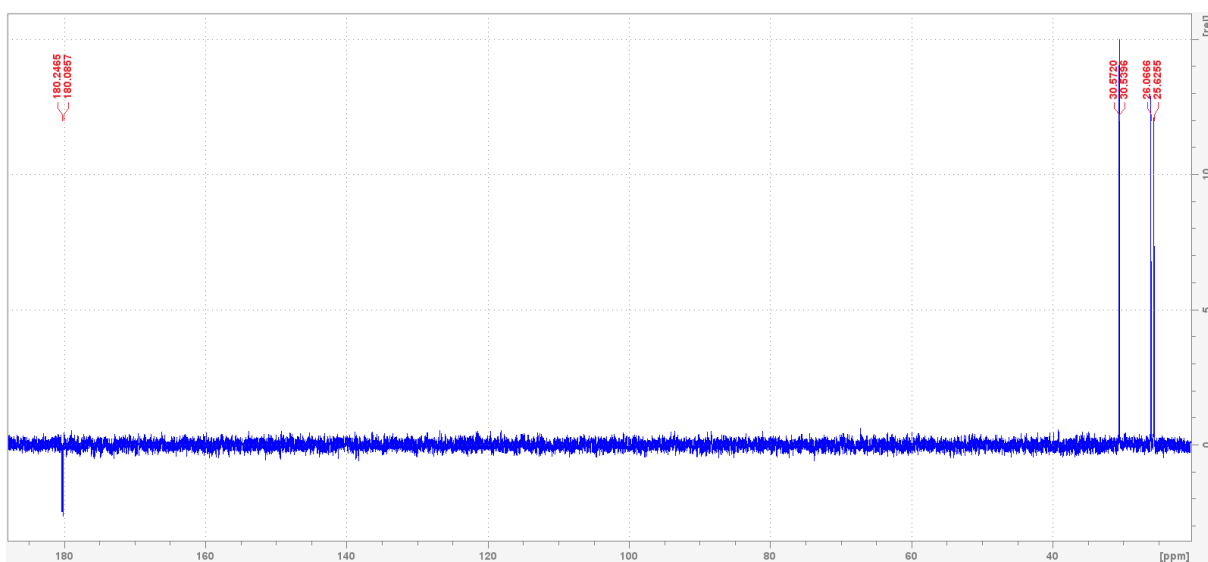


Figure 45.  $^{13}\text{C}$  NMR (101 MHz,  $\text{D}_2\text{O}$ ) of TCEP=Se

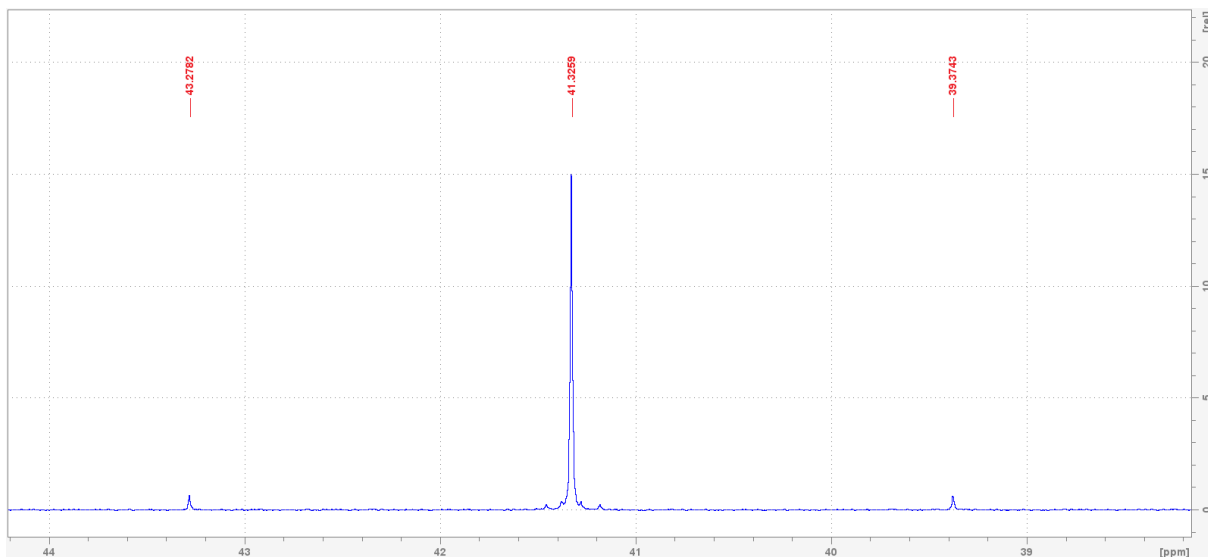


Figure S46.  $^{31}\text{P}$  NMR (162 MHz,  $\text{D}_2\text{O}$ ) of TCEP=Se

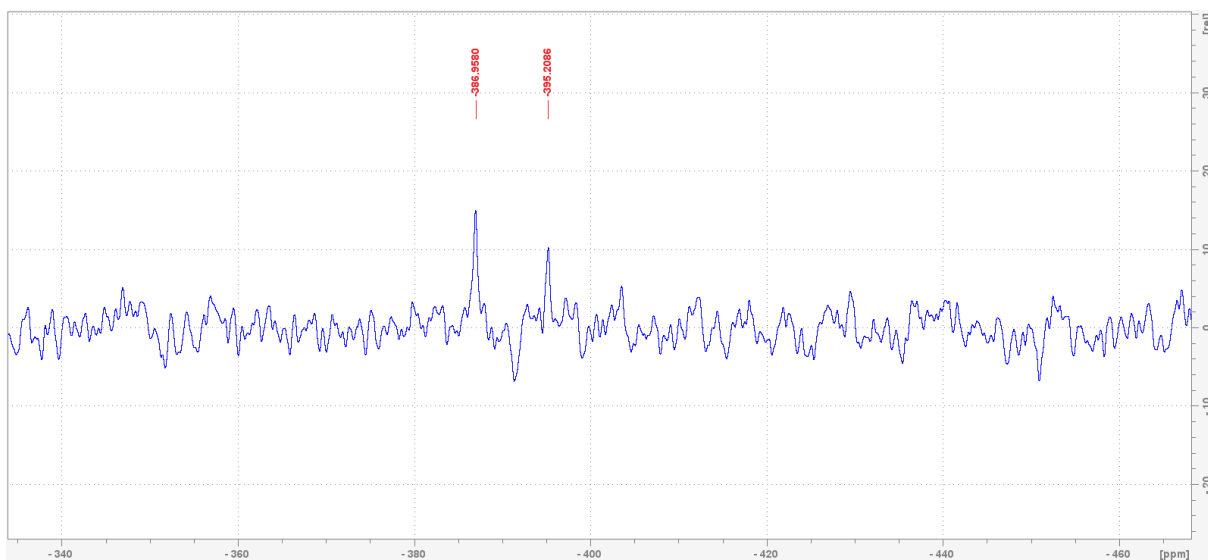


Figure S47.  $^{77}\text{Se}$  NMR (76 MHz,  $\text{D}_2\text{O}$ ) of TCEP=Se

### 5.15.5. TCEP=Te

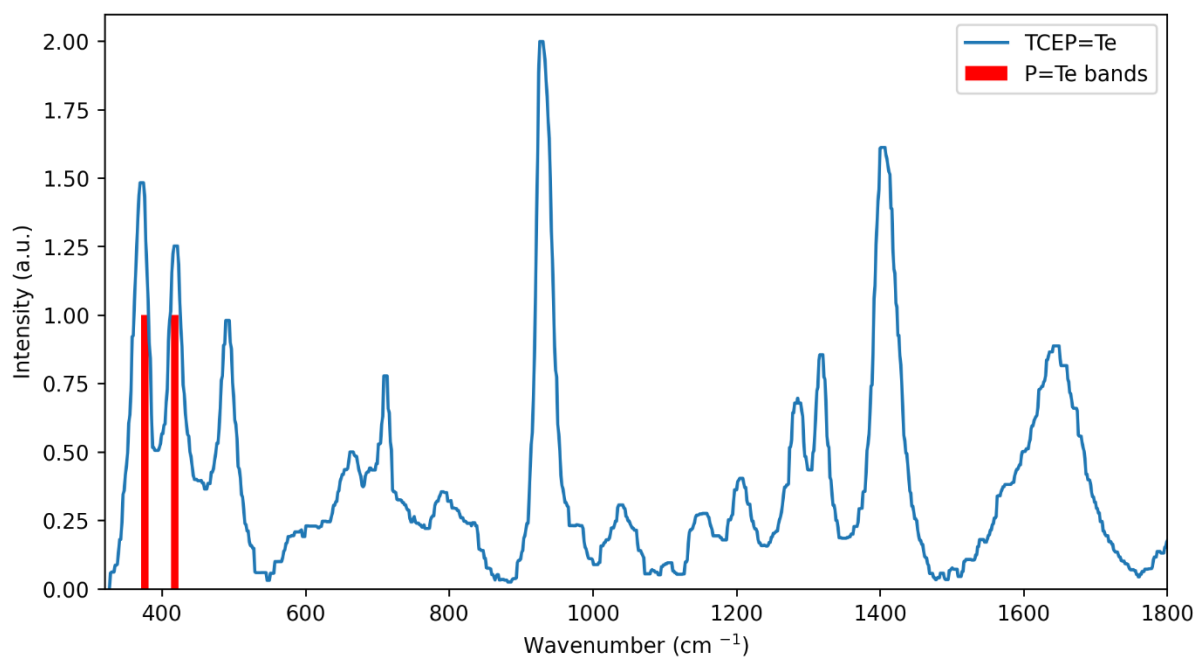


Figure S48. Reference Raman spectrum for TCEP=Te, (a.u. = arbitrary units)

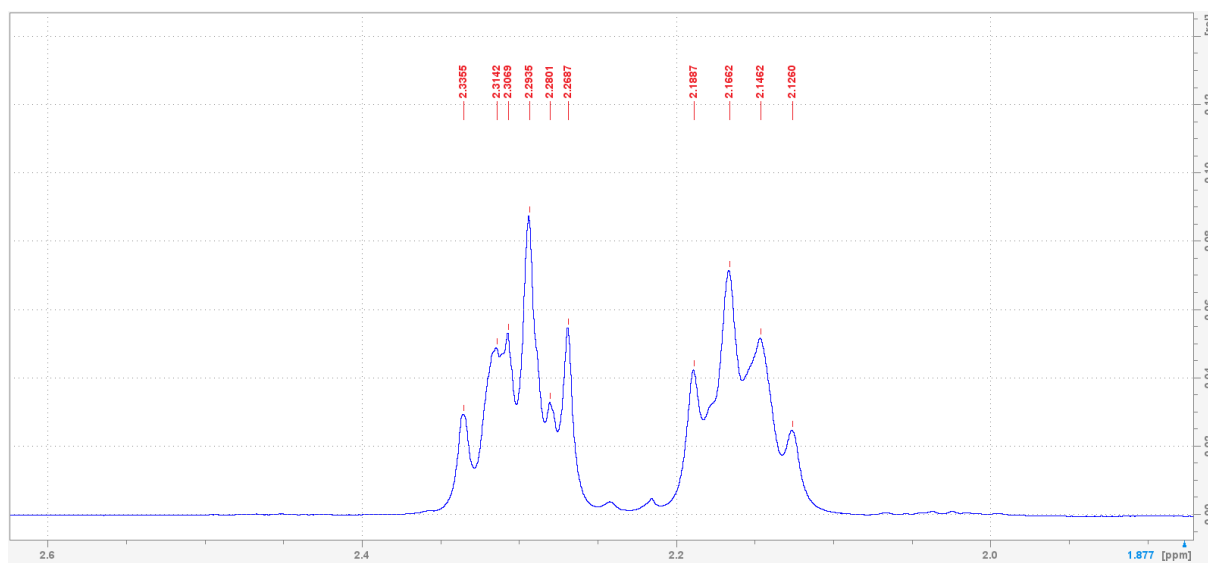


Figure S49. <sup>1</sup>H NMR (400 MHz, D<sub>2</sub>O) of TCEP=Te

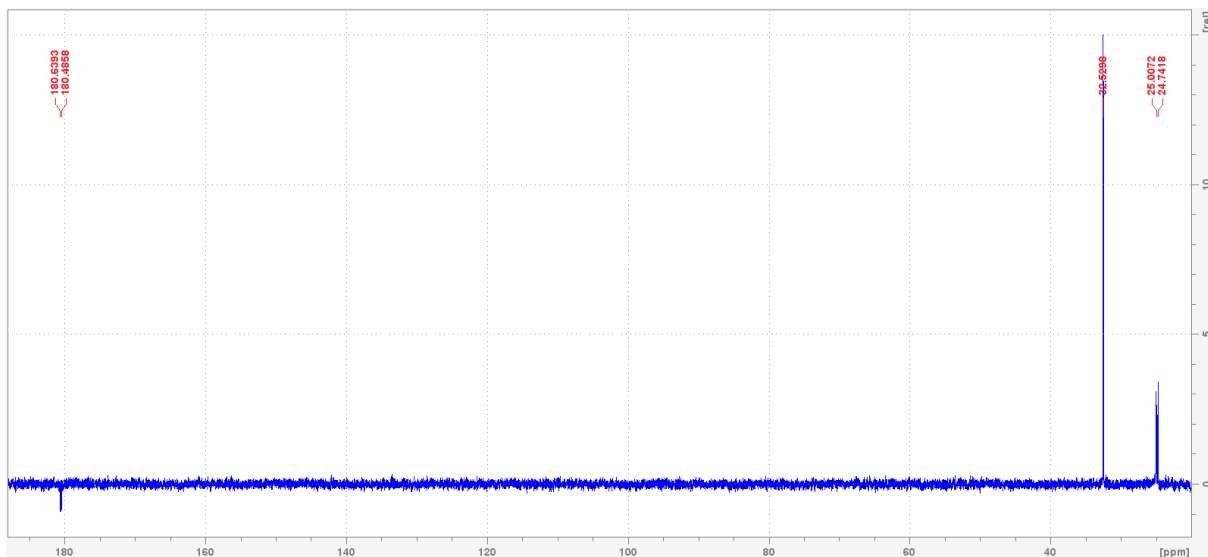


Figure S50.  $^{13}\text{C}$  NMR (101 MHz,  $\text{D}_2\text{O}$ ) of TCEP=Te

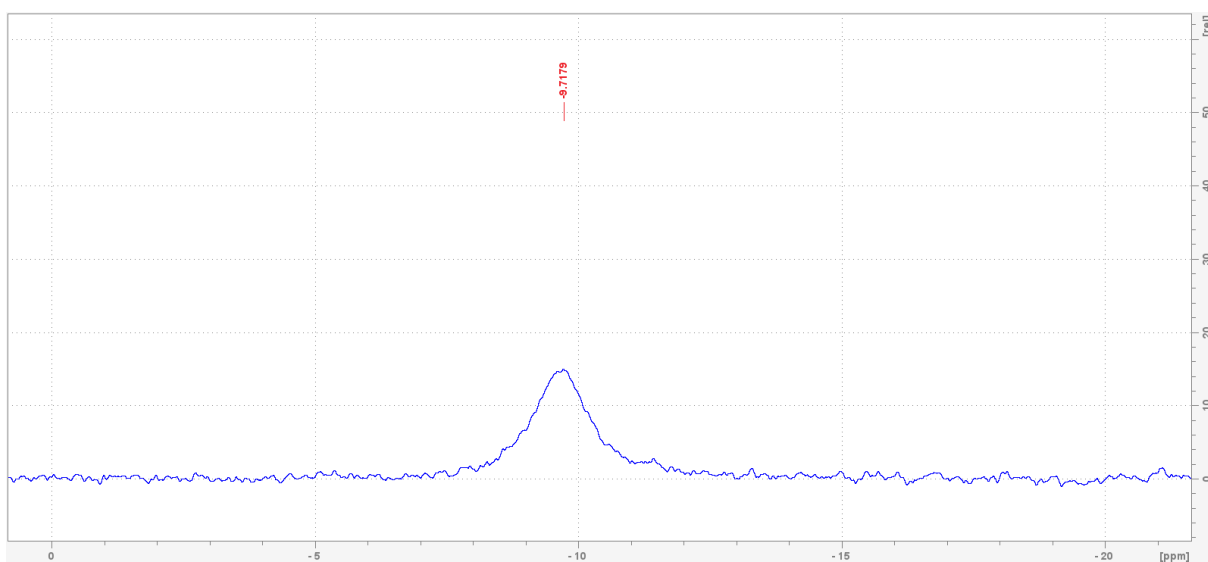


Figure S51.  $^{31}\text{P}$  NMR (162 MHz,  $\text{D}_2\text{O}$ ) of TCEP=Te

### 5.15.6. CdS

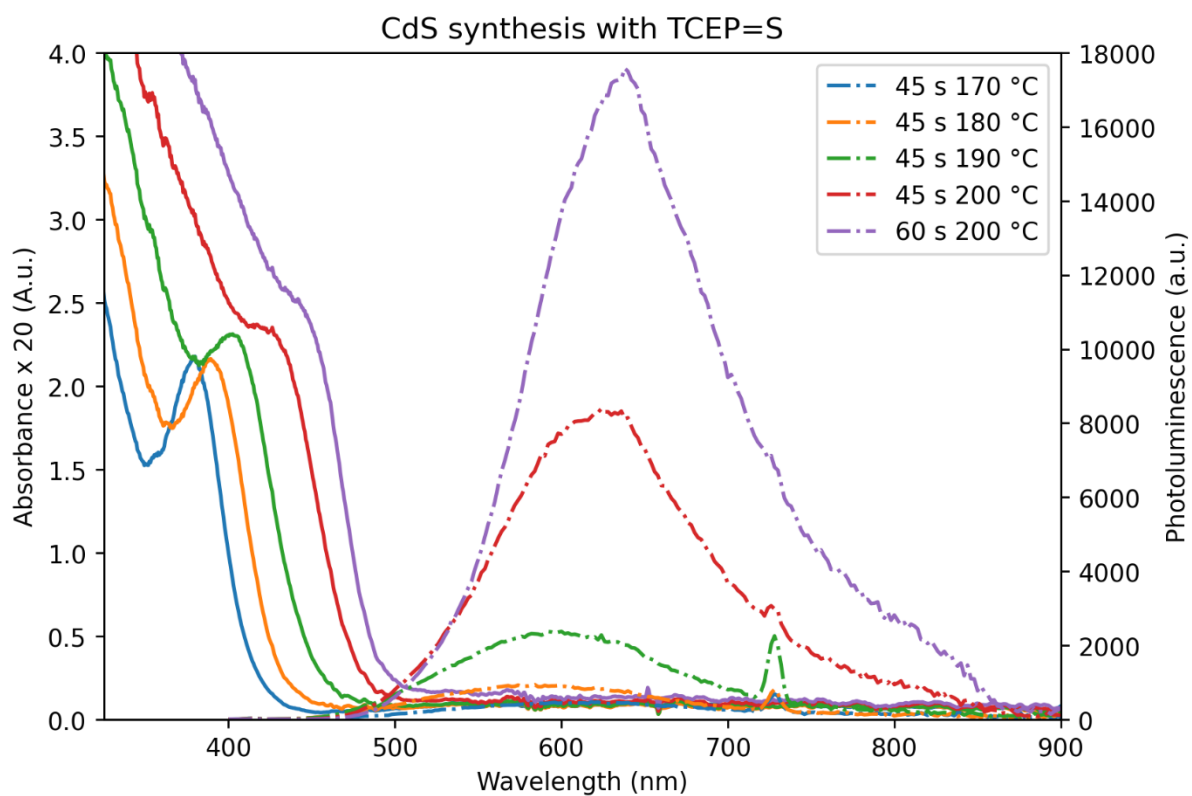


Figure S52. UV/Vis and photoluminescence spectra for the synthesized CdS QDs, (A.u. = Absorbance units, a.u. = arbitrary units)

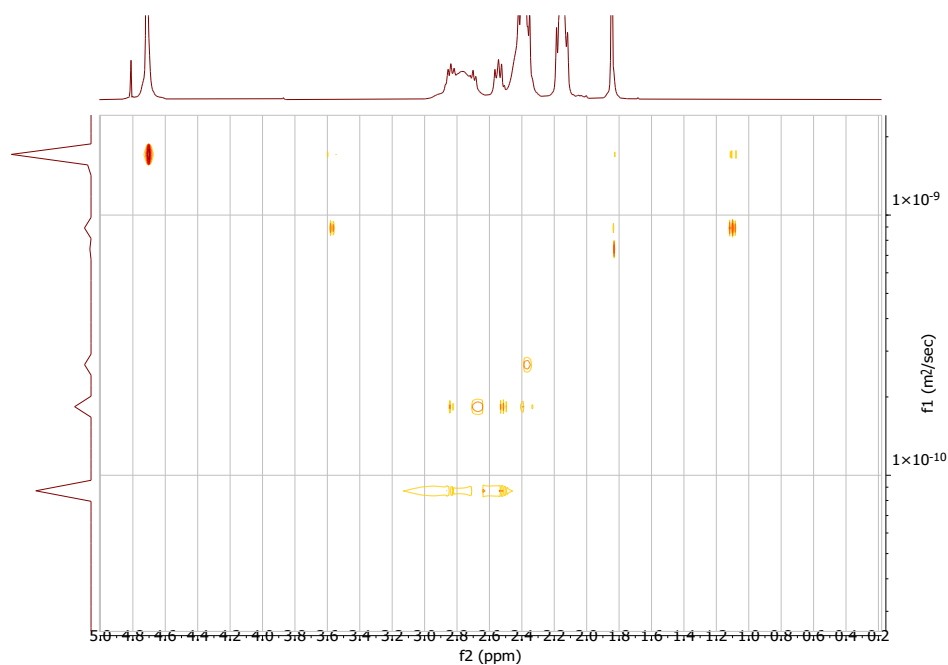


Figure S53. DOSY measurement of CdS QDs

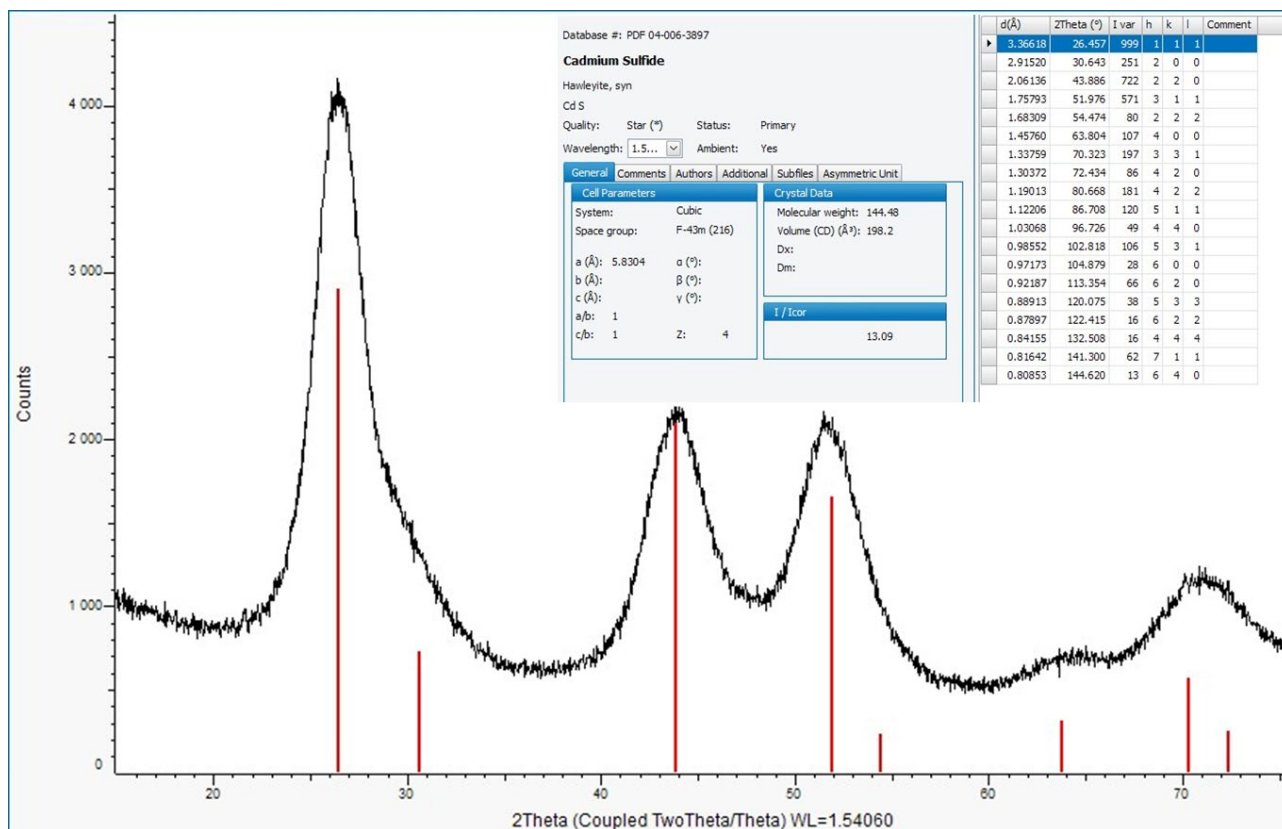


Figure S54. Powder XRD analysis of CdS, tune cell, and its peak references

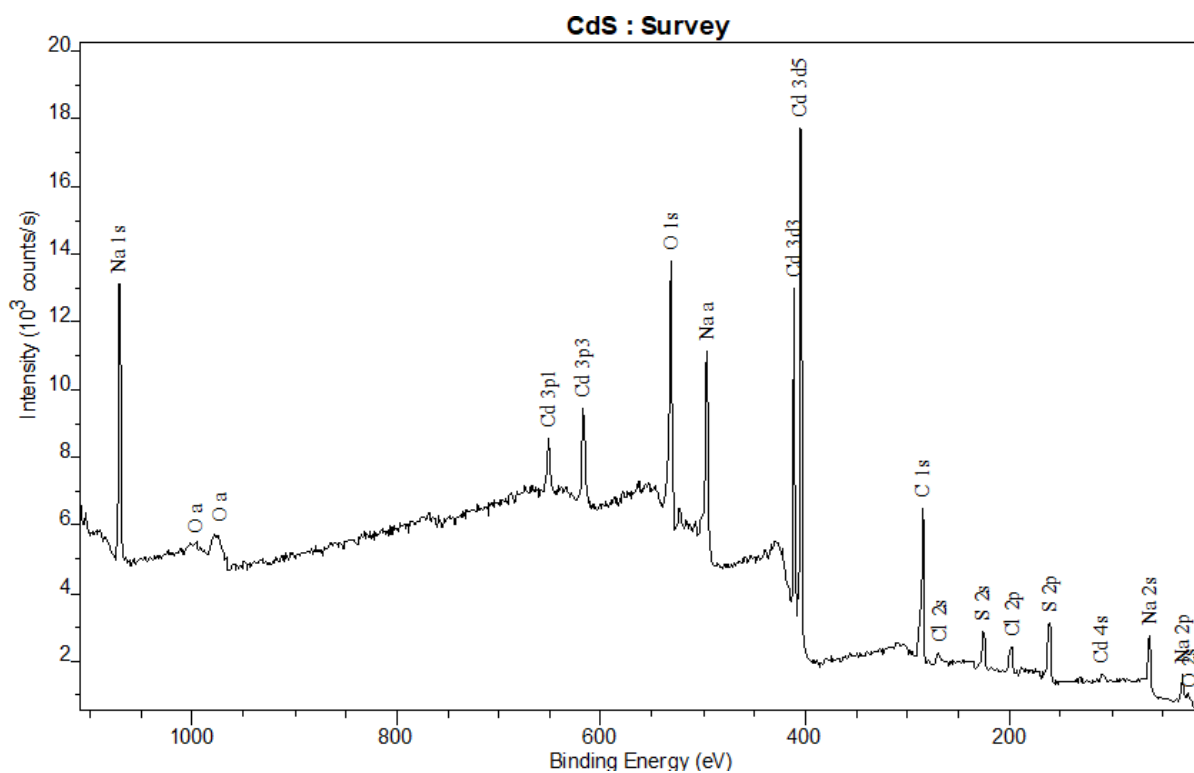


Figure S55. CdS QDs XPS analysis

### 5.15.7. CdSe core

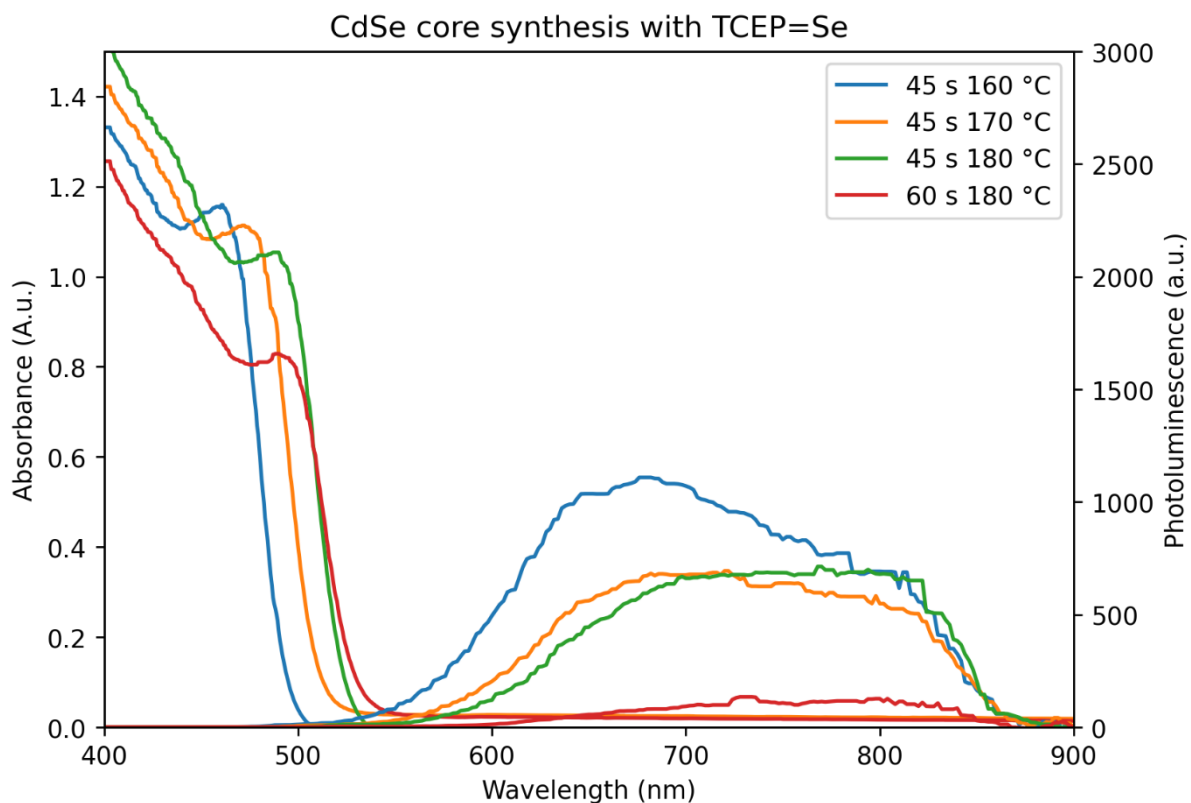


Figure S56. UV/Vis and photoluminescence spectra for the synthesized CdSe QDs, (A.u. = Absorbance units, a.u. = arbitrary units)

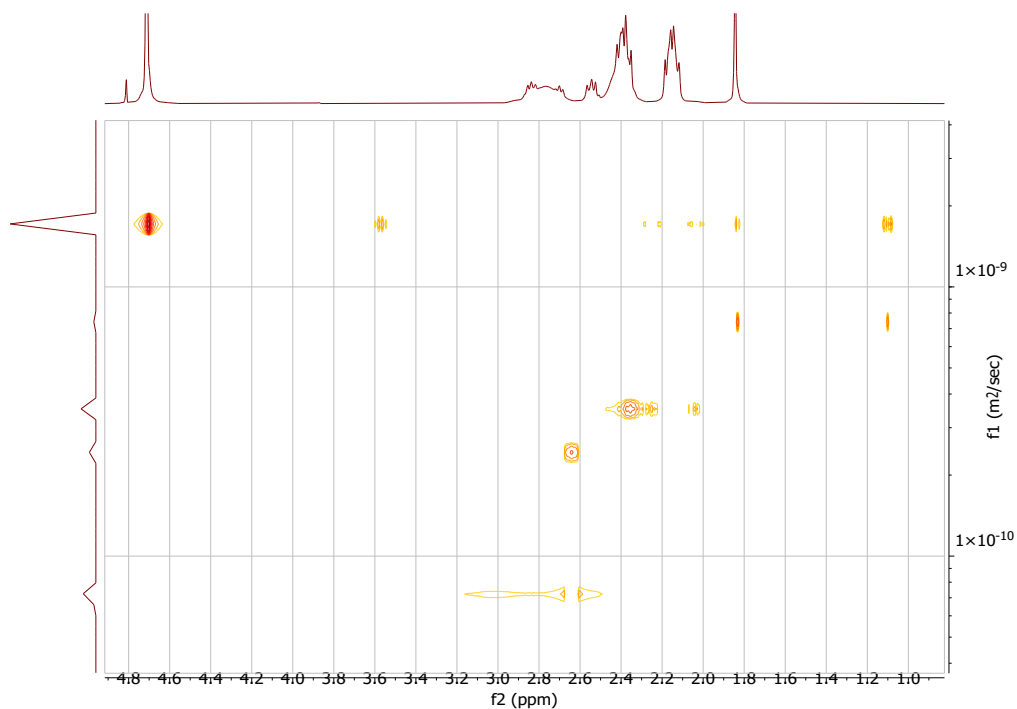
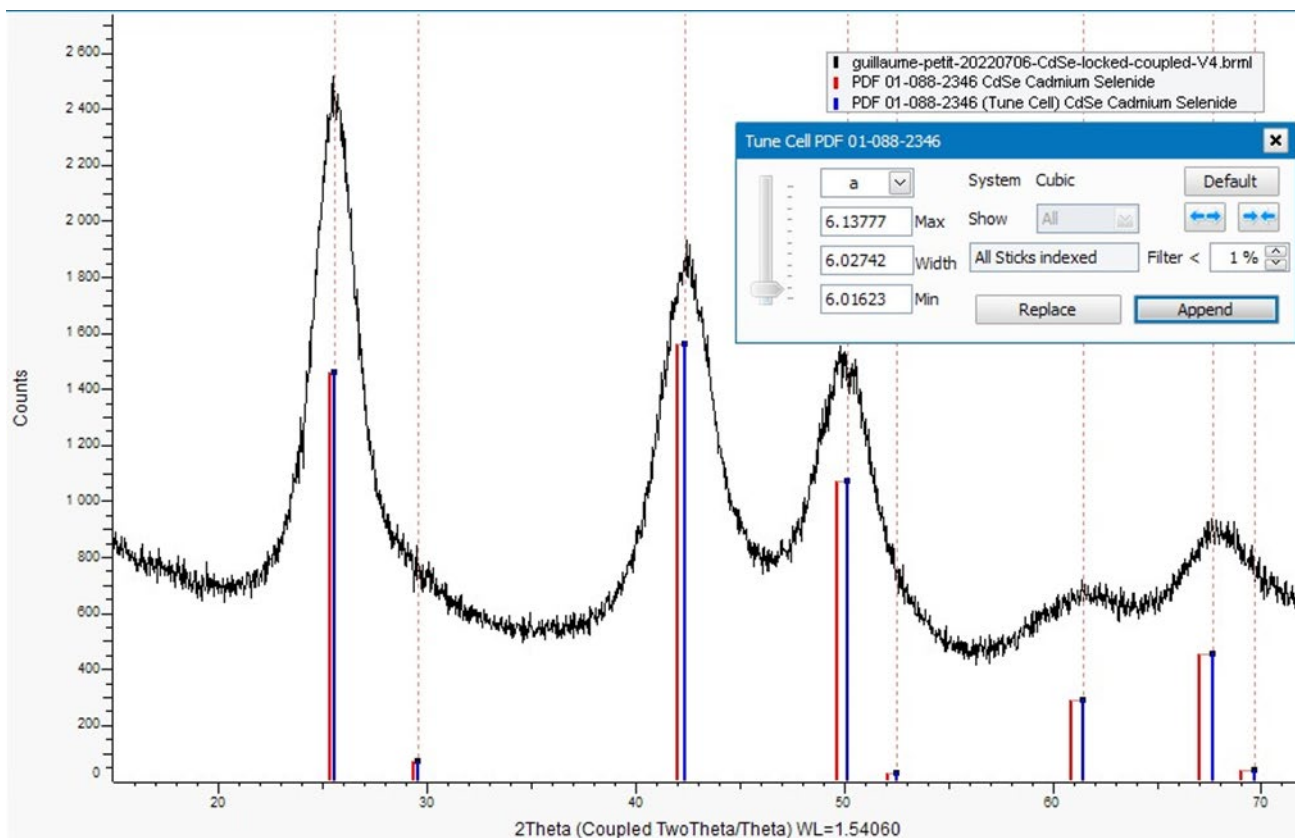


Figure S57. DOSY measurement of CdSe QDs





Database #: PDF 01-088-2346

**Cadmium Selenide**

Cd Se  
 Quality: Indexed Status: Primary  
 Wavelength: 1.5... Ambient: Yes

Cell Parameters		Crystal Data	
System:	Cubic	Molecular weight:	191.37
Space group:	F-43m (216)	Volume (CD) (Å <sup>3</sup> ):	224.42
a (Å):	6.077	Dx:	
b (Å):		Dm:	
c (Å):			
a/b:	1		
c/b:	1	Z:	4
		I / Icor	13.74

d(Å)	2Theta (°)	I var	h	k	l	Comment
3.50856	25.365	934	1	1	1	
3.03850	29.371	46	2	0	0	
2.14854	42.019	1000	2	2	0	
1.83228	49.720	687	3	1	1	
1.75428	52.093	19	2	2	2	
1.51925	60.932	186	4	0	0	
1.39416	67.080	292	3	3	1	
1.35886	69.065	25	4	2	0	
1.24046	76.775	368	4	2	2	
1.16952	82.393	213	5	1	1	
1.07427	91.622	116	4	4	0	
1.02720	97.164	214	5	3	1	
1.01283	99.024	13	6	0	0	
0.96086	106.582	174	6	2	0	
0.92673	112.444	85	5	3	3	
0.91614	114.451	11	6	2	2	
0.87714	122.851	53	4	4	4	
0.85095	129.707	162	5	5	1	
0.84273	132.144	8	6	4	0	
0.81207	143.085	299	6	4	2	

Figure S58. Powder XRD analysis of CdSe, tune cell, and its peak references

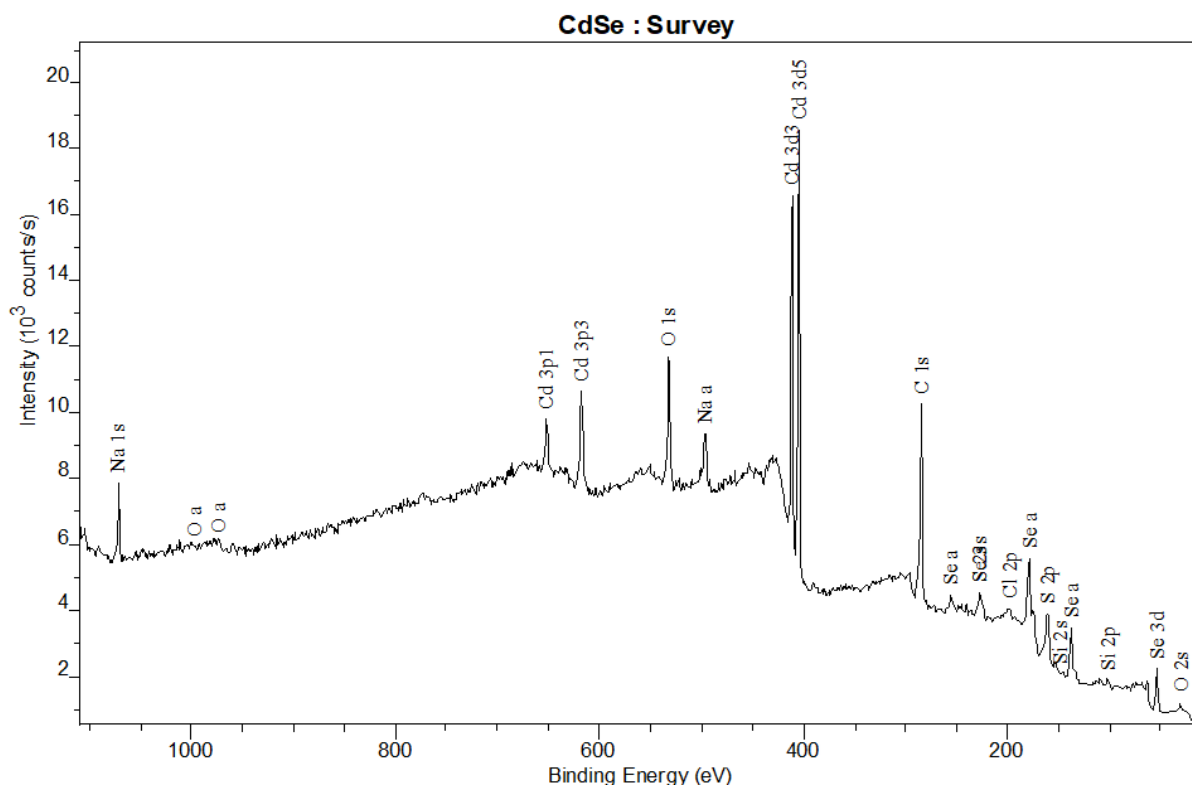


Figure S59. CdSe QDs XPS analysis

### 5.15.8. CdSe/ZnS

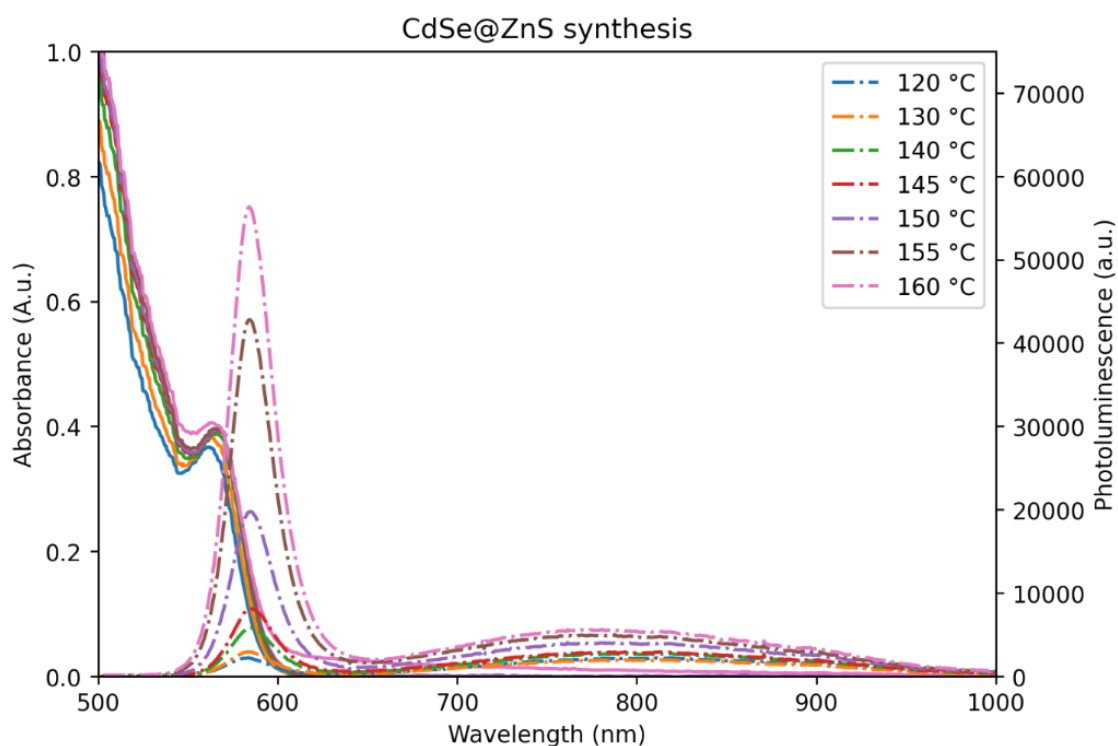


Figure S60. UV/Vis and photoluminescence spectra for the synthesized CdSe/ZnS QDs, (A.u. = Absorbance units, a.u. = arbitrary units)

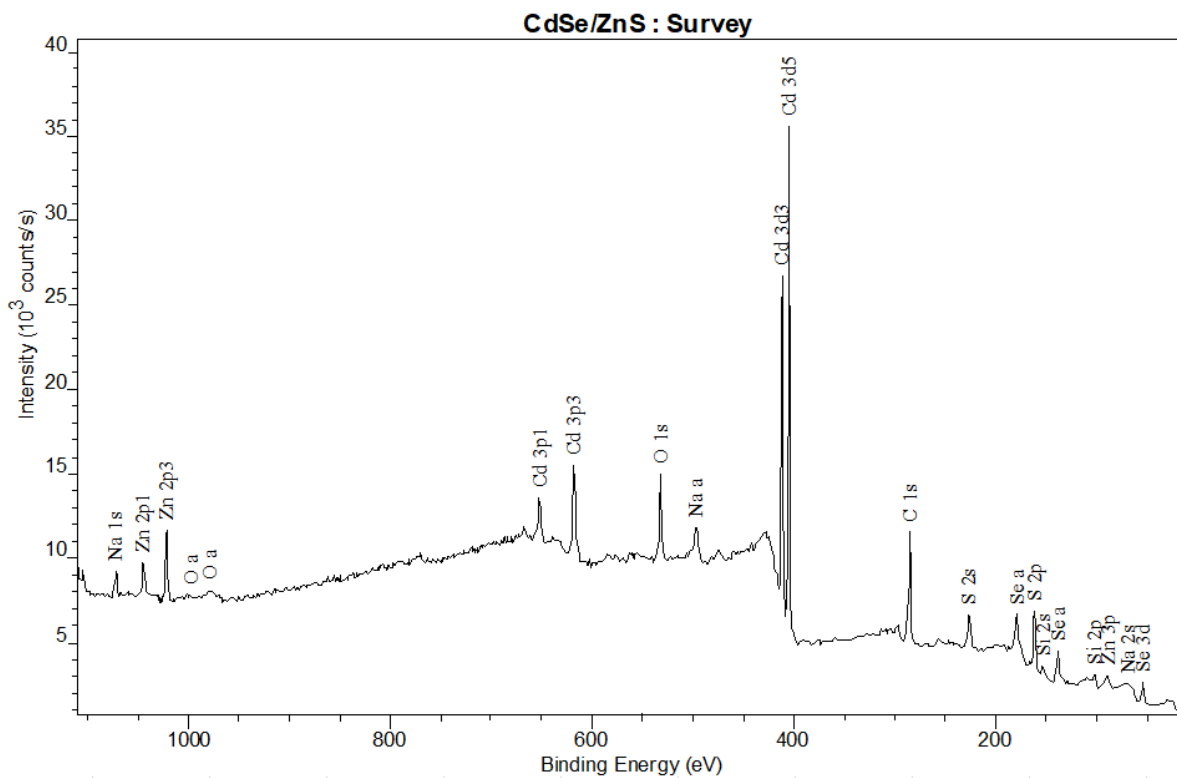


Figure S61. CdSe/ZnS QDs XPS analysis

### 5.15.9. CdTe

- Microfluidic

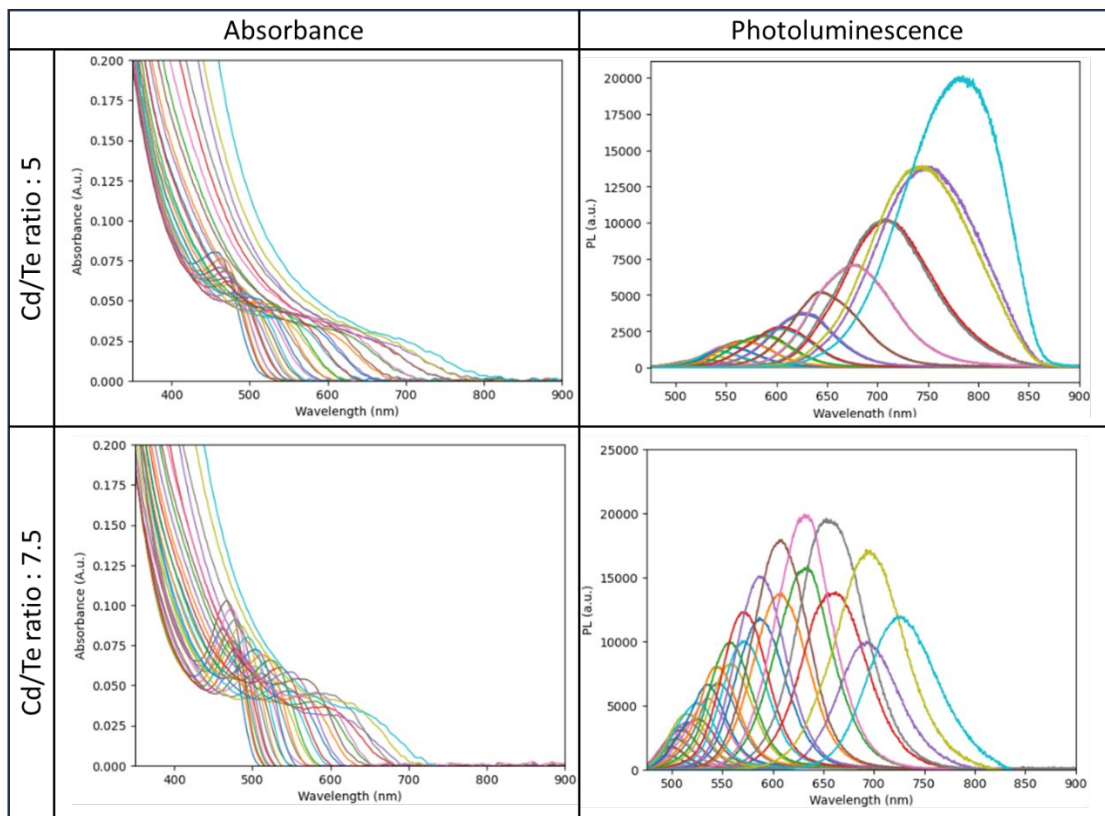
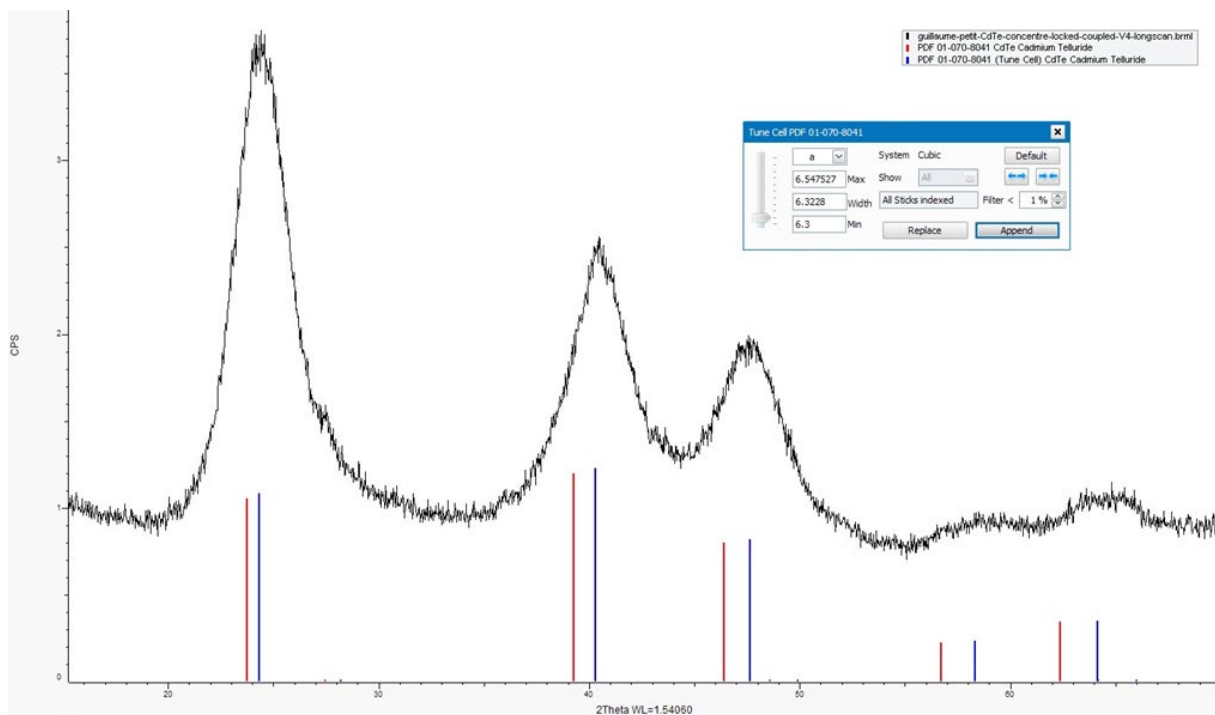


Figure S62. UV/Vis and photoluminescence spectra for the synthesized CdTe QDs, (A.u. = Absorbance units, a.u. = arbitrary units)



Database #: PDF 01-070-8041  
**Cadmium Telluride**  
 Cd Te  
 Quality: Star (\*) Status: Alternate  
 Wavelength: 1.5... Ambient: Yes

Cell Parameters		Crystal Data	
System:	Cubic	Molecular weight:	240.01
Space group:	F-43m (216)	Volume (CD) (Å <sup>3</sup> ):	272.44
a (Å):	6.4827	Dx:	
b (Å):		Dm:	
c (Å):		I / Icor	15.48
a/b:	1	Z:	4
c/b:	1		

d(Å)	2Theta (°)	I var	h	k	l	Comment
3.74279	23.754	881	1	1	1	
3.24135	27.496	3	2	0	0	
2.29198	39.277	999	2	2	0	
1.95461	46.419	668	3	1	1	
1.87139	48.613	2	2	2	2	
1.62067	56.757	190	4	0	0	
1.48723	62.389	286	3	3	1	
1.44958	64.200	5	4	2	0	
1.32328	71.199	371	4	2	2	
1.24760	76.257	201	5	1	1	
1.14599	84.470	110	4	4	0	
1.09578	89.331	187	5	3	1	
1.08045	90.950	4	6	0	0	
1.02500	97.443	148	6	2	0	
0.98860	102.371	67	5	3	3	
0.97730	104.033	4	6	2	2	
0.93570	110.820	39	4	4	4	
0.90776	116.113	113	7	1	1	
0.89899	117.930	4	6	4	0	
0.86629	125.545	202	6	4	2	
0.84398	131.763	153	7	3	1	
0.81034	143.828	25	8	0	0	

Figure S63. Powder XRD analysis of CdTe, tune cell, and its peak references

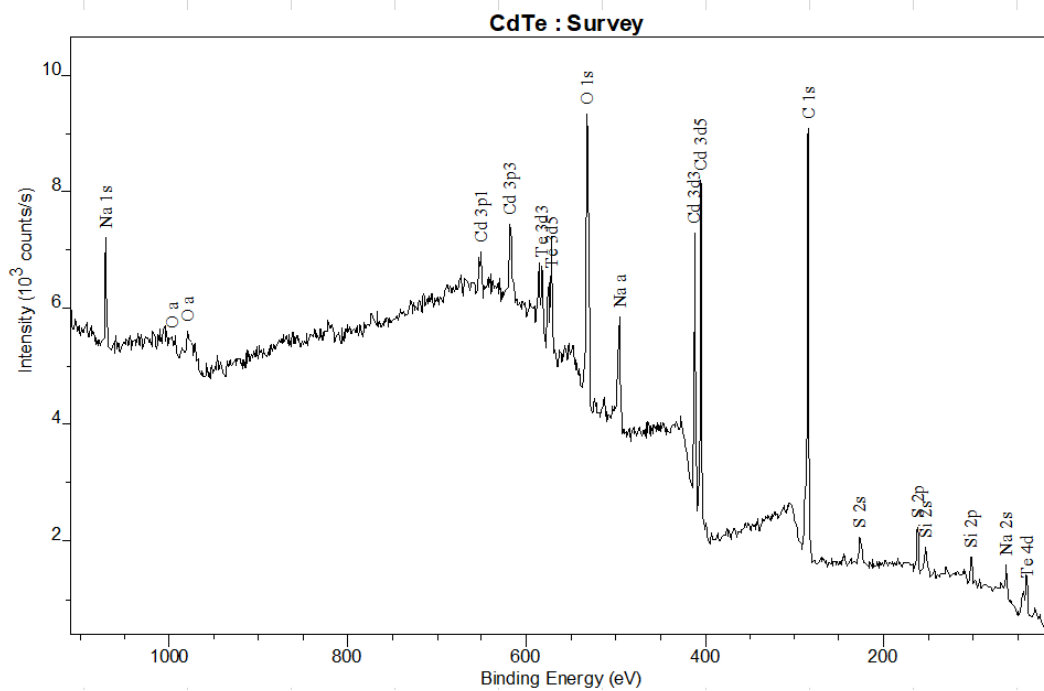


Figure S64. CdTe QDs XPS analysis

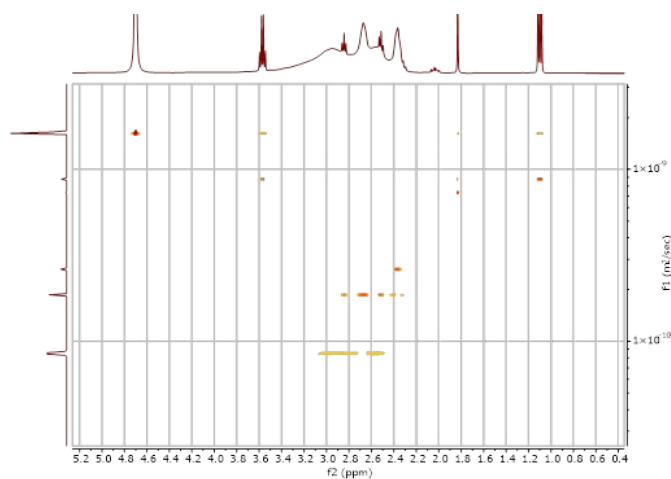


Figure S65. DOSY measurement of CdTe QDs

- Mesofluidic

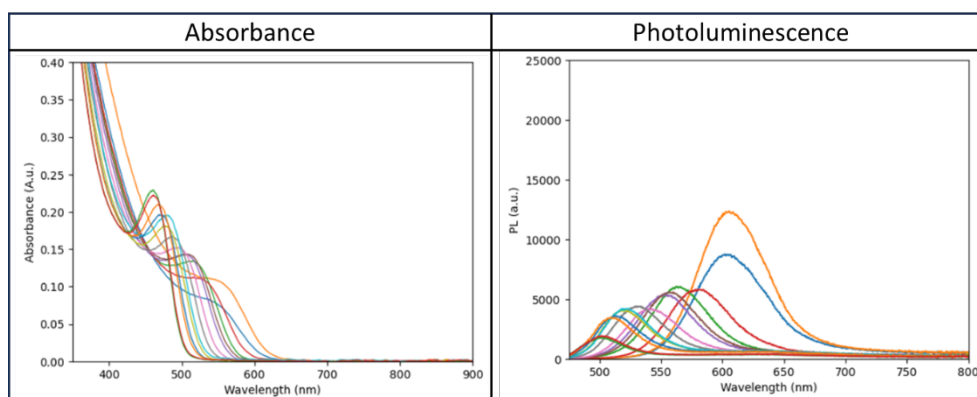


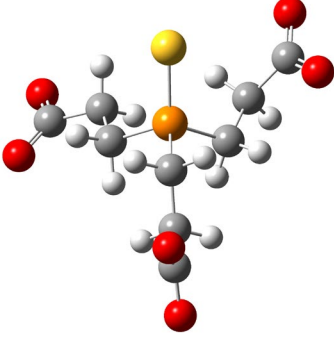
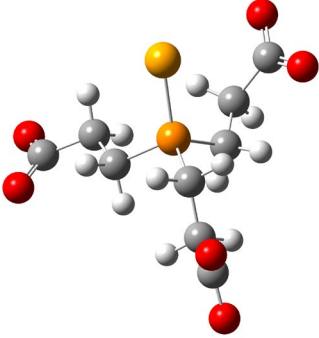
Figure S66. UV/Vis and photoluminescence spectra for the synthesized CdTe QDs, (A.u. = Absorbance units, a.u. = arbitrary units)

### 5.16. DFT calculations

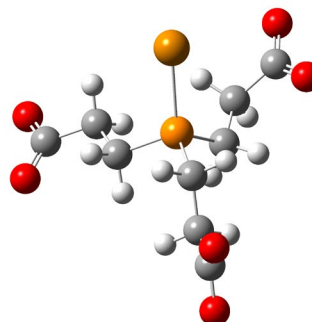
To validate the frequencies impacted by the formation of **TCEP=X** from **TCEP** and their corresponding bond, DFT calculations were performed to simulate Raman spectra. Calculations were performed using the Gaussian 16<sup>S6</sup> package and implicit solvation (SMD, solvent = water). Optimization and characterization with vibrational analysis of the stationary points were carried out at the B3LYP/6-311++ G(d/p) level of theory for C, H, O, P, S, and LANL2DZ for **Se** and **Te**. The Cartesian coordinates of the optimized molecules are provided in Table S5.

Table S5: Cartesian coordinates of the optimized forms of **TCEP=X** (X=O, S, Se, Te)

Cartesian coordinates	Molecule
C 1.85205100 0.07773900 0.74497500 H 2.20619600 1.09041200 0.95839800 H 1.97532800 -0.50556000 1.66237000 C 2.64554600 -0.54340000 -0.40682700 H 2.49919000 0.02463800 -1.33087200 H 2.29941300 -1.55919100 -0.61641900 C 4.16509700 -0.62512500 -0.18025200 C -0.18976900 1.22028200 -1.03967600 H 0.65357400 1.91141800 -1.11284100 H -0.10805600 0.52461200 -1.87936400 C -1.51084300 1.99759800 -1.11656400 H -1.65851600 2.31340500 -2.15639600 H -2.36543400 1.36775700 -0.86594500 C -0.58248700 -1.45571000 0.19938300 H -0.10925500 -1.82578700 -0.71343600 H -0.20524000 -2.06268600 1.02858600 C -2.10614600 -1.56046000 0.11007200 H -2.48496500 -0.96852600 -0.72966300 H -2.57505000 -1.14915900 1.00774700 C -2.65075200 -2.98523100 -0.08383900 C -1.58467000 3.28576300 -0.28208400 O -0.51697700 3.92180200 -0.05158100 O -3.90589200 -3.12257300 0.03935400 O 4.82916800 -1.20303300 -1.09350200 O -1.85087600 -3.92127500 -0.36561900 O -2.73982100 3.66249400 0.08059400 O 4.66410700 -0.12466600 0.86582400 P 0.04619000 0.23863900 0.49859200 O -0.61073400 0.88604600 1.72466000	<p style="text-align: center;"><b>TCEP=O</b></p>
C -1.91852200 -0.20499500 0.67962100 H -2.17296200 -1.23504000 0.94163300 H -2.12662900 0.41061400 1.55809700 C -2.73539100 0.26560400 -0.52602500 H -2.53318800 -0.35631300 -1.40223900 H -2.46711700 1.28791700 -0.80819800 C -4.25980800 0.25798600 -0.31393100 C 0.24755600 -1.12643700 -1.07114200 H -0.47962800 -1.94079600 -1.10561700 H 0.00366000 -0.43854100 -1.88572300 C 1.66572700 -1.68259100 -1.24756400 H 1.84606900 -1.80805500 -2.32217400 H 2.42497300 -0.98553600 -0.89293600 C 0.34809900 1.57357300 0.16881800 H -0.25438200 1.89792200 -0.68387000 H -0.00311600 2.12249600 1.04665600	<p style="text-align: center;"><b>TCEP=S</b></p>

<p>C 1.83021400 1.84472000 -0.08318300  H 2.16887500 1.33536700 -0.98988300  H 2.43789700 1.44713400 0.73480800  C 2.20251700 3.32749300 -0.24354700  C 1.94042600 -3.06341400 -0.63211800  O 0.98669600 -3.88716100 -0.53114700  O 3.43064400 3.56907000 -0.44880900  O -4.95863500 0.58514900 -1.32027300  O 1.29896400 4.20673900 -0.16803300  O 3.14513100 -3.31655400 -0.32763600  O -4.72729500 -0.05771400 0.81564500  P -0.08690100 -0.18841800 0.48481600  S 0.82063200 -0.92867200 2.12460400</p>	
<p>C -1.98111700 -0.26493700 0.50555600  H -2.14315800 -1.32842200 0.69677100  H -2.17713000 0.26476800 1.44061000  C -2.89657200 0.23504400 -0.61517500  H -2.69104700 -0.28821100 -1.55284100  H -2.72869700 1.29751900 -0.81350400  C -4.40171800 0.07627600 -0.33272200  C 0.15715200 -0.90157800 -1.42116200  H -0.52704800 -1.74991700 -1.48790800  H -0.15740600 -0.16937200 -2.17007100  C 1.59340900 -1.36312600 -1.69393800  H 1.73233000 -1.39897300 -2.78127900  H 2.33015100 -0.65234300 -1.31887300  C 0.13163600 1.71412400 0.00716200  H -0.52218800 2.04641700 -0.80422800  H -0.22826600 2.17512500 0.92997100  C 1.58034700 2.11075400 -0.27381900  H 1.92794600 1.67809900 -1.21464700  H 2.24218800 1.72126100 0.50678500  C 1.82473400 3.62754200 -0.34246400  C 1.96489700 -2.77045400 -1.19668800  O 1.05185900 -3.63517800 -1.07500700  O 2.96469800 3.98802600 -0.76374900  O -5.17669500 0.41605800 -1.27676300  O 0.91185800 4.41687000 0.03023800  O 3.19841700 -2.99132200 -1.00412300  O -4.77917900 -0.36167400 0.78898600  P -0.17351100 -0.09024300 0.20412300  Se 0.95119800 -0.93195300 1.88500600</p>	<p style="text-align: center;"><b>TCEP=Se</b></p> 
<p>C 2.01090300 -0.49031400 -0.43119200  H 1.99449300 -1.57645200 -0.54582500  H 2.19975900 -0.06548100 -1.41992200  C 3.08741900 -0.06306600 0.57002700  H 2.90199000 -0.50623200 1.55253000  H 3.08275100 1.02057200 0.71598100  C 4.52338500 -0.44955700 0.17180300  C -0.00514600 -0.60741300 1.72159900  H 0.58765900 -1.51724800 1.83168000  H 0.44510300 0.15619500 2.36240300  C -1.45286600 -0.87671600 2.14270900  H -1.52563900 -0.72571800 3.22619900  H -2.15141900 -0.16819200 1.69529200  C 0.28326500 1.83418900 0.05231500  H 1.04006800 2.11735900 0.78892600  H 0.63701900 2.16050500 -0.92872300</p>	<p style="text-align: center;"><b>TCEP=Te</b></p>

C -1.06089200 2.47474600 0.38859100  
 H -1.41060400 2.15411800 1.37430200  
 H -1.82667300 2.15736000 -0.32538600  
 C -1.05382100 4.01229000 0.39051300  
 C -1.97784900 -2.30137600 1.89599200  
 O -1.15174200 -3.23552700 1.69905500  
 O -2.16059400 4.57091000 0.65642200  
 O 5.43415700 -0.08618200 0.97551500  
 O 0.01911000 4.62688800 0.13292800  
 O -3.23502100 -2.45140600 1.96907500  
 O 4.71972300 -1.08792500 -0.89913100  
 P 0.28533900 -0.00667100 -0.00286100  
 Te -1.25742400 -0.86533600 -1.69172300



## 6. References

- S1 D. Bera, L. Qian, T. K. Tseng and P. H. Holloway, *Materials (Basel)*, 2010, **3**, 2260–2345.
- S2 H. Zhu, A. Prakash, D. N. Benoit, C. J. Jones and V. L. Colvin, *Nanotechnology*, 2010, **21**, 255604.
- S3 C. Würth, M. Grabolle, J. Pauli, M. Spieles and U. Resch-Genger, *Nat. Protoc.*, 2013, **8**, 1535–1550.
- S4 M. Grabolle, M. Spieles, V. Lesnyak, N. Gaponik, A. Eychmüller and U. Resch-Genger, *Anal. Chem.*, 2009, **81**, 6285–6294.
- S5 J. C. Champarnaud-Mesjard, S. Blanchandin, P. Thomas, A. Mirgorodsky, T. Merle-Méjean and B. Frit, *J. Phys. Chem. Solids*, 2000, **61**, 1499–1507.
- S6 W. Wan, M. Zhang, M. Zhao, N. Rowell, C. Zhang, S. Wang, T. Kreouzis, H. Fan, W. Huang and K. Yu, *Nat. Commun.*, 2020, **11**, 4–11.
- S7 E. Article, S. Dery, P. S. Reddy, L. Dery, R. Mousa and R. N. Dardashti, *Chem. Sci.*, 2015, **6**, 6207–6212.